RIPRAP STABILITY IN CHANNELS

by

John Spurgeon Watkins

B.S.C.E., SOUTHERN METHODIST UNIVERSITY, 1963

A thesis submitted to the Faculty of the Graduate
School of the University of Colorado in partial
fulfillment of the requirements for the degree of
Master of Science
Department of Civil Engineering

1968

PAP 273

This Thesis for the Master of Science Degree by

John Spurgeon Watkins

has been approved for the

Department of

Civil Engineering

by

____

____

Date ______________________________

Watkins, John Spurgeon (M.S., Civil Engineering)

Riprap Stability in Channels

Thesis directed by Dr. Warren DeLapp

Riprap is used in channels to dissipate the excessive energy of flow which would otherwise erode the channel and thereby decrease flow efficiency. Flow efficiency or discharge capacity is apt to be reduced at points of scour by such forms of discontinuity as vorticies and boils which introduce air into the water as well as impede its downstream movement. Several theories have been proposed in an attempt to arrive at meaningful design criteria for the size of riprap needed in a given situation. Because the problem is so complex, reliable experimental data concerning riprap is scarce.

In this study, the writer attempts to analyse the problem on the basis of forces resulting from boundary velocity distribution at the riprap surface. Velocity profiles were measured and recorded with the aid of a differntial pressure cell for the following two conditions:

1) Initial instability—defined as the removal of several pieces of riprap from their original location leaving a scour hole or cavity.

2) Scour to a depth equal to the largest size of riprap present in the test category.

The information obtained by this research will lay the groundwork for future studies in riprap gradation. This provides an interesting comparison with formulations published to date for specifying riprap sizes in prototype design. The tests discussed only concern size categories which fall near the size versus velocity curves shown at the end of the report. However, it must be noted that the curves published by the U.S. Bureau of Reclamation and others represent the 50 per cent passing material in a well graded riprap sample. The pressure distribution immediately above the rock surface is investigated to check possible uplift tendencies. Static pressure wall ports and a multiple Prandtl tube probe were used.

Shape as a parameter was investigated by comparing data taken from both cobbles and angular material. Careful measurements of physical characteristics were made on a random sample from each size category of test material. Measurements included volume, weight, and major axial dimensions. Photographs were also taken before and after one erosion test for each size category. An attempt was made to compute the scale factors of material measured as a preliminary step for proposed model tests of full scale riprap gradations.

This abstract is approved as to form and content.

Signed______________________________

Faculty member in charge of dissertation

ACKNOWLEDGMENTS

Sincere thanks are extended to the U.S. Bureau of Reclamation for the use of the Hydraulics Branch research facilities and equipment. The writer is particularly indebted to Al Peterka, Jim Carlson, M. E. Day, Phil Enger, Tom Rhone, and many of the members of the Hydraulics Branch who spent hours helping the writer in equipment adjustment and data analysis. Special thanks go to Dr. Warren DeLapp for directing the thesis, and to Mary Ann Watkins for typing and general encouragement.

NOMENCLATURE

A_c = Cross-sectional area of the contracted jet of the flow, $ft.^2$

a, b, c = axial dimensions: longest, intermediate, and shortest, respectively, inches.

c, c_1, c_2 = Constants of variation.

c_c = Coefficient of energy loss which is a function of the contraction of the submerged flow jet under the baffle, dimensionless.

c_v = Coefficient of energy loss which is a function of velocity of flow, dimensionless.

D = depth of the velocity jet under the baffle (modified from baffle opening for jet contraction), ft.

d = Characteristic linear dimension for sediment size, inches.

d_s = Diameter of equivalent weight sphere, inches.

d_c = Edge of equivalent weight cube, inches.

d_{sc} = A linear size measurement which combines characteristics of both cube edge and sphere diameter (see eq. 1.4, p. 6).

f = Frequency of repetition, cycles per second, of similar velocity fluctuations.

g = Acceleration of gravity.

h_A = Amplitude of the velocity head fluctuation, fps.

h_B = Energy loss at the baffle, ft.

K = Special coefficient of variation developed by Hedar (see p. 10).

L = Characteristic eddie length as defined by Dryden, ft. (see p. 26).

n = Porosity, dimensionless.

p_o = Static pressure, psi.

p_s = Stagnation pressure, psi.

q = Discharge per foot of channel width, cfs/ft.

q_j = Jet discharge per foot of width under the baffle, cfs/ft.

$R(y)$ = Correlation coefficient of longitudinal fluctuation of velocity (component normal to the flow tube section, see p. 26).

s = Shape factor, dimensionless.

sp. gr. = Specific gravity, dimensionless.

u = Total longitudinal velocity component at a point, fps.

$\bar{u}$ = Mean longitudinal velocity component at a point, fps.

$u' = u - \bar{u}$ = Turbulence fluctuations about the mean velocity at a point in the flow, fps.

$\dot{V}$ = Volume of riprap material, ft^3.

$\bar{V}$ = Mean point velocity, fps.

v = Mean velocity in the channel of flow, fps.

v_b, v_m = Mean water velocity for incipient or beginning motion of a given size aggregate, fps or meters/sec.

y = Effective depth of flow, ft.

y_v = Vertical distance from a median point in the rock surface profile to a given point in flow velocity, inches.

W = Weight of individual rock, lbs.

W_{sc} = Equivalent weight combining characteristics of both cube and sphere (see eq. 1.3, p. 6), lbs.

α = Slope of channel at the centerline in the direction of flow, dimensionless.

γ_s = Unit weight of stone, lbs/ft.^{3}

γ_w = Unit weight of water, lbs/ft^3.

Θ = Position function, dimensionless.

μ = Dynamic viscosity of water, lb-sec/ft^2.

π = 3.14159

ρ = Term used for natural slope of randomly placed rubble (similar to angle of repose, see eq. 1.12, p. 11).

ρ = Density of stone, lb-sec^2/ft^4(see eq. 1.13, p. 13).

ρ_s = Density of stone, lb-sec^2/ft^4.

ρ_w = Density of water, lb-sec^2/ft^4.

σ = Density of water (see eq. 1.13, p. 13), lb-sec^2/ft^4.

ϕ = Natural angle of repose of material measured from the horizontal.

tan ϕ = Coefficient of internal friction.

TABLE OF CONTENTS

LIST OF TABLES

LIST OF FIGURES

FIGURE		PAGE
	Velocity Profiles	
17	3/4 to 1 1/2 inch cobbles	93
18	1 1/2 to 3 inch cobbles	94
19, 20	3 to 6 inch cobbles	95
21, 22	6 to 9 inch cobbles	97
23, 24, 25	3 to 6 inch angular	99
26, 27	1 1/2 to 3 inch angular	102
28, 29	6 to 9 inch angular	104
30, 31, 31A	Scour Cross Sections	106
32, 33	Envelope Velocity Curves	109
34	U. S. Bureau of Reclamation Velocity Curve .	111
35	U. S. Army Corps of Engineers Velocity Curve	112
36	Andersson's Summary of Velocity Curves . . .	113
37	Pi-term Array	114

CHAPTER 1

BACKGROUND AND THEORETICAL CONSIDERATIONS

Riprap protection is an important feature of water conveying systems. Since early times, man has known that he could protect his property from erosion by placing rocks and other forms of rubble in the area of scour. As the population density along waterways became heavier, the need for more sophisticated methods of providing erosion protection was made evident.

It is the objective of the writer to approach the problem in a pragmatic manner to ascertain what the problems involve, and how the modern researcher can pursue the following questions:

a. What are the factors of stability?

b. What stability factors are significant to the designer?

Techniques for choice of riprap size and specifications have lacked the basic information which could be found in the laboratory. This deficit of information is partially due to the difficult problem of isolating any of the many parameters responsible for the erosion of riprap. The equipment used in this study establishes boundary velocity conditions by using a sluice gate type of movable baffle to induce a submerged jet along the riprap surface. This study investigates only the conditions present on the stream bed and does not consider embankment problems.

Riprap Stability

The immediate question arises; what are the stability requirements of riprap? Riprap has been defined as..."a layer, facing or protective mound of stones randomly placed to prevent erosion, scour or sloughing of a structure or embankment; also the stone so used (1)*." The Bureau of Public Roads broadened this definition to include mortared and grouted riprap, concrete in bags, concrete slab riprap and stone riprap for foundation protection(2). These descriptions point to the importance of weight and flexibility for stability. Closely related to weight is the effective size, gradation, shape and general proportions of the overall blanket. Finally, the manner of placement may be the sole reason for instability of the blanket, and a major factor in the cost as well.

Along with the physical characteristics of the blanket, the behavior of the riprap when exposed to hydrodynamic forces must be analysed. Turbulence resulting from various forms of roughness, velocity patterns, and the resulting pressure fields in the fluid all result in significant forces which can dislodge portions of the protective blanket.

Cost is a dominant consideration in every aspect of riprap construction. Consequently, the handling of the heavier pieces becomes an expensive factor in placement. Conflicting with this desire for less weight however, is the fact that none of the other parameters seem to be a sufficient substitute for weight as a stablizing factor. Riprap blankets have failed when the thickness was doubled to compensate for the use of lighter materials. Another

* Numbers found in brackets, as (1), refer to the bibliography on page 39.

substitute for weight has been the use of various techniques to increase the size of the unit, for example: tieing several sections together with wire screen, cable and mortar to link individual or groups of stones or manmade materials into one flexible unit (2) (3) (4). Naib (5) and Carey (4) give information about other forms of manmade riprap which have great promise for the future. Also very important is the type of foundation constructed for the riprap. The type of soil filter used can be instrumental in determining whether or not the bank will erode between the larger portions of riprap (2) (6) (7). Length of the riprap blanket is determined by estimates of the area affected by eroding forces such as high velocity jets, turbulent eddies and vortices (2). Side slope, centerline grade and hydraulic radius all play an important part in this analysis. Better methods of predicting future sources of change in the watercourse and their effect on stability requirements would be of considerable help to the riprap designer. For the purposes of this report, however, the discussion will be restricted to some of the more fundamental stability parameters of riprap. These parameters shall include rock size (weight and volume), shape (round versus angular), and water velocity and pressure variations with depth and time.

Riprap Failure Sequence

An analysis of the sequence of events occurring at the time of riprap failure should shed some light on the areas for study. From general observations in the laboratory and natural stream beds, it has been noted that as the velocity at the riprap surface is increased, there is a slight rearranging of the material according to shape. A slight quivering becomes increasingly evident among the smaller rocks.

The quivering seems to be directly related to the cross-sectional area of the individual rock exposed to the current and its position with relation to adjacent segments. Failure is often initiated by the removal of a key stone behind which a line of other stones has been formed by current patterns. A whole line at a time may fail and wash downstream a significant distance. A portion of the blanket is then cratered, and its resistance to future erosion reduced. The larger the stone size, the less warning occurs before failure. The stone may be lifted suddenly high into the current of flow, as in Figure 4B. To the contrary, the larger material, if it is shaped right, may merely adjust slightly to a more stable position and remain stationary.

PARAMETERS OF STABILITY

From the above sequence, it can be seen that certain difficult-to-define non-uniform parameters exist in the riprap installation that make analysis difficult. The rock shape and position may vary considerably. Velocity currents can form in a myriad of different patterns and time sequences. Fluctuations in flow cause multiple variations of pressure forces on the riprap.

Shape

Shape can be described as stream rounded cobbles, hereafter referred to as "cobbles", and quarry-blasted, crushed "angular" material. Shape can also be significantly categorized by dimension ratios separating rods, disks and blades from spheres (7) (8) (9) (10). Ratio limits should be determined for maximum variations allowable in length to width thickness. The Army Corps of Engineers makes the following comments about shape: "The shape of rock that tends to break due to quarry operations or other reasons into elongated or slabby particles needs to be controlled by provisions in the specifications. It is desirable not to have stone whose long dimension materially exceeds their short dimension." Cubical stones "nest" together best and are most resistant to movement. Limitations should be specified as follows:

a. Stones having the ratio of longest to shortest dimensions greater than two should not exceed twenty-five per cent of the total.

b. Stones having the ratio of longest to shortest dimensions greater than three should not exceed five per cent of the total riprap material. (11)

Gradation

Gradation follows directly as the next point of interest. There is the question of which portion of the gradation should make up the largest portion of the blanket—the larger sizes or the fifty per cent passing or some other portion of the blanket? Should this be determined by gross volume or weight? What is the most desirable per cent of smalls to be included? The Bureau of Public Roads, the U.S. Army Corps of Engineers, and the Bureau of Reclamation have all written specifications for riprap.

Rock Size

The specification of the size of individual pieces of riprap is further complicated by the different methods used. One method that seems to be prevalent specifies size by the diameter of sphere of volume and weight equal to that of the individual stone (11).

Reduced to equation form:

(1.1) $$\text{Weight} = W = (\gamma_s \pi d_s^3)/6$$

where γ_s = unit weight of stone, lb/ft^3

d_s = diameter of equivalent weight sphere.

(1.2) $$d_s = (6W/\gamma_s \pi)^{\frac{1}{3}}$$

$$d_s = (W/0.52\ \gamma_s)^{\frac{1}{3}}$$

A second form combines the characteristics of both cube and sphere as follows (11):

(1.3) $$\text{Weight} = W_{sc} = \frac{1}{2}\left[d_c^3 \gamma_s + \gamma_s (\pi d_s^3/6)\right],$$

where d_c = edge of equivalent weight cube.

Calling the new dimension d_{sc}, for cube and sphere dimensions combined, and solving for it:

(1.4) $$d_{sc} = [2W/(1 + \pi/6)\gamma_s]^{\frac{1}{3}} = (W/0.76\ \gamma_s)^{\frac{1}{3}}$$

Conversion from one to the other form may be made by applying the appropriate factor:

(1.5) $$d_s = 1.13\ d_{sc}.$$

For studying the various size to velocity curves, both forms of d will be used (d_s for cobbles and d_{sc} for angulars) since the curve shifts according to the size parameter used.

Blanket Thickness

Blanket thickness is directly related to the particle size. Some designers (11) specify that the thickness of the riprap layer shall be equal to or greater than one hundred per cent passing or 1.5 times fifty per cent passing, whichever results in the greater thickness. The object is to be sure that all stones are fully contained within the riprap layer.

Velocity as Index to Current Erosion Potential

Riprap installations are surrounded by varying pressure and velocity fields resulting from turbulent flow in and around the rocks that make up the blanket of protection. Of main interest to those concerned with riprap throughout its history has been the so-called competent velocity at which riprap erodes. Much terminology and data have been drawn from the closely related subject of sediment transport. Competent condition is the term used by Berry (12) to describe the limiting case between the vibration of bed-load and the start of uninterrupted movement of the pebble.

The cause or indicators of the forces present in a given situation have been separated into two general categories. These are velocity scour and turbulent boil or scour. Both forms relate to flow characteristics in the channel.

Velocity versus Riprap Size

The use of velocity as an indicator of riprap size requirements in a channel has been widely practiced. The number of particular velocities considered significant are almost as numerous as the originators. The mean velocity was generally considered a good index until a number of researchers presented velocity-versus-size curves that showed how sensitive the upper range of sizes were to even a slight change in velocity. From these curves, (Figures 34 and 35) it can be seen how a slight error in the velocity chosen as critical could radically change the stability capability of the riprap layer.

Berry (12) defines a competent mean velocity, sometimes known as the critical mean velocity, as the velocity at which a certain size sediment on a channel bottom is just moved. He states that there is a limitation to mean-velocity criteria in that it does not bear a constant relationship to the bottom velocity. It is the bottom velocity which is the probable controlling factor in bedload transportation. Likewise bottom velocity is significant in riprap instability.

Another reference to the mean velocity was made by Etcheverry (13) in 1915. He states: "Bottom velocity is approximately 0.75 of the mean velocity." This figure was used by Peterka (14) in estimating velocities present in several prototype examples which both survived and failed under excessive flow conditions.

Berry (12) reports that ..."Bogardi, on the basis of his experimental studies in Iowa, found that:

(a) The roughness factor denoting the bed friction varies independently from the critical mean velocity as well as from the critical bottom velocity. He therefore concluded, that from the point of view of bed friction alone, it is the same to characterize the competent condition by the mean velocity as by the bottom velocity.

(b) Within the limits of his experiments, for the same bed-load the competent mean and bottom velocities were not influenced by the width of the flume. From this viewpoint also, there is no difference whether we use the critical mean or competent bottom velocities for the criteria for start of movement.

(c) He further found that for the same bed-load material the competent bottom velocity does not depend upon the depth of water in the channel. On the contrary, however, the mean velocity varies with the depth of water, increasing with increasing depth of water."

Berry (12) further reports that..."as a result of analysing Gilbert's experimental data, Rubey has shown that it is the velocity in the immediate vicinity of the particle on the stream bed that is significant for the start of bed-load movement. He defines the bed-velocity as the velocity at the boundary between the thin film of laminar flow on the stream bed and the main mass of turbulent water above it."

The "sixth-power law" represents a commonly used relation between the eroding power of the current and variation of the velocity. John Leslie (12), Wilfred Airy (15), and S. V. Isbash (16) have been credited for contributing to the development of this relationship. The sixth-power law states that the weight required for stability varies as the sixth power of the velocity acting on the rock. Isbash's curve interpreting the power law is found in Figures 35 and 36. Figure 35 also gives several arbitrary curves presented for use in specific situations. Campbell says, "To estimate the required size of rock which is stable for a given velocity, the fifty per cent passing is used." "A coefficient $E_s = 1.20$ is used as the basis of the Isbash curve." (17) (See Figure 35) Superimposed on the chart will be found data points resulting from the present research for comparison.

Berry (12) introduced the following relation:

$$V_b = 0.51\sqrt{d} \qquad (1.6)$$

where d represents sediment sizes from a quarter of an inch to twenty-six inches. Some data points from this curve may be found on Figure 35. The bed-load material represented is of an average specific gravity of 2.65. Movement includes rolling or sliding on a bed of the same size, and for average turbulence and particle shapes.

Figure 36 summarizes the findings of Soren Andersson (18). For ease of comparison, notation is changed to coincide with that used throughout this report. The following is an excerpt from Andersson's report:

"SHIELD'S (1936)

(1.7)
$$d = \frac{\gamma_w}{\gamma_s - \gamma_w}\left[\frac{y \sin \alpha}{0.06}\right]$$

where α = ∠ slope of channel in the direction of flow.

MEYER, PETER & MULLER (1948)

(1.8)
$$d = \left[\frac{\gamma_w}{\gamma_s - \gamma_w}\right]\left[\frac{y \sin \alpha}{0.03 \text{ to } 0.047}\right],$$

where 0.03 must be assigned to complete rest and 0.047 to a situation in which material transport is zero. The last value was obtained by extrapolation of the test values in measurements of material transport.

SUNDBORG (1956)

(1.9)
$$d = \frac{\gamma_w}{\gamma_s - \gamma_w}\left[\frac{3}{2}\frac{y}{c_1 c_2}\right]\left[\frac{\sin \alpha}{\tan \phi \cos \alpha - \sin \alpha}\right]$$

where c_1 and c_2 = coefficients dependent on degree of turbulence and state of density of the material (normally, $c_1 \cdot c_2 = c$ may be fixed at 0.087).

HEDAR (1960, 1962)

(1.10)
$$d = \frac{\gamma_w}{\gamma_s - \gamma_w}\left[\frac{1}{K}\right]\left[\frac{v_m}{\log\left(\frac{14.83\, y}{d}\right)}\right]^2\left[\frac{1}{\tan \phi \cos \alpha - \sin \alpha}\right]$$

where v_m = mean velocity of water, m/sec

K = coefficient evaluated by Hedar = 7.5 . For the two equations above, ϕ = angle of natural slope of the stones.

ISBASH (1936)

$$(1.11) \quad d = \frac{\gamma_w}{\gamma_s - \gamma_w} \left[\frac{v_m^2}{2g}\right]\left[\frac{1}{1.44}\right]$$

where g = acceleration of gravity, m/sec^2." (18)

The coefficient 1.44 has been obtained empirically on the assumption that the blocks of stone are dumped pell-mell in running water. Andersson further states that his illustration of the above equations and others represent flow on a gentle slope at a depth of water equal to twenty rock diameters (Figure 36).

The California Highway Department, in a publication entitled Bank and Shore Protection in California Highway Practice (3), gives specifications for choosing rock size where current velocity governs. Since theirs is for embankment rather than channel bottom protection, it is only mentioned here for general interest. Their nomograph (found in the Appendix) is based on the following equation:

$$(1.12) \quad W = \frac{2\,(10)^{-5}\,V^6\,\overline{sg}_r\,\csc^3(\rho-\alpha)}{(\overline{sg}_r - 1)^3}$$

where V = velocity of the stream near the bank to be protected

$\overline{sg}_r$ = specific gravity of the stones

ρ = 70° for randomly placed rubble

α = embankment face slope

W = minimum weight in pounds of outside stone for no damage.

It is interesting to note that the emphasis is on weight and velocity with a correction factor for specific gravity. They have related random-shaped boulders and broken stone to some of the commonest geometric shapes which form a shape spectrum extending from fully rounded to fully angular. Tabulations of factors for precisely defined shapes will provide a basis for interpolation of approximate or intermediate variations (see table and illustration of shapes in Appendix).

The U.S. Bureau of Public Roads has published a report summarizing various uses of riprap for bank protection (2). Their stone-weight versus velocity curves were taken from the same original source as that used by Campbell (19) published and supplemented from time to time by the U.S. Army Corps of Engineers at the Waterways Experiment Station in Vicksburg, Mississippi. For better comparability, the supplementary curves added by Campbell were superimposed on the figure used by the U.S. Bureau of Public Roads along with data points from Berry (12), Peterka (14), and the present research.

M. G. Hiranandani, director of the Central Water and Power Research Station at Poona, India, has written a review and comparison of his findings during visits to hydraulic research laboratories in the United States, United Kingdom and France with his activities at the Poona Research Station (20). He tells of experiments that were conducted at the CWPRS, Poona, in 1940, for determining the size of stone which should be used to represent the stone of block protection given in prototype structures at bridges or else at weirs and falls. "Tests with stones were made both for angular stones and rounded stones. The velocities required for initial continuous movement, and also for general movement were observed. The stones were laid over a smooth bed and alternatively on fixed layers of stones of the same size. The data collected during these experiments for angular stones and for initial movement enabled the following correlation to be established." (20)

(1.13)

$$\frac{Dia.}{d} = 0.1145\left[\frac{V^2}{gd}\cdot\frac{\rho}{\sigma-\rho}\right]$$

(1.14)

$$Dia. = 0.1145\left[\frac{V^2}{g}\cdot\frac{\gamma_s}{\gamma_w-\gamma_s}\right]$$

where d = depth of flow in feet

Dia. = size of stone-diameter in feet

v = average velocity in feet per second

ρ = density of the stone

σ = density of the water.

"The specific gravity of stones used in these experiments varied from 2.94 to 2.83 giving a mean value of 2.89. With this specific gravity and an assumed conversion factor of 0.4, the equation reduces to the form: $Dia. = 0.0019\, v^2$." (20) (1.15)

The values obtained from this relation are plotted on the curve of the U.S. Bureau of Reclamation. The trend of this curve appears to be similar to that of the U.S. Bureau of Reclamation. (Figure 34)

It should be observed here that the transporting power of water is different from its erosive power and the two should not be confused. As Berry (12) describes it, transporting power must overcome the weight, and erosive power must break the cohesive bonding of the material. "The latter varies as the square of the bottom velocity while the former varies as the sixth power of the velocity." It has been observed that in many cases of removal of slightly cohering material, the resistance is a mixture of both, and the power of removing material will vary as some rate between v^2 and v^6. It is the cohesive force that causes a major difference between prototype and laboratory results. Impurities found only in the prototype waters form various kinds of bonding on the riprap material affecting the erosion patterns of the smaller crushed material and, in particular, the filter blanket underneath.

Discharge may be a pertinent parameter for riprap instability. Joonejo (21) concluded from his study of rock movement under flowing water that..."for a given slope and sample, the loss of material increases as the discharge increases." This problem of varying discharge is investigated in the present study.

Dimensionless parameters are often used to help describe significant characteristics of hydraulic systems. These parameters are arrived at by dimensional analysis of a variety of combinations of geometric, kinematic and dynamic dimensions. Reynolds and Froude numbers are familiar dimensionless ratios often used. Vennard (23) and Streeter (24) both give excellent developments of dimensional analysis including the Buckingham II-theorem.

Buckingham showed that, if n variables were functions of each other, k equations of their exponents could be written. Dimensional analysis would assemble the variable into (n-k) dimensionless groups which are functionally related. Buckingham designated these dimensionless groups by the capital Greek letter Pi (II). The II-theorem offers an advance notice of how many groups are to be expected and some clue as to their formulation.

CHAPTER 2

LABORATORY EQUIPMENT AND PROCEDURE

Tests were made in the large flume at the U.S. Bureau of Reclamation's Hydraulic Laboratory in Denver, Colorado. As can be seen in Figure 2, only a portion of the flume was used for the actual test section in order to cut down on the amount of rock that would have to be handled. Of the overall flume which is four feet wide by eight feet deep by eighty feet long, the test section containing gravel was reduced to two feet of width and twenty-eight feet of length. The test scour section extended downstream from the baffle approximately ten feet, but only a portion of this section was usually affected by the submerged jet. One side of the flume is glass-walled thus lending itself very well to sectional erosion tests. The baffle carriage and adjacent equipment (Figures 1 and 2) were already assembled for use in previous tests concerning the cleaning of manmade salmon spawning beds in canals (22).

The fundamental function of the equipment used for this study was to provide a relatively homogenous velocity jet in the region near the boundary of the rock surface. In this way, it was hoped that the velocity most signficant for the scour of the particular rock would become more evident. By reducing the number of variables, the research engineer can better examine a complex problem. The passage of the water under the baffle makes negligible the effect of the upstream velocity distribution on the test section scour. Turbulence, though certainly present, is of a much more uniform pattern than found in the field. Turbulent surging often appears to be the major cause for severe scour in prototype structures.

Analysis of the surge pattern requires a model of the specific situation in each different individual structure, and thus cannot be dealt with in a general study of this type. Figure 1 shows a schematic representation of how the velocity of the submerged jet was increased by lowering the baffle and thereby increasing the differential head which drives the jet.

Several discharges were used to determine its effect on riprap instability. The Bureau Laboratory uses a typical recirculating system where the water is driven by centrifugal pumps through a pipe system to the model and finally dumped back into a large capacity sump. Discharge was measured by a standard Venturi Meter connected to a mercury differential manometer. Twenty-five cubic feet per second was the maximum flow that could be produced by the system.

Velocity distribution was recorded in the vertical plane parallel to and passing through the centerline of the two foot cross section. The one foot scale was included in the pictures showing the scour patterns (Figures 5 through 9) to indicate the channel centerline. The vertical velocity profile was measured first with one Prandtl type pitot-static tube and later with two such tubes mounted in tandom, one above the other. In the latter case, the two tubes were spaced a vertical distance apart equal to the largest size of material in the category being tested. For the six to nine inch angular material, the tube spacing was reduced to give more velocity readings for the velocity jet.

The horizontal velocity distribution was assumed to be symmetrical about the centerline. Since the flume sides were relatively smooth compared to the rock surface in the bottom and considering the magnitude of the velocity in the jet, the symmetry assumption was considered adequate.

Velocity is measured by recording the differential pressure represented by the total (stagnation) pressure minus the static pressure:

$$v = \sqrt{2g\left[p_s - p_o\right]/\gamma} \qquad (2.1)$$

where p_s = stagnation pressure

p_o = static pressure (23).

For this study differential pressure transducers of one and five pounds per square inch capacity were used to measure the velocity head. Several brands of tape recorders were used to produce a graphical record of the pressure fluctation with time. Part of the tests were recorded through an averaging circuit, but for the most part, the pressure differential noted above or velocity head was averaged by eye. The resulting data compared favorably with that obtained with the averaging circuit. Even the mean value recorded using the averaging circuit did not remain constant. The recorders were recalibrated before each test velocity profile and at the conclusion of the test to check for zero drift and span settings. Recording inaccuracies, when noted, were prorated between calibrations with added weight given readings with a high degree of fluctuation. Experience has shown that large, frequent pen movements tend to shift the zero setting slightly and sometimes change the span setting. A sample of the recordings may be found in Figures 10, 11, and 12.

Reduction of velocity was done by estimating the area on either side of a straight hairline etched on plastic which was placed over the recording trace for a given point. The line was adjusted by eye until approximately equal areas were bound by the trace and the hairline. If drift was noted so that the hairline was not parallel to the grid, the points at which the beginning and ending of the trace intersected the hairline for a particular measurement were noted, and average reading taken at the mid-point on the hairline. In this way, the average velocity at a point for several seconds was taken. Velocity profiles were drawn (Figures 17 through 29) showing the vertical profile of the velocity measured relative to an arbitrarily defined datum. The datum was defined as a maximum envelope level line at the extremities of the riprap surface for tests 1 through 12. For the remainder of the tests, the datum was taken as a preset level line that approximated the average rock surface. That is, some rocks projected above the line and some fell below.

The two states of stability shall be defined as follows:

1. Initial instability shall be that condition when several rocks move from their initial positions indicating a condition of unbalanced forces.

2. Maximum scour shall be restricted to one maximum screen size dimension of the category being tested.

Test Procedure

1. Rocks were sized in categories according to specified screen sizes. The cobbles and angular material were tested separately.

2. Random samples were picked from each category, identified by number and sized as discussed above. The volume was measured by water displacement. The physical features a, b, c, and V may be found in Tables 1 through 12.

3. Rocks were placed in the flume at a prescribed depth according to the datum used, and the plan view was photographed (Figures 5 through 9).

4. Flow was established with the baffle wide open.

5. The velocity of the submerged jet was increased slowly for constant discharge by lowering the baffle. Time was allowed for the backwater time lag of the system so that the effect of each incremental gate closure could be identified. Otherwise the critical value of velocity for instability might be passed by.

6. The baffle opening was recorded for the condition of initial instability as discussed previously.

7. The opening was also measured for complete scour to a depth equal to the larger screen size of the category being tested.

8. The velocity profile was then taken.

9. The water depths both upstream and downstream were taken from time to time during the velocity measurements.

10. Discharge readings were also made periodically to check against any drift resulting from changing tailwater conditions.

11. Pictures were then made after the maximum scour to show the erosion pattern of the numbered sample rocks.

12. Profiles were drawn of the cross section under the baffle and along the channel centerline to indicate the depth of scour and to estimate the effective flow area under the baffle.

Separate tests were run using several different discharges and depths for several material categories to establish the effect of discharge and blanket thickness as variables to be related to scour velocities. Velocity tests were run twice for most of the rock categories. Rock blanket thickness, discharge and rock placement were kept as nearly identical as possible.

CHAPTER 3

RESULTS AND CONCLUSIONS

Data Analysis

Riprap shape determines how the separate pieces will fit together and equally important, how stable it is when exposed to hydraulic forces. The importance of shape has been observed, but practical methods of its determination have been lacking. Several methods are recommended in this report as being helpful in relating a particular riprap sample shape to a simple sphere or rectangular solid.

Description of riprap in place in the prototype is mostly in the form of pictures. A few measurements of size have been made in the field. Ball, Lancaster, and Schuster (25) of the U.S. Bureau of Reclamation discuss a technique used at Grand Coulee Dam in the Columbia Basin Project. "Groups of rocks at various stations on both sides of the tailrace banks were located by survey and marked before high water of May, 1949. Individual rocks of the groups varied in shape and weight and were chosen at random to represent a general gradation of riprap in the area. After the flood season, a re-survey noted the movement of the rocks that remained. Many of the rocks and some groups were not recovered because of readjustments of the riprap cover. Those rocks moved and recovered after the flood indicate the extent of readjustment (25)." In a similar manner, rocks from each category in this study tested were numbered, weighed, and the volume and three axial dimensions measured. The numbered rocks were picked at random from the surface of the test section. After they were measured, they were returned to the top layer with the expectation that they would be the first rocks to become unstable and scour. Their movement during scour was traced with pictures taken both before and after scour (Figures 5 through 9).

Riprap shape can be described several ways. Zingg (7) developed a classification of particle shapes based on the four general shapes shown below.

Class	Shape	b/a	c/b
I	Disks	$> 2/3$	$< 2/3$
II	Spherical	$> 2/3$	$> 2/3$
III	Blades	$< 2/3$	$< 2/3$
IV	Rodlike	$< 2/3$	$> 2/3$

Both Zingg [1935] and later Krumbein [1941]. gave descriptions of riprap shape based on ratios or combinations of the axial dimensions where a, b, and c are, respectively, the major, intermediate, and minor axes; the axes being measured at right angles to each other. Krumbein (7) defines sphericity as the cube root of the ratio of the volume of the circumscribing sphere. This reduces to bc/a^2. Theoretically, the closer the rock is to a sphere, the closer the b and c dimensions are to being equal to a. This does not take into consideration the possibility of the rock approaching cubical proportions. It is for just such a problem that the Buckingham II-theorem proves useful.

The pragmatic approach to studying a hydraulic system involves such tools as dimensional analysis. Applying the Buckingham II-theorem to the riprap study, the first step is to identify the possible variables. Letting S equal some stability index,

(3.1)

$$S = \phi(D, d, a,b,c, V, s, \theta, n, h_B, y_v, q, \bar{v}, f, W, \rho_s, \rho_w, h_A, \mu)$$

where the geometric parameters are identified as:

D = depth of the velocity jet under the baffle (includes contraction of the jet) [L]

d = diameter of a sphere of weight equivalent to the riprap [L]

a, b, c, = axial dimensions; longest, intermediate, and shortest, respectively [L]

V = volume of riprap $[L^3]$

s = shape factor [dimensionless]

θ = position = ϕ(shape, nesting, etcetera) [dimensionless]

n = porosity [dimensionless]

h_B = drop in energy head across the baffle [L]

where kinematic parameters are identified as:

q = discharge per foot of channel width $[L^3/T/L]$

$\bar{v}$ = mean point velocity [L/T]

f = frequency [1/T]

y_v = vertical distance from rock surface to significant point velocity for scour [L]

where dynamic parameters are identified as:

W = weight [F]

ρ_s = density of riprap $[FT^2/L^4]$

ρ_w = density of water $[FT^2/L^4]$

h_A = amplitude of the velocity head fluctuations [L]

μ = dynamic viscosity of the water $[FT/L^2]$

According to Buckingham's II-theorem, there must be three repeating variables since there are three fundamental dimensions, length, force and time present. Usually, a variable is chosen from each of the three categories listed above. In the case of riprap, it would be desirable to have Π-terms representing physical features, hydraulic forces, and a combination of the two.

Physical characteristics can be formed into Π-terms directly since they are for the most part, a function of length.

(3.2) $$\Pi_1 = \frac{a + b + c}{3d}$$

(3.3) $$\Pi_2 = \frac{a + b + c}{3y_v}$$

(3.4) $$\Pi_3 = \frac{V}{a\ b\ c}$$

The third pi term is suggested by the need to compare the rocks' actual shape to a rectangular solid of the same axial dimensions.

The hydraulic force terms are a little more difficult to see without some prior knowledge of dimensionless parameters. Beginning with a familiar ratio, the Froude number, h_B, $\bar{v}$, and g are used. If $\Pi_4 = \phi_4[\bar{v}^x, g^y, \rho_s^z, h_B^{-1}]$ with $\bar{v}$, g and ρ_s the repeating variables, then according to Buckingham's Π-theorem:

$$\Pi_4 = \phi_4\left[(L/T)^x, (L/T^2)^y, (FT^2/L^4)^z, L^{-1}\right]$$

F: $z = 0$

L: $x + y - 4z - 1 = 0$

T: $-x - 2y + 2z = 0$

$x = 1 - y = -2y$

$y = -1, \quad x = 2$

(3.5) $$\Pi_4 = \frac{\bar{v}^2}{h_B}$$

For II_5, the last term in equation 3.5 was changed to D ; and g changed to h_B as a repeating variable

$$II_5 = \phi_5 \left[\bar{v}^x, h_B^y, \rho_s^z D^{-1} \right]$$

$$II_5 = \phi_5 \left[(L/T)^x, (L)^y, (FT^2/L^4)^z, L^{-1} \right]$$

F: $z = 0$

L: $x + y - 4z - 1 = 0$

T: $-x + 2z = 0$

$x = 2\ (0) = 0$ thus $y = 1$

(3.6) $II_5 = h_B/D$

By inspection;

(3.7) $$II_6 = \frac{\bar{v}^2}{Dg}$$

A combination of hydraulic and physical characteristics can be evaluated by inspection from II_4 in equation 3.5:

(3.8) $$II_7 = \bar{v}^2/dg.$$

A number of other II-terms could be developed, but the present study will be limited to these seven. (Tables 15 through 21)

To formulate an equation with the pi terms, another II-term involving S is needed. But since S is defined as an index, it should remain dimensionless. Thus,

(3.9) $$II_8 = S$$ and since

(3.10) $$S = C \left[II_1 \cdot II_2 \cdot II_3 \cdot II_4 \cdot II_5 \cdot II_6 \cdot II_7 \cdot \ldots \cdot II_{17} \right],$$

where C = constant,

the researcher must make some decisions about which terms can be measured and which factors are of negligible consideration for riprap design.

Referring back to the list of possible variables, other Π-terms to be concerned with, in particular, are those factors which deal with turbulence. The amplitude term (h_A) and frequency term (f) might be linked together in an expression called the scale of turbulence. H. L. Dryden (26) found that a characteristic length was needed in the specification of turbulence. This length was a measure of the magnitude of the turbulent eddies which he called their scale. He found that this length can be experimentally measured by using a correlation coefficient of longitudinal fluctuations u_1' and u_2' measured at two points whose transverse distance is y. Expressed in equation form:

$$R(y) = \frac{\overline{u_1' \ u_2'}}{\sqrt{\overline{u_1'^2}} \sqrt{\overline{u_2'^2}}} \tag{3.11}$$

where u = total velocity fluctation

$\overline{u}$ = mean velocity fluctuation

$u' = u - \overline{u}$ = turbulence fluctuations over and above the mean velocity

$\sqrt{\overline{u'^2}}$ = root-mean-square value of excess turbulence fluctuation.

The quantity which is characteristic of the scale of turbulence is given as:

$$L = \int_0^\infty R(y)dy. \tag{3.12}$$

It is a measure of the magnitude of the clots of fluid which move together as a unit and thus describe the size of individual eddies. This technique has one difficult requirement for the researcher. It states that y is to varied from zero to infinity, and the root-mean-square value computed for at least a sufficient number of points in-between. This task would have been out of the question with the present instrumentation available. Consequently, the scale of turbulence was not taken for the present report.

The idea of a relationship between turbulence and uplift persisted. As the research progressed, the phenomena of a sudden upward thrust was repeated several times. The problem became one of measuring pressure fields down in the riprap and at its surface. The surface profile could be measured with the dual-tube probe, but no way was found to measure pressure among the rocks at the centerline of the channel. The wall ports below the riprap surface were subject to a variety of possible velocity vectors rebounding off of the adjacent rocks as well as just the static pressure head. The water column readings did not fluctuate enough to warrant transducer recording. At any rate, in situations where fluctuations were observed, several readings were taken and averaged. To see if a trend could be established, the data was plotted. From the plottings, Figures 13 through 16, it can be seen that a trend of uplift pressure would be difficult to confirm. All but the smallest size material show the higher pressure for final scour at the port farthest below the rock surface. But this is not the case at the next port above. The pressure was higher above the rock surface for about half the cases of initial instability. This would have to be reversed for uplift to take place. Finally, it is recognized that ports adjacent to rocks below the surface probably do not indicate the true static pressure at these points because of variation in the direction of the velocity vectors around the rocks.

Another point of interest is the profile drag of the material. As was briefly mentioned in the first chapter, rocks should in general be placed in such a way as to have a minimum number of points projecting significantly above the mean rock surface. The problem of surface drag effects is the reason behind this requirement. Such rocks would be more subject to scour than the others in the blanket. The surface drag magnitude could be established experimentally by rigging one individual rock with a system of spring and levers or even an electrical system which would record its movement. Yet this approach would be difficult to correlate to the overall riprap blanket. Here again is the problem of extreme variation of sample condition where random sampling is recommended.

Attention is now directed back to the factors considered significant and measurable for the present study. Referring to the II-terms again, the following factors are required: a, b, c, d, h_B, $\overline{v}$, and D. The first four terms have already been discussed since they could be measured before flow tests in the flume could begin. The last three terms all concern the velocity jet at the boundary of the riprap surface.

The h_B term represents the drop in head across the baffle. The energy on either side of the baffle is distributed as shown in the equation 3.13 for a unit width section.

$$y_1 + \frac{v_1^2}{2g} = y_2 + \frac{v_2^2}{2g} + h_1 \qquad (3.13)$$

where y_1 & y_2 = upstream and downstream depth

v_1 & v_2 = upstream and downstream velocity

h_1 = energy loss at the baffle

If the unit width areas of flow for upstream and downstream are assumed to be y_1 and y_2, respectively, then the continuity equation can be stated:

$$q = v_1 \, y_1 = v_2 \, y_2 \, . \tag{3.14}$$

Combining equations 3.13 and 3.14, and solving for v_2,

$$v_2 = \frac{c_v \sqrt{2g(y_1 - y_2)}}{\sqrt{1 - (y_2/y_1)^2}} \, . \tag{3.15}$$

The corresponding flow rate can then be stated as

$$q = \frac{c_v \, c_c \, A}{\sqrt{1 - (y_2/y_1)^2}} \sqrt{2g(y_1 - y_2)} \tag{3.16}$$

where c_v accounts for the energy loss, h_1

c_c accounts for the contraction of the submerged jet.

The depths were measured with stilling well manometers attached to static ports located at the base of the riprap blanket. Standard hook type point gauges were used to measure the depth of the water relative to the base of the riprap layer on the flume floor. The respective depth readings of the manometer wells were related by using a standard Wye Level to establish a level line. The distance from the flume floor was also established with a level rod accurate to 0.01 foot. Before continuing, it seems pertinent to discuss the aspect of accuracy as it pertains to this research effort.

Validity of results in research depends heavily on the judgement shown in evaluating the accuracy of data measurements. Extreme care must be exercised in some very delicate measurements such as those made at the point of initial instability, while other measurements may be by necessity, rather arbitrarily taken. For example, the stilling well gauges may be read to the nearest 0.001 foot. Water surface elevation for undulating flow may be good to the nearest

0.1 foot with some reservation for the time of recording. To add to the problem, the backwater effect must be observed. To accomplish a realistic set of data, the stilling well measurements were read at least before and after the velocity profile was taken and sometimes more frequently as the circumstance warranted. The observed trend can be described as an asymptotic approach to a constant depth achieved upon the return to the steady state or equilibrium force condition. This return time for the present system was short enough that by the time a vertical velocity traverse of the jet was made, the flow system was sufficiently stabilized that the depth readings then recorded could be safely used. The difference $y_1 - y_2$ was used as the parameter h_B.

The boundary of the submerged jet was made evident by air bubbles in the flow. The jet contained very few if any air bubbles, whereas the turbulent portion above it contained many bubbles which stood out very well when illuminated by flood lamp (Figure 4B). The fluid interface was traced on the glass wall in order to estimate how much jet contraction existed. The coefficients c_v and c_c were assumed to be combined in a single term c. This coefficient, then, is equal to the ratio of the vertical dimension from the flume floor to the fluid interface, divided by the vertical distance of the baffle edge above the floor (Figure 1). The cross section was roughly plotted by eye using vertical measurements from the baffle edge to the rock surface at three inch intervals. Subtracting the mean riprap blanket thickness from the height of the contracted jet boundary gives the parameter D. This information was all measured for the tests following: 10D, 11B, 11D, 12D, 14B, 15B, 16B, 19B, 20B. If tests can be continued over a longer time period, the initial instability test and the final scour test will be run separately, pausing between to allow the flume to drain so that the cross section of the initial instability surface can be recorded.

Using equation 3.16, the above measurements and the discharge measured by the Venturi meter, the total flow under the baffle can be checked. By integrating the vertical velocity traverse with a planimeter and dividing by D, the mean velocity of the jet is determined. If the area of the jet is assumed to be that at the recorded cross section and determined by planimeter, then the flow in the jet is represented by the equation

(3.17) $q_j = \overline{v}_{mean} \ A_c$,

where A_c = contracted area of flow.

The difference of the total flow minus the jet flow should provide a fair estimate of the water moving through the riprap. This latter flow should in turn give some indication of the relative stability according to size and shape categories.

The velocity profiles must be investigated next to see if a significant velocity exists. The velocity in the profiles represents a condition which results after the forces causing instability reach equilibrium. Consequently, the velocity recorded for both instability and final scour for each test represents a span of values from slightly less than instability velocity to slightly less than the final scour velocity. The measurements at each point represent an average value of the velocity head at that point. Velocity head fluctuations were highest at the boundaries, both at the riprap surface and at the water interface between the jet and the backwash, from the submerged hydraulic jump downstream from the test section (Figure 4B). The shape or divergence angle of the upper and lower portions of the velocity traverse were affected by a change in the tailwater condition and by discharge variation. In attempting to find a significant velocity most affecting scour, several tests were run for the same size riprap at different discharges. Curves from the different discharges are compared in Figures 19, 20, 21, 22, 24, and 25. Final scour was hard to duplicate. As a result of this fact plus the different berm formation of scoured material downstream, the position of the curve is shifted with respect to the datum. Consequently, there is quite a difference in the shape and maximum velocity for the final scour curves. A good example is found in Tests 20 and 21 where the final scour was different due to the existence of a slightly higher differential head across the baffle in Test 20. This resulted in a higher maximum velocity than in Test 21. There was a slightly higher berm formed in Test 20 downstream from the velocity probes elevating the velocity curve relative to the assumed datum. Both tests were conducted for conditions approaching the extreme capacity of the flume allowing little leeway for adjustment. During both tests, the downstream wheels (Figure 2) of the carriage holding the movable baffle were forced into the air by the tremendous force of the water on the baffle.

Special note should be made of the riprap thickness indicated in Figures 24 - 29. Theoretically, the thickness of the rock blanket should not affect the velocity it takes to scour the blanket to a depth that is less than riprap depth. In the current study, however, the small material used to help block flow through the riprap was not present. As a result, the profile drag was not as great and a higher velocity was required for movement (see Test 15A, Figure 24).

The use of the double probe in Tests 17 through 21 gives a more accurate picture of the rapid fluctuations at a given time. By spacing the two Prandtl tubes in such a way as to duplicate velocity measurements in the center region of the jet, a check was made on the data from each separate tube.

The velocity significant for the initial instability was difficult to establish. Point velocities selected for study included the maximum jet velocity, the mean jet velocity, and the velocity at an arbitrary point which usually was placed at an abrupt change in the velocity gradient. This last point was signified by the sign, ⊕. Point plots based on maximum jet velocity and the so called arbitrary velocity best fit the envelope conditions shown in Figures 32 and 33 when the average diameter per category was used. (Tables 13 and 14)

Finally, in order to establish some model scale for size projections to larger riprap material, the II-terms must be developed further. Figure 37 gives the general variation of II-terms with the different sizes and shapes tested.

Evaluation Outline of Tests by Number Taken From Daily Reports

1A. Good shape. Too low discharge for size of rock. Too much influence per rock on velocity profile. Difficult to duplicate scour test.

1B. Not plotted since velocity probe was not at the maximum contraction or throat of the jet.

2A and 2B. No Test 2A was run. Actual sequence follows: Tests 1A and 1B were run. Prandtl tube moved upstream to throat of jet. Discharge slowly built up to same as that of Test 1. Profile 2B then taken over scour of Test 1B.

3A. Good correlation with similar test, 2B. Flow in rocks prevents profile from returning to zero at rock surface.

4A. Fairly good correlation with lower discharge in 3A. With higher discharge, larger baffle opening provided needed velocity, thus not as dependent on each rock's position at the centerline.

4B. Not run.

5A. Good profile.

5B. Trouble with rock berm near probe. Definitely affected shape of curve.

6A. Good profile. Maximum velocity reduced by low discharge.

6B. Needs more data points in critical gradient either side of maximum velocity.

7A. Good profile. Good correlation with high discharge profile in Test 8A.

7B. Good profile. Some scatter for maximum velocities due to rock #4 projecting into current directly under probe.

8A. Best profile for 3 to 6 inch cobbles for initial instability.

8B. Good profile. Rocks numbered 1 and 11 interfered with probe reading in scour.

9A and 9B. Not plotted. Discharge too low even to move 6 to 9 inch cobbles for scour test.

10A and 10C. Good agreement. Appears to be slight shift in datum.

10B and 10D. Slightly higher maximum velocity on Test 10D. Test 10B should have more measurements in region of maximum velocity, but good profile at riprap surface showing velocity gradient.

11A and 11C. Same as 10A and 10C.

11B and 11D. Good agreement in maximum velocities.

12A, 13A, 14A, 15A, 16A, 17A. Good general agreement in all but Test 15A where initial scour data was questionable. Movable baffle would not raise high enough for twenty-two second-foot discharge resulting in some instability as this discharge was being obtained.

12B, 13B, 14B, 15B, 16B, 17B. Good agreement in all but lower discharge tests, numbers 16B and 17B. For Test 16B, rock number 15 affected lower profile data.

18A and 19A. Slight shift in velocity magnitude. Also vertical translation of profile. Cause traced to difference in moved rock formation.

18B and 19B. Good agreement for final scour tests.

20A and 21A. Largest material tested. Almost too big for flume. Profile shape definitely affected by individual rock position.

20B and 21B. Same as 20A and 21A.

Conclusions and Recommendations

The choice of the diameter affected the plot in Figures 32 and 33 noticeably. The U.S. Army Corps of Engineers' curves (Figure 35) are based on equivalent diameter as developed in equations 1.2 and 1.4. The weight used in finding the equivalent diameter is plotted parallel to the diameter. The diameter also represents the fifty per cent passing size of stone as measured in a sieve analysis. V_m represents the mean velocity and V_s, the velocity against the stone. The U.S. Bureau of Reclamation (Figure 34) recommends that..."most of the stone should be of the size indicated by the curve (14)." The U.S. Bureau of Reclamation also uses the equivalent diameter and weight for parallel ordinates. The velocity used is an estimated bottom velocity. Andersson's curves (Figure 36) are based on the equations as outlined on pages 10 and 11. The curve envelopes of Figures 32 and 33 represent higher values of velocity for failure of a given size. The writer believes this difference to be due to the lack of graded material filling the voids in the material tested. Since the curves obtained from other sources all represent some form of gradation, a true comparison could not be made until a sieve analysis was made available on a random sample from each gradation represented.

Estimates of discharge in the gravel proved to be difficult. Differences in the estimated and actual effective cross section are believed to be the reason that, for instance, the discharge in the jet for Test 19 was greater than the total measured discharge in the flume (Tables 22 and 23). The discharge computed on the basis of equation 3.16 is too high because the correct value of c_v was never estimated. A computer program entitled "AREVEL" was used to compute the information (Tables 22 and 23). This program is found in the Appendix along with other computer programs used to calculate shape characteristics and II-terms for physical features.

The plot of the pi terms proved indecisive. More rock sizes are needed to provide any sort of trend. For the angular material, the v^2/dG terms vary inversely with the size since d or the equivalent diameter is in the denominator. The v^2/dG varies directly with the riprap size. The depth of the jet is reduced as the velocity is increased by moving the baffle down while holding discharge constant. This term reflects the special conditions imposed on this specific system used for tests and does not show promise for prototype applications. The term h_B/D varies directly with the material size. This trend is expected since the differential head must increase across the baffle as the velocity increases. This increase in h_B combined with the previously discussed decrease in D accounts for the increase in h_B/D. This term, too, is restricted for use in the present study system of a submerged jet under a baffle. The II-terms representing the physical characteristics found in Tables 15 through 20 are difficult to use in their present form. They represent values for each individual rock per random sample per category. As such they must be lumped together in such a way as to best represent the category in question. A form of statistical analysis such as standard deviation would seem appropriate. This part of data reduction is recommended for the first phase of the overall study of riprap. The term "model study" can only be applied to this study in a general sense in that the rock sample in the flume did not similate prototype riprap.

A basic research project of this type is merely a first step in a series of studies aimed at improving riprap design criteria. The next step after the scale projection of size will be tests to determine optimum gradation for the general case of a submerged jet such as used in this study. Next, a series of tests on different specific situations would be appropriate. For example, the jet which occurs downstream from a chute with no energy dissipator other than riprap could be studied by building a deck under the baffle and lowering the tailwater conditions to increase velocity. The velocities resulting should be high enough to provide data from the present level flume system.

In conclusion, the writer recommends that any approach to the problem of riprap should be made with a research program based on principles of random selection of data. This data should be systematically analysed by methods of modern statistical techniques made possible by the use of the new high speed digital computors. For the mass of data especially concerning the velocity profiles and turbulent pressure fluctuations, a direct system of digitized tape recording as well as line recordings would be very useful. Then data could be directly entered into the computor for analysis.

The present study is considered by the writer to be a meaningful beginning. The velocities in general are a valid representation of the conditions defined by the study. The initial instability velocities are believed to be more reliable than the final scour velocities. More rock sizes will need to be tested before this phase of the general study can be considered complete.

BIBLIOGRAPHY

1. U. S. Army, Office, Chief of Engineers. Shore Protection Planning and Design. Beach Erosion Board, Technical Report No. 4, U. S. Government Printing Office, Washington, D. C., 1961. p. 392.

2. Searcy, James K. Use of Riprap for Bank Protection. U. S. Department of Transportation, Bureau of Public Roads Publication, Hydraulic Engineering Circular No. 11, U. S. Government Printing Office, Washington, D. C., June, 1967.

3. California Highway Department. Bank and Shore Protection in California Highway Practice. Department of Public Works Publication, November, 1960. pp. 112-119.

4. Carey, Walter C. "Construction Problems in Comprehensive River Stabilization, " ASCE Water Resources Engineering Conference, Mobile, Alabama. March, 1965. pp. 25-27.

5. Naib, S. K. A. "Equilibrium of Talus Blocks Downstream of Stilling Basins," Water Power, Vol. 19, No. 10, October, 1967. pp. 407-410.

6. U. S. Army Engineer Waterways Experiment Station, CE. Investigation of Filter Requirements for Underdrains. Vicksburg, Mississippi, December, 1941.

7. Karpoff, K. P. "The Use of Laboratory Tests to Develop Design Criteria for Protective Filters," Earth Laboratory Report No. EM-425. Bureau of Reclamation, United States Department of the Interior, Denver, Colorado, June 20, 1955.

8. Krumbein, W. C. "Measurement and Geological Significance of Shape and Roundness of Sedimentary Particles," Journal of Sedimentary Petrology, Vol. 11, No. 2, 1941. pp. 64-72.

9. Mavies, F. T. and Laushey, L. M. "A Reappraisal of the Beginnings of Bed Movement-Competent Velocity," Proceedings, International Association for Hydraulic Structures Research, Stockholm, Sweden, 1948.

10. Wadell, Hakon. "Volume, Shape, and Roundness of Rock Particles," Journal of Geology, Vol. 40, 1932. pp. 443-451.
"Sphericity and Roundness of Rock Particles," Journal of Geology, Vol. 41, 1933. pp. 310-331.
"Volume, Shape, and Roundness of Quartz Particles," Journal of Geology, Vol. 43, 1935. pp. 250-280.

11. U. S. Army, Office, Chief of Engineers. Criteria for Graded Stone Riprap Channel Protection. Draft Report, U. S. Government Printing Office, Washington, D. C., 20 April, 1966. pp. 1-12.

12. Berry, N. K. "The Start of Bed Load Movement." Thesis, Graduate School, University of Colorado, 1948.

13. Etcheverry, B. A. Irrigation Practice and Engineering, 1st Edition, Volume II. New York; McGraw-Hill Book Company, 1915. p. 56.

14. Peterka, A. J. Hydraulic Design of Stilling Basins and Energy Dissipators. USBR Water Resources Technical Publication, Engineering Monograph No. 25. U. S. Government Printing Office, Washington, D. C., 1964.

15. Airy, Wilfred, discussion of paper, "On Rivers Flowing into Tideless Seas, Illustrated by the River Tiber," by William Shelford. Proceedings, Institution of Civil Engineers, Vol. 82, 1885. p. 25.

16. Isbash, S. V. "Construction of Dams by Depositing Rock in Running Water," Transactions, Second Congress on Large Dams, Vol. 5, 1936. pp. 123-136.

17. Campbell, Frank B. Hydraulic Design of Rock Riprap. Miscellaneous Paper No. 2-777. U. S. Army Engineer, Waterways Experiment Station, Vicksburg, Mississippi, February, 1966.

18. Andersson, Soren. "Stability of Armour Layer of Uniform Stones in Running Water," Sartryck Och Preliminara Rapporter, No. 6, Swedish Geotechnical Institute, Stockholm, Sweden, 1964. pp. 21-27.

19. U. S. Army Engineer Waterways Experiment Station, CE, Hydraulic Design Criteria. Vicksburg, Mississippi, 1957. Vol. 2, pp. 712-1.

20. Hiranandani, M. G. A Visit to Hydraulic Research Laboratories in the United States, United Kingdom and France. Ministry of Irrigation and Power, 20 Bombay Road, Poona, Government of India, 1959. pp. 97, 154.

21. Joonejo, Nazir Ahmad. "Movement of Stones Under Flowing Water." Thesis, Graduate School, University of Colorado, 1966.

22. Carlson, E. J. "Baffle Gate Method for Cleaning Salmon Beds in Canals," XII Congress of International Association for Hydraulic Research (IAHR), September, 1967, Fort Collins, Colorado. Vol. 3. pp. 453-462.

23. Vennard, John K. Fluid Mechanics, 4th Edition. New York; John Wiley & Sons, Inc., July, 1965. p. 197.

24. Streeter, Victor L. Fluid Mechanics, 4th Edition. New York; McGraw-Hill Book Company, 1966. pp. 183-204.

25. U. S. Bureau of Reclamation. Study of Height and Frequency of Waves Acting on Tailrace Slopes and Riverbanks During 1949 Flood Season, Grand Coulee Dam, Columbia Basin Project. Hydraulic Laboratory Report No. 336, U.S. Government Printing Office, Washington, D. C. November 28, 1952.

TABLE 1

PHYSICAL CHARACTERISTICS OF RIPRAP
3/4 TO 1 1/2 INCH COBBLES

```
005 REM    AXIAL  DIMENSIØNS(IN)   WT   VØL
007 REM     A       B        C     LBS  ML
010 DATA  2.125, 1.875, 1.125, .24, 44
020 DATA  2.125, 1.875,  .875, .17, 30
030 DATA  2.250, 1.625,  .625, .14, 25
040 DATA  2.500, 1.625,  .750, .16, 28
050 DATA  1.250, 1.000,  .750, .04,  9
060 DATA  2.000, 1.500, 1.000, .16, 30
070 DATA  2.125, 1.375, 1.125, .17, 30
080 DATA  1.875, 1.750, 1.125, .20, 34
090 DATA  2.125, 1.250, 1.125, .14, 25
100 DATA  1.500, 1.250, 1.125, .09, 15
110 DATA  1.375, 1.250, 1.000, .08, 14
120 DATA  1.625, 1.750, 1.000, .11, 20
130 DATA  1.250, 1.000,  .500, .03,  4
140 DATA  2.000, 1.625,  .625, .13, 22
150 DATA  1.125, 1.000,  .750, .04,  7
160 DATA  1.375, 1.000,  .875, .05, 10
170 DATA  1.750, 1.250,  .625, .07,  6
180 DATA  1.875, 1.625, 1.000, .19, 27
190 DATA  2.500, 1.625, 1.000, .17, 30
200 DATA  2.000, 1.750,  .750, .18, 27
210 DATA  1.375, 1.000, 1.000, .07, 11
220 DATA  2.125, 1.500, 1.000, .18, 28
230 DATA  1.875, 1.375,  .750, .10, 22
240 DATA  2.250, 1.625, 1.125, .22, 41
250 DATA  1.375, 1.250, 1.000, .09,  8
260 DATA  1.500, 1.000, 1.000, .07, 11
270 DATA  2.250, 1.375, 1.000, .17, 34
280 DATA  2.000, 1.500, 1.250, .17, 30
290 DATA  2.000, 1.500,  .875, .13, 24
300 DATA  1.875, 1.500, 1.125, .16, 27
310 DATA  2.000, 1.625,  .875, .11, 23
320 DATA  2.625, 1.500, 1.000, .18, 40
330 DATA  1.500, 1.375, 1.000, .09, 18
340 DATA  2.125, 1.500, 1.250, .19, 39
350 DATA  2.375, 1.500, 1.125, .16, 28
360 DATA  2.375, 1.500, 1.375, .25, 44
```

TABLE 2

PHYSICAL CHARACTERISTICS OF RIPRAP
1 1/2 TO 3 INCH COBBLES

```
005 REM   AXIAL DIMENSIØNS(IN)       WT    VØL
007 REM    A        B        C       LBS   ML
010 DATA  3.000, 2.375, 1.625,   .56,   95
020 DATA  4.500, 3.875, 1.875,  1.57,  265
030 DATA  3.750, 2.875, 1.625,   .81,  135
040 DATA  2.625, 2.125, 1.000,   .33,   62
050 DATA  3.000, 1.750, 1.750,   .42,   80
060 DATA  3.375, 2.500, 1.625,   .67,  120
070 DATA  3.000, 2.500, 1.875,   .69,  122
080 DATA  3.250, 1.875, 1.625,   .41,   74
090 DATA  2.750, 2.000, 1.375,   .43,   75
100 DATA  3.250, 2.750, 1.125,   .56,  100
110 DATA  3.000, 2.000, 1.750,   .49,   90
120 DATA  3.250, 2.375, 1.250,   .59,  105
130 DATA  4.000, 2.250, 2.000,   .84,  145
140 DATA  4.000, 3.250, 1.500,  1.17,  230
150 DATA  3.500, 2.250, 1.375,   .54,   95
160 DATA  4.375, 2.750, 1.000,   .59,  105
170 DATA  2.500, 2.125, 1.250,   .33,   64
180 DATA  2.750, 2.500, 1.750,   .52,   95
190 DATA  2.500, 1.875, 1.000,   .28,   52
200 DATA  4.000, 3.000, 1.750,  1.12,  210
210 DATA  2.625, 1.875, 1.250,   .34,   60
220 DATA  4.750, 2.000, 1.875,   .91,  160
230 DATA  3.000, 2.750, 1.125,   .48,   88
240 DATA  3.125, 2.250, 1.500,   .66,  120
250 DATA  2.000, 1.750, 1.250,   .24,   45
260 DATA  2.375, 2.000, 1.250,   .26,   48
270 DATA  2.000, 1.625, 1.625,   .26,   50
280 DATA  2.250, 1.750, 1.125,   .23,   42
290 DATA  5.000, 3.375, 1.750,  1.49,  260
300 DATA  3.875, 3.000, 2.000,  1.39,  250
310 DATA  3.500, 2.625, 2.000,  1.04,  180
320 DATA  3.500, 2.125, 2.000,   .77,  130
330 DATA  2.875, 1.750, 1.000,   .27,   52
340 DATA  2.750, 2.250, 1.500,   .48,   84
350 DATA  2.750, 1.875, 1.125,   .26,   48
360 DATA  2.500, 1.875, 1.125,   .24,   45
```

TABLE 3

PHYSICAL CHARACTERISTICS OF RIPRAP

A. 3 TO 6 INCH COBBLES

```
005 REM   AXIAL DIMENSIØNS (IN)  WEIGHT VØLUME
007 REM    A       B       C       LBS     ML
010 DATA  5.625, 5.375, 1.375, 2.325, 400
020 DATA  6.875, 4.375, 2.625, 3.053, 530
030 DATA  7.625, 5.375, 3.000, 5.578, 890
040 DATA  6.000, 3.500, 2.500, 2.470, 315
050 DATA  7.375, 3.250, 3.250, 4.395, 510
060 DATA  6.000, 4.750, 3.625, 4.370, 690
070 DATA  4.750, 3.875, 1.375, 1.610, 220
080 DATA  5.500, 3.875, 1.500, 1.678, 220
090 DATA  6.000, 4.375, 2.625, 3.785, 530
100 DATA  5.625, 5.375, 1.375, 2.325, 400
110 DATA  6.625, 4.750, 3.250, 4.705, 695
120 DATA  7.625, 5.750, 3.500, 7.515, 1170
130 DATA  5.500, 4.000, 2.625, 2.600, 322
140 DATA  6.125, 3.875, 2.000, 2.148, 420
150 DATA  4.750, 4.125, 2.625, 2.371, 250
160 DATA  6.375, 6.125, 4.250, 7.277, 1100
170 DATA  6.938, 6.500, 2.625, 5.355, 730
```

B. 6 TO 9 INCH COBBLES

```
005 REM   AXIAL DIMENSIØNS (IN)  WEIGHT VØLUME
007 REM    A       B       C       LBS     ML
010 DATA  11.750, 10.000, 4.500, 23.08, 3840
020 DATA  11.500,  8.000, 5.500, 25.02, 4230
030 DATA   9.250,  8.750, 5.125, 21.01, 3480
040 DATA   9.125,  8.750, 5.875, 23.75, 3840
050 DATA   8.500,  6.750, 5.250, 13.44, 2380
060 DATA  11.000,  7.500, 5.500, 23.69, 3950
070 DATA  11.500,  8.500, 5.625, 23.46, 4140
080 DATA   8.750,  7.750, 6.500, 20.42, 3445
090 DATA   9.500,  7.875, 4.875, 14.75, 2425
100 DATA   9.250,  7.875, 4.000, 12.65, 2090
110 DATA  11.375, 8.750,  4.500, 19.72, 3340
120 DATA  11.625, 7.875,  4.000, 15.84, 2730
130 DATA  10.875,  9.375, 4.500, 19.62, 3340
140 DATA  10.750,  6.625, 4.625, 15.19, 2530
150 DATA   8.000,  7.000, 6.625, 15.68, 2620
160 DATA  10.750,  5.625, 4.000, 12.47, 2060
170 DATA  10.375,  7.375, 5.125, 13.61, 2260
180 DATA  10.750,  6.750, 5.875, 14.45, 3130
```

TABLE 4

PHYSICAL CHARACTERISTICS OF RIPRAP
1 1/2 TO 3 INCH ANGULAR RIPRAP

005	REM	AXIAL DIMENSIØNS(IN)			WT	H ØF CYL VØL	
007	REM	A	B	C	LBS	H1	H2
010	DATA	4.375,	2.500,	2.000,	1.23,	1.910,	1.925
020	DATA	4.750,	3.000,	2.000,	1.46,	1.910,	1.926
030	DATA	6.000,	2.000,	1.750,	1.35,	1.910,	1.926
040	DATA	4.250,	2.625,	1.000,	.54,	1.909,	1.916
050	DATA	5.500,	3.000,	2.750,	1.72,	1.909,	1.925
060	DATA	6.000,	2.875,	2.875,	1.94,	1.908,	1.928
070	DATA	5.000,	2.750,	2.750,	1.38,	1.908,	1.920
080	DATA	5.500,	3.250,	1.500,	1.00,	1.907,	1.918
090	DATA	5.000,	3.000,	2.750,	1.78,	1.907,	1.926
100	DATA	4.500,	3.000,	1.625,	1.50,	1.907,	1.922
110	DATA	4.750,	2.875,	2.500,	1.28,	1.906,	1.919
120	DATA	5.500,	3.750,	1.250,	1.26,	1.906,	1.919
130	DATA	6.250,	2.750,	2.500,	2.09,	1.906,	1.927
140	DATA	6.250,	3.000,	2.750,	2.24,	1.906,	1.928
150	DATA	4.500,	3.500,	2.500,	1.27,	1.905,	1.918
160	DATA	4.000,	3.250,	1.500,	.90,	1.904,	1.917
170	DATA	6.000,	3.000,	2.500,	2.02,	1.904,	1.924
180	DATA	6.500,	2.750,	2.000,	2.05,	1.904,	1.927
190	DATA	4.500,	2.500,	2.500,	1.94,	1.904,	1.919
200	DATA	5.000,	2.250,	1.625,	1.43,	1.904,	1.919
210	DATA	4.000,	3.000,	3.000,	1.30,	1.903,	1.918
220	DATA	5.000,	2.375,	1.250,	.54,	1.903,	1.909
230	DATA	6.250,	3.500,	1.500,	1.42,	1.903,	1.918
240	DATA	5.500,	2.500,	2.500,	2.63,	1.903,	1.920
250	DATA	4.750,	3.750,	2.000,	1.35,	1.902,	1.916
260	DATA	7.750,	3.500,	1.750,	2.01,	1.902,	1.930
270	DATA	5.500,	3.500,	1.750,	1.75,	1.902,	1.922
280	DATA	5.250,	3.500,	2.250,	1.87,	1.901,	1.921
290	DATA	4.500,	2.750,	2.625,	1.80,	1.901,	1.920
300	DATA	8.250,	2.500,	1.750,	1.56,	1.901,	1.918
310	DATA	5.750,	3.000,	2.500,	1.81,	1.900,	1.920
320	DATA	6.500,	3.250,	2.000,	2.08,	1.900,	1.922
330	DATA	5.500,	2.875,	2.250,	2.15,	1.900,	1.923
340	DATA	4.500,	3.500,	1.250,	1.06,	1.900,	1.910
350	DATA	5.250,	1.750,	1.375,	.97,	1.900,	1.910
360	DATA	5.250,	3.250,	1.500,	1.11,	1.900,	1.911
370	DATA	4.500,	3.000,	2.250,	1.43,	1.899,	1.914
380	DATA	5.000,	3.500,	2.000,	1.33,	1.899,	1.913
390	DATA	5.000,	2.625,	2.500,	1.28,	1.899,	1.913

TABLE 5

PHYSICAL CHARACTERISTICS OF RIPRAP
3 TO 6 INCH ANGULAR

```
005 REM    AXIAL  DIMENSIØNS(IN)    WT     VØL
007 REM     A       B        C      LBS    ML
010 DATA   8.750, 6.000, 3.750, 6.06,  980
020 DATA   5.000, 4.250, 2.000, 1.62,  250
030 DATA   7.000, 4.250, 3.750, 4.94,  880
040 DATA   9.000, 4.000, 3.250, 6.78, 1160
050 DATA   5.500, 3.500, 3.250, 1.71,  300
060 DATA   9.250, 5.750, 2.500, 5.10,  860
070 DATA   7.500, 5.250, 3.375, 5.86, 1000
080 DATA   7.000, 4.500, 3.750, 4.55,  760
090 DATA   7.000, 4.000, 2.000, 2.08,  320
100 DATA   5.000, 4.000, 3.250, 3.30,  540
110 DATA   5.000, 4.375, 4.000, 4.01,  660
120 DATA   5.000, 3.875, 2.500, 1.46,  200
130 DATA   9.375, 5.000, 4.000, 8.05, 1310
140 DATA   5.500, 5.375, 3.125, 4.01,  560
150 DATA   8.000, 4.750, 3.375, 5.08,  800
160 DATA   7.125, 4.625, 3.750, 4.51,  750
170 DATA   7.125, 6.000, 2.000, 3.59,  570
180 DATA   8.000, 4.625, 3.375, 5.00,  840
190 DATA   5.375, 4.500, 2.500, 2.20,  420
200 DATA   6.750, 4.750, 3.000, 4.47,  730
210 DATA   9.000, 4.500, 2.750, 5.02,  720
220 DATA   7.500, 4.625, 3.875, 5.80,  960
230 DATA   5.375, 4.75,  3.250, 3.62,  560
240 DATA   5.500, 3.000, 2.500, 2.77,  440
250 DATA   5.250, 4.000, 4.000, 2.95,  530
260 DATA   7.000, 5.125, 3.250, 4.76,  830
270 DATA   6.500, 4.500, 3.875, 3.74,  660
280 DATA   4.750, 3.125, 3.125, 1.88,  320
290 DATA   6.000, 4.375, 3.375, 3.87,  650
300 DATA   7.500, 5.000, 3.500, 5.63,  920
310 DATA   5.750, 3.000, 2.000, 1.82,  350
320 DATA   6.000, 3.750, 2.750, 2.95,  480
330 DATA   6.000, 5.000, 3.500, 3.04,  730
340 DATA   5.750, 4.000, 3.750, 5.31,  880
350 DATA   5.375, 3.000, 1.500,  .94,  180
360 DATA   9.500, 5.500, 3.875, 6.58, 1020
```

TABLE 6

PHYSICAL CHARACTERISTICS OF RIPRAP
6 TO 9 INCH ANGULAR

```
005 REM    AXIAL DIMENSIØNS (IN)     WEIGHT   HT ØF EQ CYL
007 REM      A        B         C      LBS       H1      H2

010 DATA 12.500,  7.250,   7.250,   40.14,   1.420,   1.836
020 DATA  8.750,  6.250,   5.000,   19.56,   1.418,   1.616
030 DATA 12.500,  9.250,   7.250,   29.40,   1.418,   1.780
040 DATA 12.000,  8.250,   6.125,   25.71,   1.415,   1.682
050 DATA 12.750,  8.125,   5.375,   25.92,   1.415,   1.685
060 DATA 13.750,  8.000,   7.250,   26.93,   1.414,   1.700
070 DATA 10.750, 10.375,   5.625,   27.12,   1.412,   1.698
080 DATA  8.500,  7.375,   5.000,   19.68,   1.411,   1.617
090 DATA  9.250,  8.750,   7.750,   31.47,   1.410,   1.730
100 DATA 10.375,  7.250,   5.875,   22.55,   1.408,   1.641
110 DATA  9.625,  7.750,   6.125,   26.82,   1.406,   1.694
120 DATA 11.500,  7.750,   6.875,   24.50,   1.404,   1.651
130 DATA 11.250,  8.625,   5.000,   27.51,   1.400,   1.678
140 DATA  9.250,  6.750,   5.750,   16.68,   1.405,   1.582
150 DATA 13.500,  6.375,   6.125,   20.62,   1.405,   1.622
160 DATA 14.750,  8.250,   7.250,   45.37,   1.420,   1.889
170 DATA 14.000,  9.000,   7.125,   35.56,   1.564,   1.927
180 DATA  9.500,  9.500,   7.250,   32.77,   1.555,   1.900
190 DATA  9.500,  6.125,   4.125,   16.50,   1.566,   1.740
200 DATA 10.250,  7.750,   5.994,   25.10,   1.563,   1.820
210 DATA 11.000,  8.000,   6.750,   39.79,   1.515,   1.915
220 DATA 11.250,  9.000,   8.750,   33.93,   1.508,   1.859
230 DATA 10.750,  7.750,   5.750,   18.81,   1.502,   1.697
240 DATA  9.000,  6.625,   6.500,   24.76,   1.500,   1.761
250 DATA 14.250, 10.000,   4.750,   25.63,   1.499,   1.767
260 DATA 10.500,  7.000,   7.000,   22.12,   1.502,   1.737
270 DATA  8.500,  8.250,   6.250,   17.66,   1.499,   1.685
280 DATA 12.750,  8.125,   6.250,   27.84,   1.488,   1.777
290 DATA 10.000, 10.000,   5.750,   23.26,   1.485,   1.724
300 DATA 10.000,  9.500,   8.000,   27.02,   1.484,   1.765
310 DATA 17.000,  9.125,   7.375,   27.28,   1.484,   1.765
320 DATA  9.250,  7.750,   7.000,   21.52,   1.482,   1.705
330 DATA 10.125,  9.125,   4.500,   18.81,   1.473,   1.666
340 DATA 13.750,  8.750,   6.000,   26.86,   1.470,   1.753
350 DATA 10.000,  8.250,   7.000,   18.03,   1.468,   1.650
360 DATA 14.250,  7.750,   4.875,   24.52,   1.468,   1.726
```

TABLE 7A

SHAPE CHARACTERISTICS
3/4 TO 1 1/2 INCH COBBLES

ZING CLASSIFICATIØNS: PER CENT PER CATEGØRY

I DISK	II SPHERICAL	III BLADE	IV RØDLIKE
8.33333	16.6667	41.6667	33.3333

RØCK NUMBER	ZING CLASS	BC/A↑2 SPHERICITY	VØL CU FT
1	III	.467128	1.55364 E-3
2	III	.363322	1.05930 E-3
3	III	.200617	8.82750 E-4
4	I	.195	9.88680 E-4
5	IV	.48	3.17790 E-4
6	III	.375	1.05930 E-3
7	II	.342561	1.05930 E-3
8	III	.56	1.20054 E-3
9	II	.311419	8.82750 E-4
10	IV	.625	5.29650 E-4
11	IV	.661157	4.94340 E-4
12	III	.662722	7.06200 E-4
13	III	.32	1.41240 E-4
14	III	.253906	7.76820 E-4
15	IV	.592593	2.47170 E-4
16	IV	.46281	3.53100 E-4
17	III	.255102	2.11860 E-4
18	III	.462222	9.53370 EZ•
19	I	.26	1.05930 E-3
20	III	.328125	9.53370 E-4

TABLE 7B

SHAPE CHARACTERISTICS
3/4 TO 1 1/2 INCH COBBLES (CON'T)

RØCK NUMBER	ZING CLASS	BC/A↑2 SPHERICITY	VØL CU FT
21	IV	.528926	3.88410 E-4
22	III	.33218	9.88680 E-4
23	III	.293333	7.76820 E-4
24	IV	.361111	1.44771 E-3
25	IV	.661157	2.82480 E-4
26	II	.444444	3.88410 E-4
27	II	.271605	1.20054 E-3
28	IV	.46875	1.05930 E-3
29	III	.328125	8.47440 E-4
30	IV	.48	9.53370 E-4
31	III	.355469	8.12130 E-4
32	I	.217687	1.41240 E-3
33	IV	.611111	6.35580 E-4
34	IV	.415225	1.37709 E-3
35	II	.299169	9.88680 E-4
36	II	.365651	1.55364 E-3

SPHERICITY CLASSIFICATIØN = [C*B]/A↑2

PERCENT--0.0 TØ 0.1 = 0
PERCENT--0.1 TØ 0.2 = 2.77778
PERCENT -0.2 TØ 0.3 = 22.2222
PERCENT -0.3 TØ 0.4 = 30.5556
PERCENT - 0.4 TØ 0.5 = 22.2222
PERCENT - 0.5 TØ 0.6 = 8.33333
PERCENT - 0.6 TØ 0.7 = 13.8889
PERCENT - 0.7 TØ 0.8 = 0
PERCENT - 0.8 TØ 0.9 = 0
PERCENT - 0.9 TØ 1.0 = 0

TABLE 8A

SHAPE CHARACTERISTICS
1 1/2 TO 3 INCH COBBLES

ZING CLASSIFICATIØNS: PER CENT PER CATEGØRY

I DISK	II SPHERICAL	III BLADE	IV RØDLIKE
8.33333	16.6667	55.5556	19.4444

RØCK NUMBER	ZING CLASS	BC/A↑2 SPHERICITY	VØL CU FT
1	IV	.428819	3.35445 E-3
2	III	.358796	9.35715 E-3
3	III	.332222	4.76685 E-3
4	III	.30839	2.18922 E-3
5	II	.340278	2.82480 E-3
6	III	.356653	4.23720 E-3
7	IV	.520833	4.30782 E-3
8	II	.288462	2.61294 E-3
9	IV	.363636	2.64825 E-3
10	III	.292899	.003531
11	II	.388889	3.17790 E-3
12	III	.281065	3.70755 E-3
13	II	.28125	5.11995 E-3
14	III	.304688	8.12130 E-3
15	I	.252551	3.35445 E-3
16	I	.143673	3.70755 E-3
17	III	.425	2.25984 E-3
18	IV	.578512	3.35445 E-3
19	III	.3	1.83612 E-3
20	III	.328125	7.41510 E-3

TABLE 8B (CONTINUED)

SHAPE CHARACTERISTICS
1 1/2 TO 3 INCH COBBLES

RØCK NUMBER	ZING CLASS	BC/A↑2 SPHERICITY	VØL CU FT
21	III	.340136	2.11860 E-3
22	II	.166205	5.64960 E-3
23	III	.34375	3.10728 E-3
24	III	.3456	4.23720 E-3
25	IV	.546875	1.58895 E-3
26	III	.443213	1.69488 E-3
27	IV	.660156	1.76550 E-3
28	III	.388889	1.48302 E-3
29	III	.23625	9.18060 E-3
30	III	.399584	8.82750 E-3
31	IV	.428571	6.35580 E-3
32	II	.346939	4.59030 E-3
33	I	.21172	1.83612 E-3
34	III	.446281	2.96604 E-3
35	III	.278926	1.69488 E-3
36	III	.3375	1.58895 E-3

SPHERICITY CLASSIFICATIØN = [C*B]/A↑2

PERCENT--0.0 TØ 0.1 = 0
PERCENT--0.1 TØ 0.2 = 5.55556
PERCENT -0.2 TØ 0.3 = 25
PERCENT -0.3 TØ 0.4 = 44.4444
PERCENT - 0.4 TØ 0.5 = 13.8889
PERCENT - 0.5 TØ 0.6 = 8.33333
PERCENT - 0.6 TØ 0.7 = 2.77778
PERCENT - 0.7 TØ 0.8 = 0
PERCENT - 0.8 TØ 0.9 = 0
PERCENT - 0.9 TØ 1.0 = 0

TABLE 9A

SHAPE CHARACTERISTICS
3 TO 6 INCH COBBLES

ZING CLASSIFICATIØNS: PER CENT PER CATEGORY

I DISK	II SPHERICAL	III BLADE	IV RØDLIKE
12.5	12.5	56.25	18.75

RØCK NUMBER	ZING CLASSIFICATIØN	BC/A↑2 SPHERICITY	VØL CU FT
1	III	.23358	.014124
2	I	.242975	1.87143 E-2
3	III	.277345	3.14259 E-2
4	II	.243056	1.11227 E-2
5	II	.194197	1.80081 E-2
6	IV	.478299	2.43639 E-2
7	III	.23615	7.76820 E-3
8	III	.192149	7.76820 E-3
9	III	.31901	1.87143 E-2
10	III	.23358	.014124
11	IV	.351727	2.45405 E-2
12	III	.346144	4.13127 E-2
13	III	.347107	1.13698 E-2
14	I	.206581	1.48302 E-2
15	III	.479917	8.82750 E-3
16	IV	.640523	.038841

SPHERICITY CLASSIFICATIØN = [C*B]/A↑2

PERCENT--0.0 TØ 0.1 = 0
PERCENT--0.1 TØ 0.2 = 12.5
PERCENT -0.2 TØ 0.3 = 43.75
PERCENT -0.3 TØ 0.4 = 25
PERCENT - 0.4 TØ 0.5 = 12.5
PERCENT - 0.5 TØ 0.6 = 0
PERCENT - 0.6 TØ 0.7 = 6.25
PERCENT - 0.7 TØ 0.8 = 0
PERCENT - 0.8 TØ 0.9 = 0
PERCENT - 0.9 TØ 1.0 = 0

TABLE 9B

SHAPE CHARACTERISTICS
6 TO 9 INCH COBBLES

ZING CLASSIFICATIØNS: PER CENT PER CATEGORY

I DISK	II SPHERICAL	III BLADE	IV RØDLIKE
0	16.6667	44.4444	38.8889

RØCK NUMBER	ZING CLASSIFICATIØN	BC/A↑2 SPHERICITY	VØL CU FT
1	III	.325939	.13559
2	IV	.332703	.149361
3	III	.524105	.122879
4	IV	.617377	.13559
5	IV	.490484	8.40378 E-2
6	IV	.340909	.139475
7	III	.361531	.146183
8	IV	.657959	.121643
9	III	.425381	8.56268 E-2
10	III	.368152	7.37979 E-2
11	III	.304311	.117935
12	III	.233091	9.63963 E-2
13	III	.356718	.117935
14	II	.265143	8.93343 E-2
15	IV	.724609	9.25122 E-2
16	II	.1947	7.27386 E-2
17	IV	.35114	7.98006 E-2
18	II	.343158	.11052

SPHERICITY CLASSIFICATIØN = [C*B]/A↑2

PERCENT--0.0 TØ 0.1 = 0
PERCENT--0.1 TØ 0.2 = 5.55556
PERCENT -0.2 TØ 0.3 = 11.1111
PERCENT -0.3 TØ 0.4 = 50
PERCENT - 0.4 TØ 0.5 = 11.1111
PERCENT - 0.5 TØ 0.6 = 5.55556
PERCENT - 0.6 TØ 0.7 = 11.1111
PERCENT - 0.7 TØ 0.8 = 5.55556
PERCENT - 0.8 TØ 0.9 = 0
PERCENT - 0.9 TØ 1.0 = 0

TABLE 10A

SHAPE CHARACTERISTICS
1 1/2 TO 3 INCH ANGULAR

ZING CLASSIFICATIØNS: PER CENT PER CATEGØRY

I DISK	II SPHERICAL	III BLADE	IV RØDLIKE
28.2051	53.8462	12.8205	5.12821

RØCK NUMBER	ZING CLASS	BC/A↑2 SPHERICITY	VØL CU FT
1	II	.261224	1.00629 E-2
2	I	.265928	1.07337 E-2
3	II	9.72222 E-2	1.07337 E-2
4	I	.145329	.004696
5	II	.272727	1.07337 E-2
6	II	.229601	1.34171 E-2
7	II	.3025	8.05028 E-3
8	I	.161157	7.37943 E-3
9	II	.33	1.27463 E-2
10	I	.240741	1.00629 E-2
11	II	.31856	8.72114 E-3
12	III	.154959	8.72114 E-3
13	II	.176	.014038
14	II	.2112	1.47589 E-2
15	IV	.432099	8.72114 E-3
16	III	.304688	8.72114 E-3
17	II	.208333	1.34171 E-2
18	II	.130178	1.54297 E-2
19	II	.308642	1.00629 E-2
20	II	.14625	1.00629 E-2

TABLE 10B (CONTINUED)

SHAPE CHARACTERISTICS
1 1/2 TO 3 INCH ANGULAR

RØCK NUMBER	ZING CLASS	BC/A↑2 SPHERICITY	VØL CU FT
21	IV	.5625	1.00629 E-2
22	I	.11875	4.02514 E-3
23	I	.1344	1.00629 E-2
24	II	.206612	1.14046 E-2
25	III	.33241	.009392
26	I	.101977	.018784
27	I	.202479	1.34171 E-2
28	I	.285714	1.34171 E-2
29	II	.356481	1.27463 E-2
30	II	6.42792 E-2	1.14046 E-2
31	II	.226843	1.34171 E-2
32	I	.153846	1.47589 E-2
33	II	.213843	1.54297 E-2
34	III	.216049	6.70857 E-3
35	II	8.73016 E-2	6.70857 E-3
36	I	.176871	7.37943 E-3
37	II	.333333	1.00629 E-2
38	III	.28	.009392
39	II	.2625	.009392

SPHERICITY CLASSIFICATIØN = [C*B]/A↑2

PER CENT - 0.0 TØ 0.1 = 7.69231
PER CENT - 0.1 TØ 0.2 = 28.2051
PER CENT - 0.2 TØ 0.3 = 38.4615
PER CENT - 0.3 TØ 0.4 = 20.5128
PER CENT - 0.4 TØ 0.5 = 2.5641
PER CENT - 0.5 TØ 0.6 = 2.5641
PER CENT - 0.6 TØ 0.7 = 0
PER CENT - 0.7 TØ 0.8 = 0
PER CENT - 0.8 TØ 0.9 = 0
PER CENT - 0.9 TØ 1.0 = 0

TABLE 11A

SHAPE CHARACTERISTICS
3 TO 6 INCH ANGULAR

ZING CLASSIFICATIØNS: PER CENT PER CATEGØRY

I DISK	II SPHERICAL	III BLADE	IV RØDLIKE
13.8889	38.8889	25	22.2222

RØCK NUMBER	ZING CLASS	BC/A↑2 SPHERICITY	VØL CU FT
1	III	.293878	3.46038 E-2
2	III	.34	8.82750 E-3
3	II	.325255	3.10728 E-2
4	II	.160494	4.09596 E-2
5	II	.376033	.010593
6	I	.168006	3.03666 E-2
7	III	.315	.03531
8	II	.344388	2.68356 E-2
9	I	.163265	1.12992 E-2
10	IV	.52	1.90674 E-2
11	IV	.7	2.33046 E-2
12	III	.3875	.007062
13	II	.227556	4.62561 E-2
14	III	.555269	1.97736 E-2
15	II	.250488	.028248
16	II	.341644	2.64825 E-2
17	III	.23638	2.01267 E-2
18	II	.243896	2.96604 E-2
19	III	.3894	1.48302 E-2
20	III	.312757	2.57763 E-2

TABLE 11B (CONTINUED)

SHAPE CHARACTERISTICS
3 TO 6 INCH ANGULAR

RØCK NUMBER	ZING CLASS	BC/A↑2 SPHERICITY	VØL CU FT
21	I	.152778	2.54232 E-2
22	II	.318611	3.38976 E-2
23	IV	.534343	1.97736 E-2
24	II	.247934	1.55364 E-2
25	IV	.580499	1.87143 E-2
26	III	.339923	2.93073 E-2
27	IV	.412722	2.33046 E-2
28	II	.432825	1.12992 E-2
29	IV	.410156	2.29515 E-2
30	II	.311111	3.24852 E-2
31	I	.181474	1.23585 E-2
32	II	.286458	1.69488 E-2
33	IV	.486111	2.57763 E-2
34	IV	.453686	3.10728 E-2
35	I	.15576	6.35580 E-3
36	II	.23615	3.60162 E-2

SPHERICITY CLASSIFICATIØN = [C*B]/A↑2

PERCENT--0.0 TØ 0.1 = 0
PERCENT--0.1 TØ 0.2 = 16.6667
PERCENT -0.2 TØ 0.3 = 22.2222
PERCENT -0.3 TØ 0.4 = 33.3333
PERCENT - 0.4 TØ 0.5 = 13.8889
PERCENT - 0.5 TØ 0.6 = 11.1111
PERCENT - 0.6 TØ 0.7 = 2.77778
PERCENT - 0.7 TØ 0.8 = 0
PERCENT - 0.8 TØ 0.9 = 0
PERCENT - 0.9 TØ 1.0 = 0

TABLE 12A
SHAPE CHARACTERISTICS
6 TO 9 INCH ANGULAR

ZING CLASSIFICATIØNS: PER CENT PER CATEGØRY

I DISK	II SPHERICAL	III BLADE	IV RØDLIKE
5.55556	27.7778	13.8889	52.7778

RØCK NUMBER	ZING CLASS	BC/A↑2 SPHERICITY	VØL CU FT
1	II	.3364	.279077
2	IV	.408163	.13283
3	IV	.4292	.24285
4	IV	.350911	.179119
5	I	.268647	.181131
6	II	.306777	.191865
7	III	.505003	.191865
8	IV	.510381	.138197
9	IV	.792549	.214674
10	IV	.395703	.15631
11	IV	.512397	.193207
12	IV	.402883	.165702
13	III	.340741	.186498
14	IV	.453616	.118742
15	II	.214249	.145576
16	II	.274921	.314632
17	II	.327168	.243521
18	IV	.763158	.231446
19	II	.279952	.116729
20	IV	.442151	.17241

TABLE 12B (CONTINUED)

SHAPE CHARACTERISTICS
6 TO 9 INCH ANGULAR

RØCK NUMBER	ZING CLASS	BC/A↑2 SPHERICITY	VØL CU FT
21	IV	.446281	.268343
22	IV	.622222	.235471
23	IV	.385614	.130817
24	IV	.531636	.175094
25	III	.233918	.17979
26	II	.444444	.157651
27	IV	.713668	.124779
28	II	.31238	.193878
29	III	.575	.160335
30	IV	.76	.188511
31	II	.232861	.188511
32	IV	.634039	.149601
33	III	.400549	.129475
34	II	.277686	.189853
35	IV	.5775	.122096
36	I	.186057	.173081

SPHERICITY CLASSIFICATIØN = [C*B]/A↑2

PER CENT - 0.0 TØ 0.1 =	0
PER CENT - 0.1 TØ 0.2 =	2.77778
PER CENT - 0.2 TØ 0.3 =	19.4444
PER CENT - 0.3 TØ 0.4 =	22.2222
PER CENT - 0.4 TØ 0.5 =	22.2222
PER CENT - 0.5 TØ 0.6 =	16.6667
PER CENT - 0.6 TØ 0.7 =	5.55556
PER CENT - 0.7 TØ 0.8 =	11.1111
PER CENT - 0.8 TØ 0.9 =	0
PER CENT - 0.9 TØ 1.0 =	0

TABLE 13

VELOCITIES AT SIGNIFICANT POINTS
Cobbles

TEST	Size Category	Maximum Boundary Velocity (fps)	Distance from Datum (ft)	Velocity at d(in) from rock surface	d from Datum (ft)	Velocity at ● (fps)	Distance from Datum (ft)	Mean Boundary Velocity (fps)
	22 cfs							
11a	¾"≤d≤1½"	6.4	1.48	5.1	0.0625	5.6	0.28	5.8
11b	¾"≤d≤1½"	7.1	0.78	6.4	0.125	6.7	0.19	6.3
	22 cfs							
10a	1½"≤d≤3"	7.3	1.00	6.5	0.125	6.7	0.18	6.0
10b	1½"≤d≤3"	8.2	.89	7.5	0.25	7.4	-.02	6.4
	21 cfs							
5a	3"≤d≤6"	8.1	.92	7.7	0.25	7.6	0.18	6.5
5b	3"≤d≤6"	9.9	.43	9.9	0.5	8.8	0.02	7.1
	20.6 cfs							
8a	6"≤d≤9"	9.4	.67	9.4	0.5	8.8	0.00	7.1
8b	6"≤d≤9"	10.8	.26	9.8	0.75	10.7	0.06	7.4
	14 cfs							
4a	3"≤d≤6"	9.0	.43	8.5	0.25	8.4	0.18	6.3
	14 cfs							
7a	6"≤d≤9"	9.0	.20	6.4	0.5	9.0	0.12	6.0
7b	6"≤d≤9"	10.0	.33	10.0	0.75	10.0	0.23	6.0
	11.6 cfs							
6a	6"≤d≤9"	8.4	.19	4.5	0.5	8.4	0.19	5.1
6b	6"≤d≤9"	9.7	.19	4.7	0.75	9.7	0.19	5.7
	7.5 cfs							
1a	3"≤d≤6"	6.8	.18	6.6	0.25	6.8	0.18	4.3
	7.5 cfs							
2b	3"≤d≤6"	8.0	-.10	6.0	0.5	8.0	-.10	6.0
	7.5 cfs							
3a	3"≤d≤6"	8.2	0.00	5.3	0.25	8.2	0.00	6.0
3b	3"≤d≤6"	7.5	-.18	7.5	0.5	7.5	-.18	6.0

TABLE 14

VELOCITIES AT SIGNIFICANT POINTS
Angular

TEST NØ.	SIZE CATEGØRY	MAXIMUM JET VELØCITY [FPS]	DISTANCE FRØM DATUM [FT]	VELØCITY AT MAX RØCK DIA FRØM DAT [IN]	DISTANCE FRØM DATUM [FT]	VELØCITY AT SIGN [FPS]	DISTANCE FRØM BASE ØF VEL PRØFILE [FT]
18	1.5	9.2	1.08	8.1	.25	8	.35
19	1.5	8.2	1.23	4.7	.25	7.5	.46
18	3	10.2	.64	5.8	0	8.7	.21
19	3	11.1	.82	8.5	0	9.5	.36
12	3	8.6	.9	8.3	.5	8.2	.37
13	3	8.4	1.07	7.9	.5	8.2	.35
14	3	8.9	1.2	8.5	.5	8.1	.41
15	3	11.2	.7	11	.5	10.5	.41
16	3	8.4	.6	8.2	.5	7.1	.2
17	3	8.8	.49	8.8	.5	8	.34
12	6	10.3	.52	9	0	9	.3
13	6	10.4	.7	6.8	0	9.1	.25
14	6	10.5	.4	9.9	0	9.9	.2
15	6	10.6	.7	9.1	0	9.1	.25
16	6	8.5	.37	6.9	0	6.9	.15
17	6	9.7	.39	4.7	0	7.2	.2
20	6	10	.02	8.7	.75	10	.52
21	6	10.2	.62	9.3	.75	8.1	.35
20	9	12.9	.23	10.5	0	12.3	.4
21	9	11.4	.05	11.3	0	9	.45

TABLE 15A
3/4 TO 1 1/2 INCH COBBLES

PIE TERMS FØR PHYSICAL CHARACTERISTICS ØF RIPRAP

WHERE DIA=DIAMETER ØF SPHERE ØF WEIGHT EQUAL TØ RØCK SAMPLE
PIE 1 IS RATIØ ØF MEAN AXIS DIM AND DIA ØF = WT SPHERE
PIE 2 IS RATIØ ØF MEAN AXIS DIM AND SIGNIFICANT DEPTH
PIE 3 IS RATIØ ØF RØCK VØLUME AND ABC RECTANGULAR SØLID

RØCK NUMBER	DIA INCHES	PIE 1	PIE 2	PIE 3
1	1.69442	1.00821	6.10119	.598937
2	1.51045	1.07584	5.80357	.525042
3	1.4158	1.05947	5.35714	.667522
4	1.48023	1.0978	5.80357	.560718
5	.932532	1.07235	3.57143	.585751
6	1.48023	1.01335	5.35714	.610157
7	1.51045	1.02067	5.50595	.556863
8	1.59452	.992984	5.65476	.56199
9	1.4158	1.05947	5.35714	.510458
10	1.22193	1.05707	4.6131	.433889
11	1.17489	1.02847	4.31548	.497
12	1.30645	1.11626	5.20833	.429121
13	.847269	1.08191	3.27381	.3905
14	1.38126	1.02564	5.05952	.660847
15	.932532	1.02767	3.42262	.506204
16	1.00453	1.07845	3.86905	.507143
17	1.12375	1.07527	4.31548	.267772
18	1.56749	.956942	5.35714	.540693
19	1.51045	1.13101	6.10119	.450577
20	1.5395	.974343	5.35714	.62759

TABLE 15B
3/4 TO 1 1/2 INCH COBBLES

CONTINUED

PIE TERMS FØR PHYSICAL CHARACTERISTICS ØF RIPRAP

WHERE DIA=DIAMETER ØF SPHERE ØF WEIGHT EQUAL TØ RØCK SAMPLE
PIE 1 IS RATIØ ØF MEAN AXIS DIM AND DIA ØF = WT SPHERE
PIE 2 IS RATIØ ØF MEAN AXIS DIM AND SIGNIFICANT DEPTH
PIE 3 IS RATIØ ØF RØCK VØLUME AND ABC RECTANGULAR SØLID

RØCK NUMBER	DIA INCHES	PIE 1	PIE 2	PIE 3
21	1.12375	1.00112	4.01786	.488125
22	1.5395	1.00141	5.50595	.535981
23	1.2656	1.05352	4.7619	.694223
24	1.64599	1.01256	5.95238	.608187
25	1.22193	.988874	4.31548	.284
26	1.12375	1.03819	4.16667	.447448
27	1.51045	1.02067	5.50595	.670556
28	1.51045	1.04825	5.65476	.488125
29	1.38126	1.0558	5.20833	.557858
30	1.48023	1.01335	5.35714	.520667
31	1.30645	1.14815	5.35714	.493489
32	1.5395	1.10967	6.10119	.619842
33	1.22193	1.05707	4.6131	.5325
34	1.56749	1.03669	5.80357	.597236
35	1.48023	1.12595	5.95238	.426277
36	1.71763	1.01884	6.25	.548071

MEAN DIA ØF = WEIGHT SPHERE 1.36891 INCHES

TABLE 16A

1 1/2 TO 3 INCH COBBLES

PIE TERMS FØR PHYSICAL CHARACTERISTICS ØF RIPRAP

WHERE DIA=DIAMETER ØF SPHERE ØF WEIGHT EQUAL TØ RØCK SAMPLE
PIE 1 IS RATIØ ØF MEAN AXIS DIM AND DIA ØF = WT SPHERE
PIE 2 IS RATIØ ØF MEAN AXIS DIM AND SIGNIFICANT DEPTH
PIE 3 IS RATIØ ØF RØCK VØLUME AND ABC RECTANGULAR SØLID

RØCK NUMBER	DIA INCHES	PIE 1	PIE 2	PIE 3
1	2.25297	1.03567	11.6667	.500641
2	3.17672	1.07553	17.0833	.49454
3	2.5479	1.07932	13.75	.470168
4	1.88889	1.01471	9.58333	.67818
5	2.04698	1.05847	10.8333	.531293
6	2.39175	1.04526	12.5	.534018
7	2.41531	1.01781	12.2917	.529345
8	2.03061	1.10804	11.25	.455969
9	2.0631	.989612	10.2083	.605114
10	2.25297	1.05416	11.875	.606838
11	2.1549	1.04413	11.25	.522992
12	2.2925	.999635	11.4583	.664009
13	2.57898	1.06631	13.75	.491515
14	2.88013	1.01269	14.5833	.719672
15	2.22583	1.06702	11.875	.535318
16	2.2925	1.18139	13.5417	.5325
17	1.88889	1.03677	9.79167	.588048
18	2.19801	1.06157	11.6667	.481786
19	1.78823	1.00192	8.95833	.676867
20	2.8385	1.02754	14.5833	.610157

TABLE 168 (CONTINUED)

1 1/2 TO 3 INCH COBBLES

PIE TERMS FØR PHYSICAL CHARACTERISTICS ØF RIPRAP

WHERE DIA=DIAMETER ØF SPHERE ØF WEIGHT EQUAL TØ RØCK SAMPLE
PIE 1 IS RATIØ ØF MEAN AXIS DIM AND DIA ØF = WT SPHERE
PIE 2 IS RATIØ ØF MEAN AXIS DIM AND SIGNIFICANT DEPTH
PIE 3 IS RATIØ ØF RØCK VØLUME AND ABC RECTANGULAR SØLID

RØCK NUMBER	DIA INCHES	PIE 1	PIE 2	PIE 3
21	1.90777	1.00466	9.58333	.595048
22	2.6487	1.08544	14.375	.548071
23	2.14014	1.0708	11.4583	.578519
24	2.37979	.962969	11.4583	.694223
25	1.69867	.981159	8.33333	.62759
26	1.7446	1.07475	9.375	.493264
27	1.7446	1.0031	8.75	.577663
28	1.67475	1.02006	8.54167	.578519
29	3.12182	1.0811	16.875	.537196
30	3.05037	.969829	14.7917	.656083
31	2.76925	.978002	13.5417	.597705
32	2.50526	1.01453	12.7083	.533246
33	1.76668	1.06131	9.375	.630622
34	2.14014	1.01239	10.8333	.552223
35	1.7446	1.09863	9.58333	.504889
36	1.69867	1.07927	9.16667	.520667

MEAN DIA ØF = WEIGHT SPHERE 2.24837 INCHES

TABLE 17A

3 TO 6 INCH COBBLES

PIE TERMS FØR PHYSICAL CHARACTERISTICS ØF RIPRAP

DIA = DIAMETER ØF SPHERE ØF WT = RØCK SAMPLE
PIE 1 IS RATIØ ØF MEAN AXIS DIM AND DIA ØF = WT SPHERE
PIE 2 IS RATIØ ØF MEAN AXIS DIM AND SIGNIFICANT DEPTH
PIE 3 IS RATIØ ØF RØCK VØLUME AND ABC RECTANGULAR SØLID

RØCK NUMBER	DIA INCHES	PIE 1	PIE 2	PIE 3
1	3.58495	1.15064	31.7308	.587081
2	3.92567	1.17814	35.5769	.409579
3	4.79906	1.11133	41.0256	.441664
4	3.65798	1.0935	30.7692	.366094
5	4.43254	1.04342	35.5769	.399469
6	4.42412	1.08308	36.859	.407509
7	3.17168	1.05097	25.641	.530391
8	3.21572	1.12728	27.8846	.419893
9	4.2172	1.02754	33.3333	.469309
10	3.58495	1.15064	31.7308	.587081
11	4.53439	1.07512	37.5	.414633
12	5.30032	1.06126	43.2692	.465213
13	3.72105	1.08616	31.0897	.340209
14	3.49158	1.14561	30.7692	.539862
15	3.60844	1.06232	29.4872	.296575
16	5.24377	1.06476	42.9487	.404444

MEAN DIA ØF = WT. SPHERE IS 4.05709

TABLE 17B

6 TO 9 INCH COBBLES

PIE TERMS FØR PHYSICAL CHARACTERISTICS ØF RIPRAP

DIA = DIAMETER ØF SPHERE ØF WT = RØCK SAMPLE
PIE 1 IS RATIØ ØF MEAN AXIS DIM AND DIA ØF = WT SPHERE
PIE 2 IS RATIØ ØF MEAN AXIS DIM AND SIGNIFICANT DEPTH
PIE 3 IS RATIØ ØF RØCK VØLUME AND ABC RECTANGULAR SØLID

RØCK NUMBER	DIA INCHES	PIE 1	PIE 2	PIE 3
1	7.72019	1.13339	43.75	.443121
2	7.93068	1.05077	41.6667	.510072
3	7.48214	1.03023	38.5417	.51189
4	7.79417	1.01572	39.5833	.499487
5	6.44699	1.05993	34.1667	.482099
6	7.7876	1.02727	40	.531156
7	7.76232	1.1004	42.7083	.459412
8	7.41144	1.03444	38.3333	.476878
9	6.64997	1.11529	37.0833	.405699
10	6.31812	1.11452	35.2083	.437659
11	7.32578	1.12047	41.0417	.455005
12	6.80988	1.15029	39.1667	.454884
13	7.31338	1.12807	41.25	.444196
14	6.71544	1.09201	36.6667	.468658
15	6.78688	1.0621	36.0417	.430892
16	6.28802	1.0801	33.9583	.519658
17	6.47405	1.17778	38.125	.351646
18	6.60458	1.17974	38.9583	.447987

MEAN DIA ØF = WT. SPHERE IS 7.09009

TABLE 18A

1 1/2 TO 3 INCH ANGULAR

PIE TERMS FØR PHYSICAL CHARACTERISTICS ØF RIPRAP

WHERE DIA=DIAMETER ØF SPHERE ØF WEIGHT EQUAL TØ RØCK SAMPLE
PIE 1 IS RATIØ ØF MEAN AXIS DIM AND DIA ØF = WT SPHERE
PIE 2 IS RATIØ ØF MEAN AXIS DIM AND SIGNIFICANT DEPTH
PIE 3 IS RATIØ ØF RØCK VØLUME AND ABC RECTANGULAR SØLID

RØCK NUMBER	DIA INCHES	PIE 1	PIE 2	PIE 3
1	2.69417	1.09805	7.39583	.794908
2	2.85258	1.13932	8.125	.650802
3	2.77907	1.16946	8.125	.883231
4	2.0477	1.28193	6.5625	.727367
5	3.01274	1.24472	9.375	.408768
6	3.13606	1.24891	9.79167	.467495
7	2.79951	1.25022	8.75	.367891
8	2.51455	1.35876	8.54167	.475586
9	3.04737	1.17588	8.95833	.533953
10	2.8784	1.05672	7.60417	.792643
11	2.73019	1.23618	8.4375	.441413
12	2.7159	1.28871	8.75	.584538
13	3.21488	1.19237	9.58333	.566553
14	3.29001	1.2158	10	.494609
15	2.72306	1.28532	8.75	.382734
16	2.42778	1.20137	7.29167	.772827
17	3.17858	1.20599	9.58333	.515218
18	3.19424	1.17399	9.375	.745805
19	3.13606	1.00976	7.91667	.618262
20	2.83291	1.04427	7.39583	.951172

TABLE 18B (CONTINUED)
1 1/2 TO 3 INCH ANGULAR
PIE TERMS FØR PHYSICAL CHARACTERISTICS ØF RIPRAP

WHERE DIA=DIAMETER ØF SPHERE ØF WEIGHT EQUAL TØ RØCK SAMPLE
PIE 1 IS RATIØ ØF MEAN AXIS DIM AND DIA ØF = WT SPHERE
PIE 2 IS RATIØ ØF MEAN AXIS DIM AND SIGNIFICANT DEPTH
PIE 3 IS RATIØ ØF RØCK VØLUME AND ABC RECTANGULAR SØLID

RØCK NUMBER	DIA INCHES	PIE 1	PIE 2	PIE 3
21	2.74433	1.21462	8.33333	.483017
22	2.0477	1.40401	7.1875	.468577
23	2.82629	1.32683	9.375	.529939
24	3.47081	1.00841	8.75	.573297
25	2.77907	1.25941	8.75	.455561
26	3.17333	1.36555	10.8333	.683792
27	3.03015	1.18256	8.95833	.688232
28	3.09788	1.18361	9.16667	.560782
29	3.05874	1.07615	8.22917	.678036
30	2.91627	1.42876	10.4167	.545997
31	3.06439	1.22374	9.375	.537619
32	3.20974	1.22024	9.79167	.603628
33	3.24535	1.09131	8.85417	.749408
34	2.56386	1.20261	7.70833	.588821
35	2.48915	1.12154	6.97917	.917643
36	2.60355	1.2803	8.33333	.498233
37	2.83291	1.14723	8.125	.572465
38	2.76528	1.26569	8.75	.463696
39	2.73019	1.23618	8.4375	.494609

MEAN DIA ØF = WEIGHT SPHERE 2.86807 INCHES

TABLE 19A

3 TO 6 INCH ANGULAR

PIE TERMS FØR PHYSICAL CHARACTERISTICS ØF RIPRAP

WHERE DIA=DIAMETER ØF SPHERE ØF WEIGHT EQUAL TØ RØCK SAMPLE
PIE 1 IS RATIØ ØF MEAN AXIS DIM AND DIA ØF = WT SPHERE
PIE 2 IS RATIØ ØF MEAN AXIS DIM AND SIGNIFICANT DEPTH
PIE 3 IS RATIØ ØF RØCK VØLUME AND ABC RECTANGULAR SØLID

RØCK NUMBER	DIA INCHES	PIE 1	PIE 2	PIE 3
1	4.36704	1.41209	7.90598	.303723
2	2.81333	1.33294	4.80769	.358916
3	4.07952	1.22564	6.41026	.481289
4	4.53355	1.1948	6.94444	.604942
5	2.86449	1.4255	5.23504	.292583
6	4.12309	1.4148	7.47863	.39463
7	4.31847	1.24465	6.89103	.459142
8	3.96922	1.28069	6.51709	.392566
9	3.05774	1.41717	5.55556	.348661
10	3.56624	1.145	5.23504	.506899
11	3.80555	1.17153	5.71581	.460233
12	2.71749	1.39528	4.86111	.251936
13	4.80055	1.27589	7.85256	.426296
14	3.80555	1.22628	5.98291	.369861
15	4.11769	1.30534	6.89103	.380605
16	3.95755	1.30552	6.62393	.370318
17	3.66777	1.37459	6.46368	.406771
18	4.09596	1.30209	6.83761	.410436
19	3.11544	1.32405	5.28846	.423799
20	3.94582	1.22493	6.19658	.463069

TABLE 19B (CONTINUED)
3 TO 6 INCH ANGULAR
PIE TERMS FØR PHYSICAL CHARACTERISTICS ØF RIPRAP

WHERE DIA=DIAMETER ØF SPHERE ØF WEIGHT EQUAL TØ RØCK SAMPLE
PIE 1 IS RATIØ ØF MEAN AXIS DIM AND DIA ØF = WT SPHERE
PIE 2 IS RATIØ ØF MEAN AXIS DIM AND SIGNIFICANT DEPTH
PIE 3 IS RATIØ ØF RØCK VØLUME AND ABC RECTANGULAR SØLID

RØCK NUMBER	DIA INCHES	PIE 1	PIE 2	PIE 3
21	4.10142	1.32068	6.94444	.394445
22	4.30368	1.23925	6.83761	.435781
23	3.67796	1.21218	5.71581	.411788
24	3.36409	1.08994	4.70085	.650834
25	3.43543	1.28562	5.66239	.38498
26	4.02936	1.27191	6.57051	.434354
27	3.71816	1.33355	6.35684	.355294
28	2.95642	1.24024	4.70085	.420918
29	3.76074	1.21873	5.87607	.447664
30	4.26122	1.2516	6.83761	.427691
31	2.92463	1.22523	4.59402	.619
32	3.43543	1.21285	5.34188	.473334
33	3.47001	1.39289	6.19658	.424204
34	4.17891	1.07683	5.76923	.622537
35	2.34657	1.40276	4.22009	.45407
36	4.48853	1.40172	8.06624	.307386

MEAN DIA ØF = WEIGHT SPHERE 3.72707 INCHES

TABLE 20A

6 TO 9 INCH ANGULAR

PIE TERMS FØR PHYSICAL CHARACTERISTICS ØF RIPRAP

WHERE DIA=DIAMETER ØF SPHERE ØF WEIGHT EQUAL TØ RØCK SAMPLE
PIE 1 IS RATIØ ØF MEAN AXIS DIM AND DIA ØF = WT SPHERE
PIE 2 IS RATIØ ØF MEAN AXIS DIM AND SIGNIFICANT DEPTH
PIE 3 IS RATIØ ØF RØCK VØLUME AND ABC RECTANGULAR SØLID

RØCK NUMBER	DIA INCHES	PIE 1	PIE 2	PIE 3
1	8.60801	1.04554	18	.733975
2	6.76744	.985109	13.3333	.839423
3	7.75684	1.24621	19.3333	.500602
4	7.41641	1.18543	17.5833	.510439
5	7.43663	1.17661	17.5	.562115
6	7.53239	1.28335	19.3333	.415728
7	7.55013	1.18099	17.8333	.52847
8	6.78133	1.0261	13.9167	.761886
9	7.93541	1.08165	17.1667	.591388
10	7.09779	1.10363	15.6667	.611217
11	7.52208	1.04138	15.6667	.730731
12	7.29769	1.1933	17.4167	.467303
13	7.5863	1.09298	16.5833	.664258
14	6.41546	1.13008	14.5	.571523
15	6.8882	1.25819	17.3333	.477214
16	8.96762	1.12442	20.1667	.616258
17	8.27491	1.21351	20.0833	.468732
18	8.05259	1.08661	17.5	.611234
19	6.40641	1.02762	13.1667	.840368
20	7.36782	1.08553	15.996	.625698

TABLE 20B (CONTINUED)
6 TO 9 INCH ANGULAR
PIE TERMS FØR PHYSICAL CHARACTERISTICS ØF RIPRAP

WHERE DIA=DIAMETER ØF SPHERE ØF WEIGHT EQUAL TØ RØCK SAMPLE
PIE 1 IS RATIØ ØF MEAN AXIS DIM AND DIA ØF = WT SPHERE
PIE 2 IS RATIØ ØF MEAN AXIS DIM AND SIGNIFICANT DEPTH
PIE 3 IS RATIØ ØF RØCK VØLUME AND ABC RECTANGULAR SØLID

RØCK NUMBER	DIA INCHES	PIE 1	PIE 2	PIE 3
21	8.59077	.999134	17.1667	.780634
22	8.1465	1.1866	19.3333	.45928
23	6.69239	1.20784	16.1667	.471879
24	7.3344	1.00554	14.75	.780679
25	7.41931	1.30291	19.3333	.458987
26	7.0639	1.15611	16.3333	.529488
27	6.55314	1.16992	15.3333	.491964
28	7.62668	1.18553	18.0833	.517438
29	7.18321	1.19492	17.1667	.481841
30	7.55107	1.21396	18.3333	.428614
31	7.57521	1.47411	22.3333	.284732
32	6.99945	1.14295	16	.515154
33	6.69239	1.18294	15.8333	.538134
34	7.53613	1.26059	19	.454463
35	6.59859	1.27553	16.8333	.365337
36	7.31063	1.22539	17.9167	.555523

MEAN DIA ØF = WEIGHT SPHERE 7.40376 INCHES

TABLE 21

PI-TERMS FOR VELOCITY PARAMETERS

TEST	v_{max} (FPS)	h_B (FT)	D (FT)	d_{ave} (IN)	$v^2/h_B g$ II-4	h_B/D II-5	v^2/Dg II-6	v^2/dg II-7
COBBLES								
10D 1 1/2" TO 3"	8.63	1.01	1.76	2.25	2.29	.57	1.31	1.03
11D 3/4" TO 1 1/2"	7.00	.54	2.18	1.37	2.84	.25	.70	1.11
ANGULAR RIPRAP								
19B 1 1/2" TO 3"	11.10	1.18	1.88	2.87	3.24	.63	2.04	1.33
14B 3" TO 6"	10.50	2.14	1.46	3.73	1.60	1.47	2.35	.92
15B 3" TO 6"	10.60	1.59	1.07	3.73	2.20	1.49	3.28	.94
20B 6" TO 9"	12.90	2.42	.79	7.40	2.14	3.05	6.53	.70

TABLE 22

DISCHARGE

WHERE G = FLØW IN CUBIC FEET PER SECØND IN GRAVEL
Q = TØTAL DISCHARGE FØR UNIT WIDTH SECTIØN
F = DISCHARGE IN JET CØMPUTED BY THE CØNTINUITY EQUATIØN
E = DISCHARGE IN JET CØMPUTED BY EQUATIØN 3.16

TEST NUMBER	DISCHARGE IN RIPRAP G [CFS/FT]	TØTAL DISCHARGE IN FLUME [CFS/FT]	DISCHARGE F [CFS/FT]	DISCHARGE E [CFS/FT]
10	3.94101	10.925	6.98399	10.3367
11	10.6949	11.045	.350077	.616406
14	4.54291	11.15	6.60709	15.0458
15	1.61315	11	9.38685	8.86255
19	-3.01951	10.735	13.7545	18.7739
20	5.97264	10.91	4.93736	6.55503

TABLE 13

COMPARISON OF VELOCITY COMPUTATION

WHERE V = MEAN VELOCITY OF JET BY VELOCITY PROFILE AVERAGING
U = MEAN JET VELOCITY BY EQUATION 3.15
L = MEAN DEPTH OF JET ABOVE RIPRAP SURFACE

TEST NUMBER	V [FPS]	U [FPS]	L
10	6.71537	12.2705	1.04
11	5.83462	11.5432	.06
14	4.93067	13.4744	1.34
15	8.49489	12.3163	1.105
19	7.33574	12.0363	1.875
20	7.53795	14.7475	.655

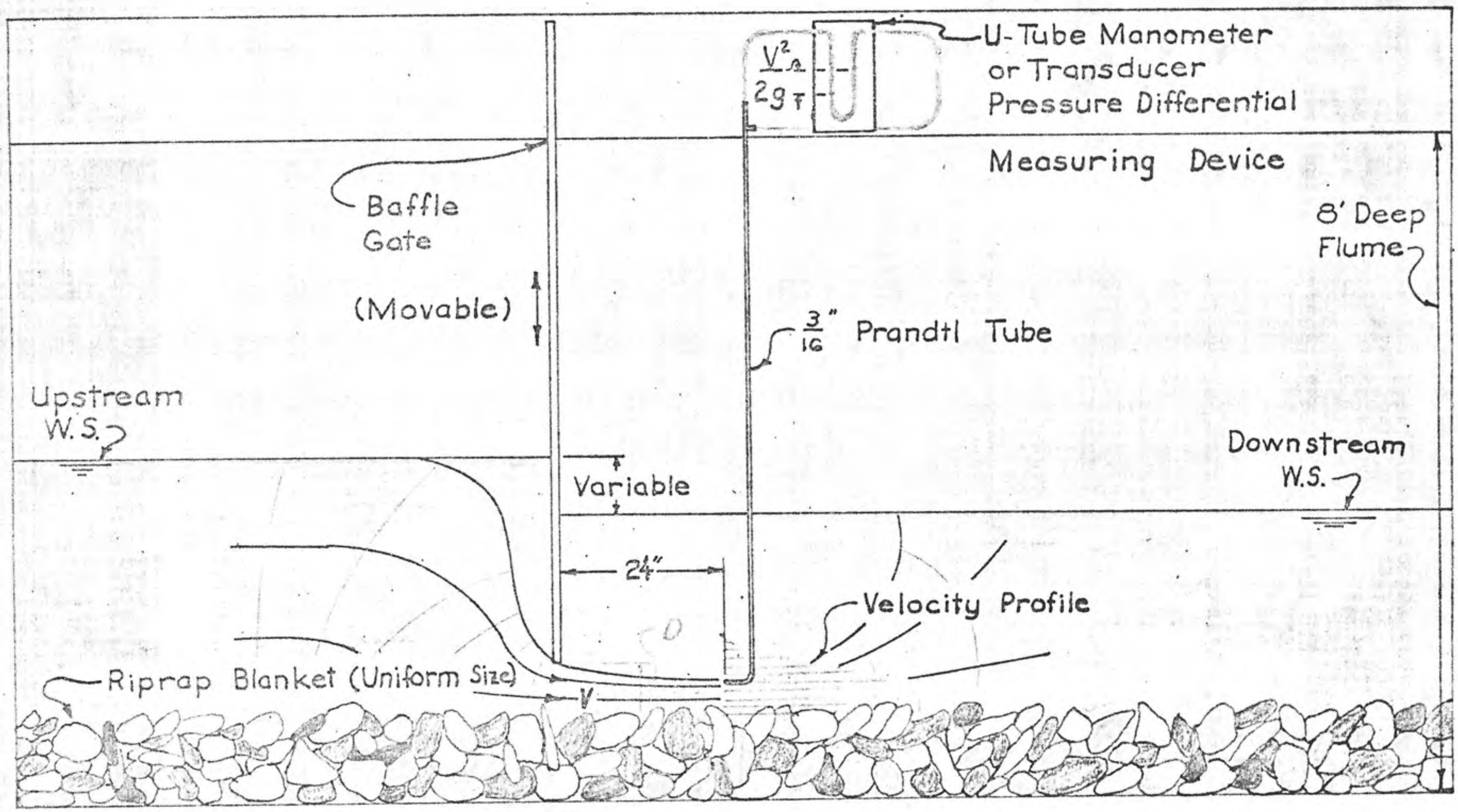

STABILITY OF RIPRAP
HYDRAULIC FLUME STUDY, 1:1 SCALE
FIGURE 1

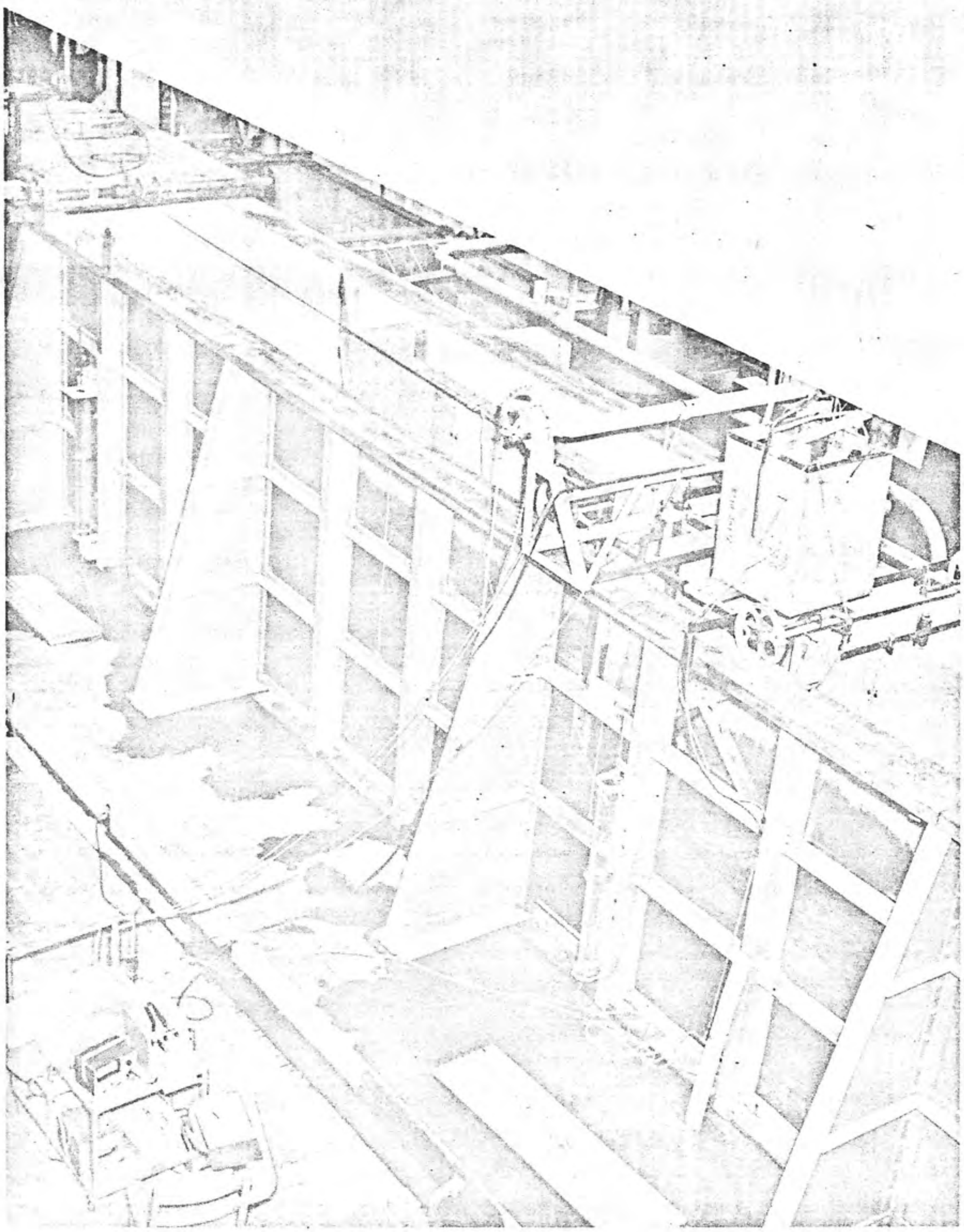

Figure 2
General view of test flume with baffle platform and test section in the center of the picture
Photo PX-D-61604NA

Figure 3
Dye test showing jet under the baffle
and differential pressure recording equipment
Photo PX-D-61605NA

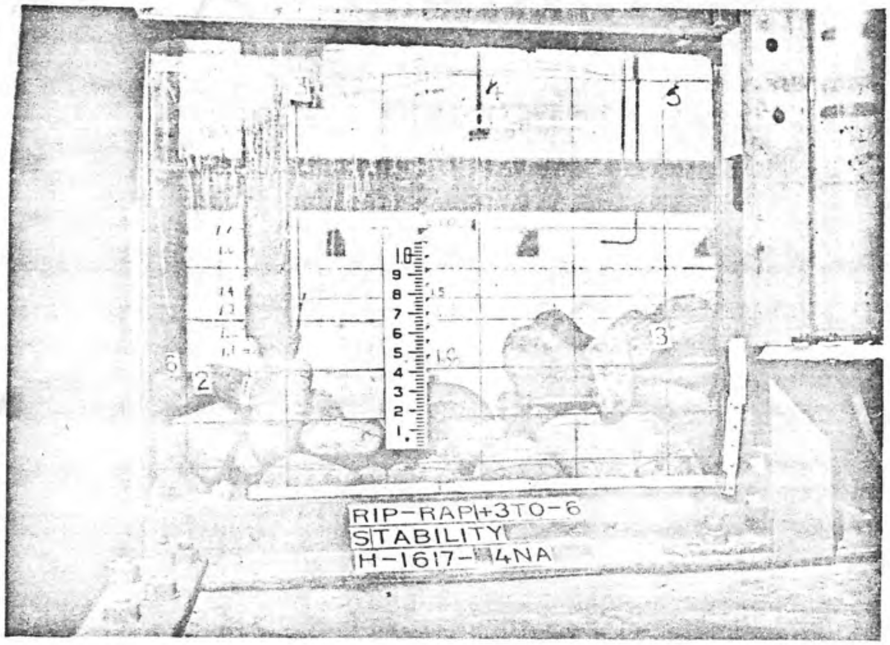

Figure 4A
3- to 6-inch cobbles
6-inch scour test profile
Photo PX-D-61606NA

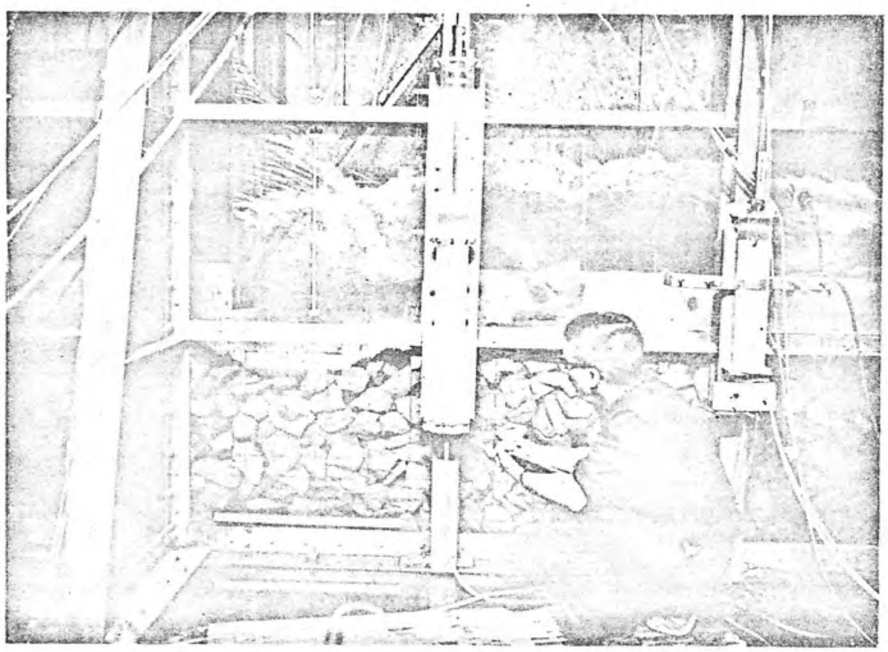

Figure 4B
3- to 6-inch angulars
6-inch scour in progress
Photo PX-D-61501NA

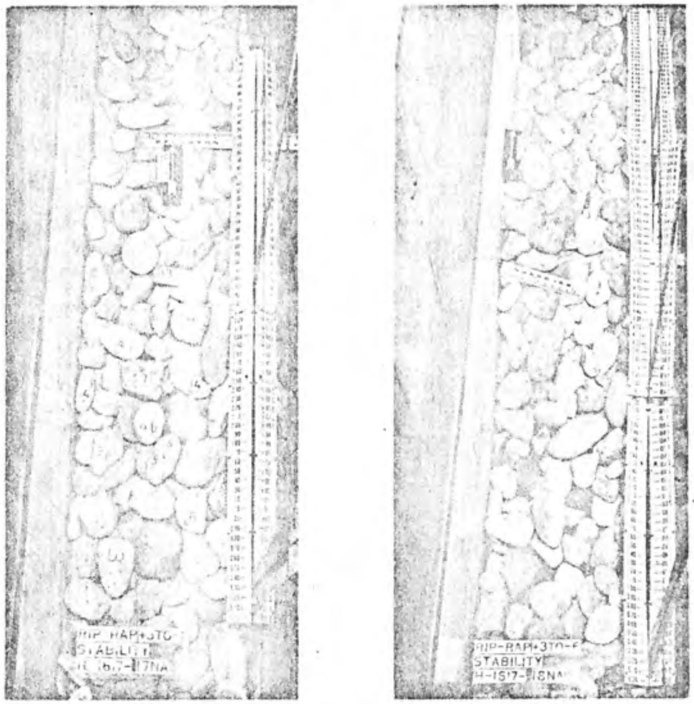

Figure 5A
Test 8
Before and after 6-inch scour
3- to 6-inch cobbles
1-foot stone layer
21-cubic-foot-per-second flow
Photos PX-D-61607NA and PX-D-61608NA

Figure 5B
Test 6
Before and after 9-inch scour
6- to 9-inch cobbles
1-foot stone layer
11.6-cubic-foot-per-second flow
Photos PX-D-61609NA and PX-D-61610NA

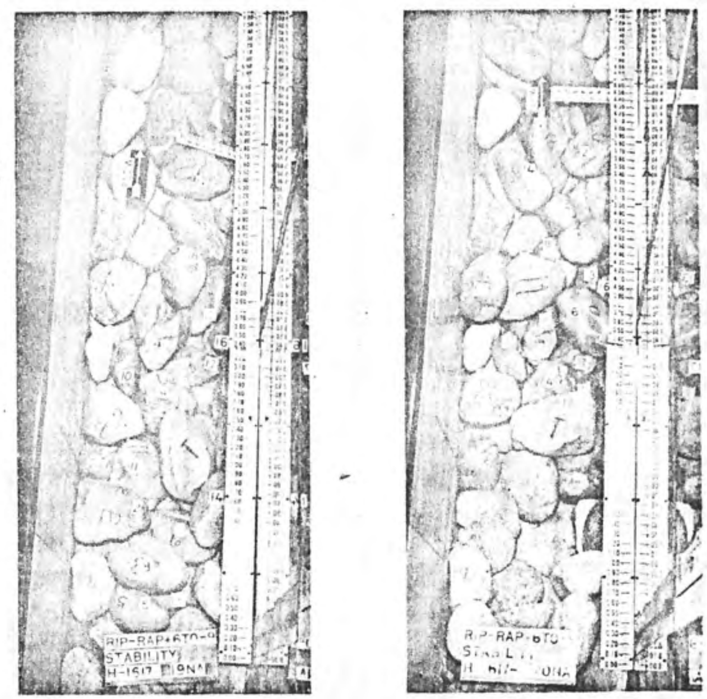

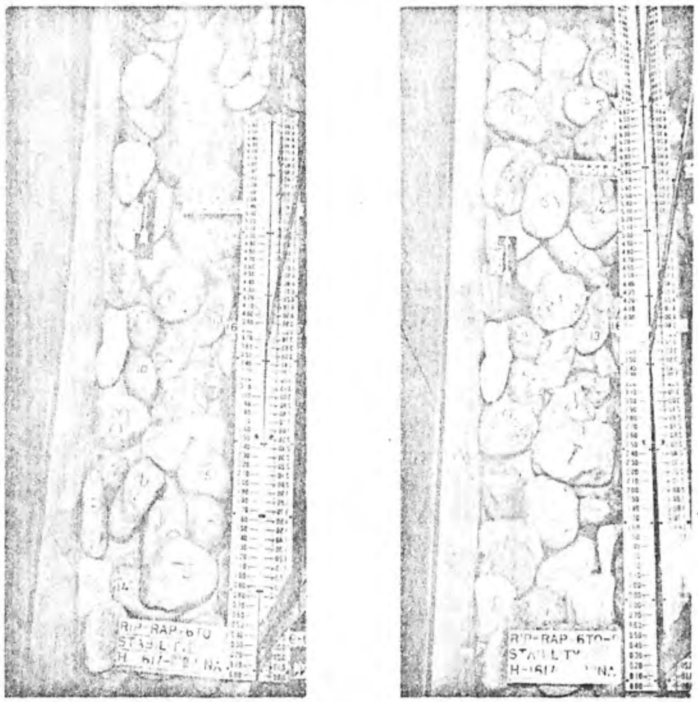

Figure 6A
Test 7
Before and after 9-inch scour
6- to 9-inch cobbles
1-foot stone layer
14-cubic-foot-per-second flow
Photos PX-D-61611NA and PX-D-61612NA

Figure 6B
Test 8
Before and after 9-inch scour
6- to 9-inch cobbles
1-foot stone layer
20.6-cubic-foot-per-second flow
Photos PX-D-61615NA and PX-D-61614NA

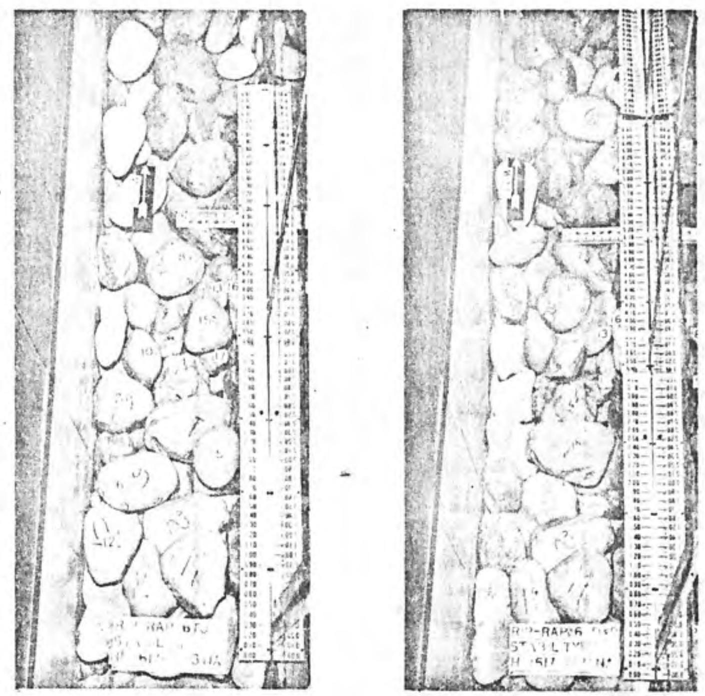

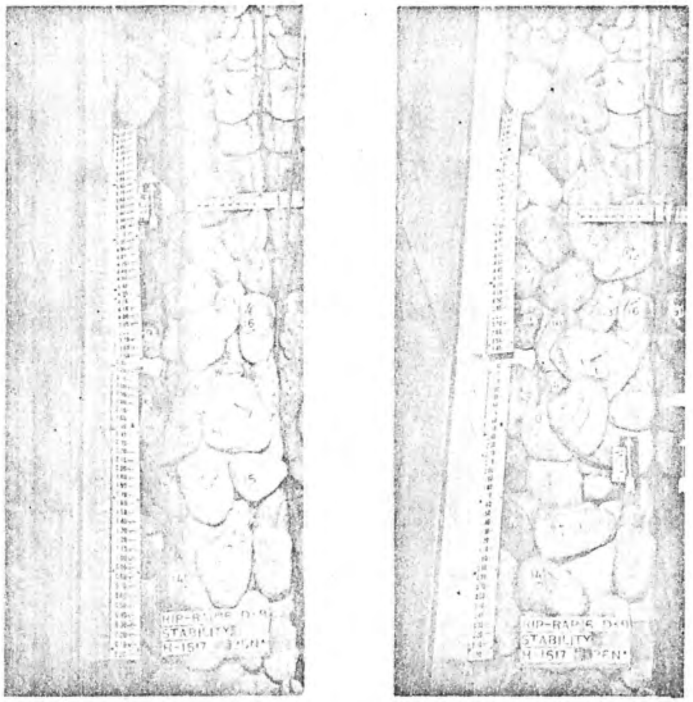

Figure 7A
Test 9
Before and after 9-inch scour
6- to 9-inch cobbles
1-foot stone layer
7.5-cubic-foot-per-second flow
Photos PX-D-61615NA and PX-D-61616NA

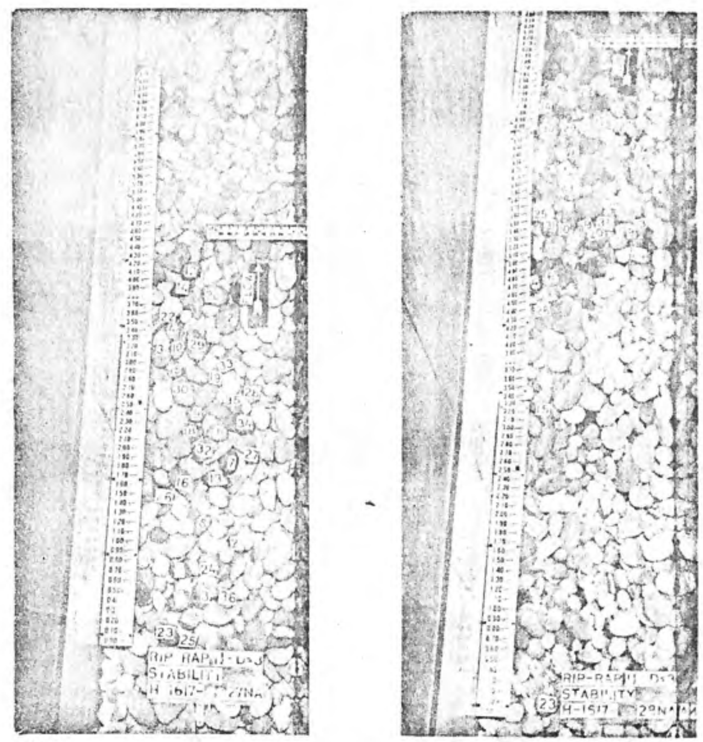

Figure 7B
Test 10
Before and after 3-inch scour
1-1/2- to 3-inch cobbles
1-foot stone layer
22-cubic-foot-per-second flow
Photos PX-D-61617NA and PX-D-61618NA

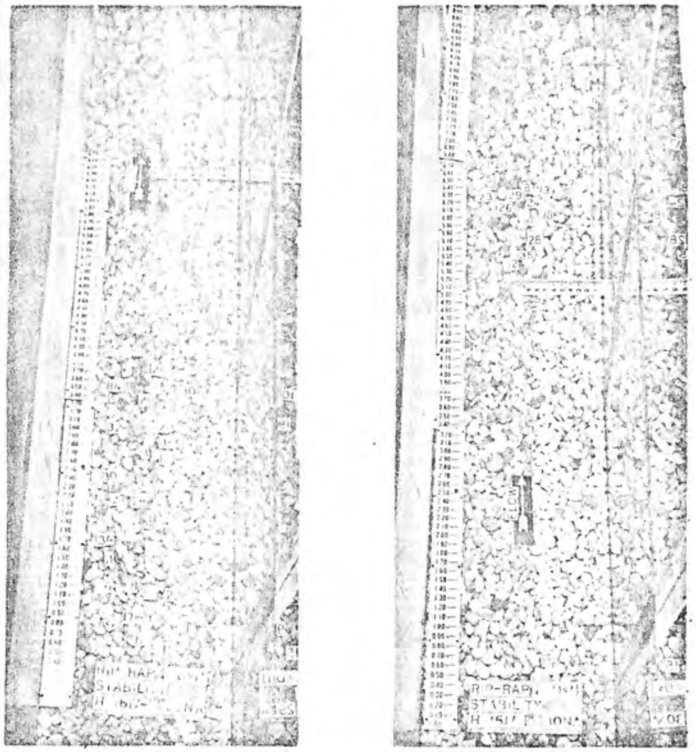

Figure 8A
Test 11
Before and after 1-1/2-inch scour
3/4- to 1-1/2-inch cobbles
1-foot stone layer
22-cubic-foot-per-second flow
Photos PX-D-61619NA and PX-D-61620NA

Figure 8B
Test 12
Before and after 6-inch scour
3- to 6-inch angulars
1-foot stone layer
22-cubic-foot-per-second flow
Photos PX-D-61621NA and PX-D-61622NA

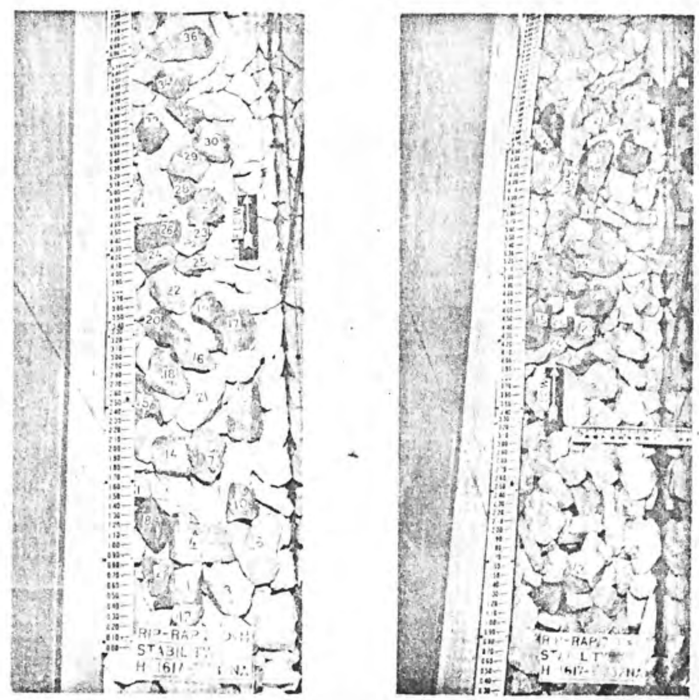

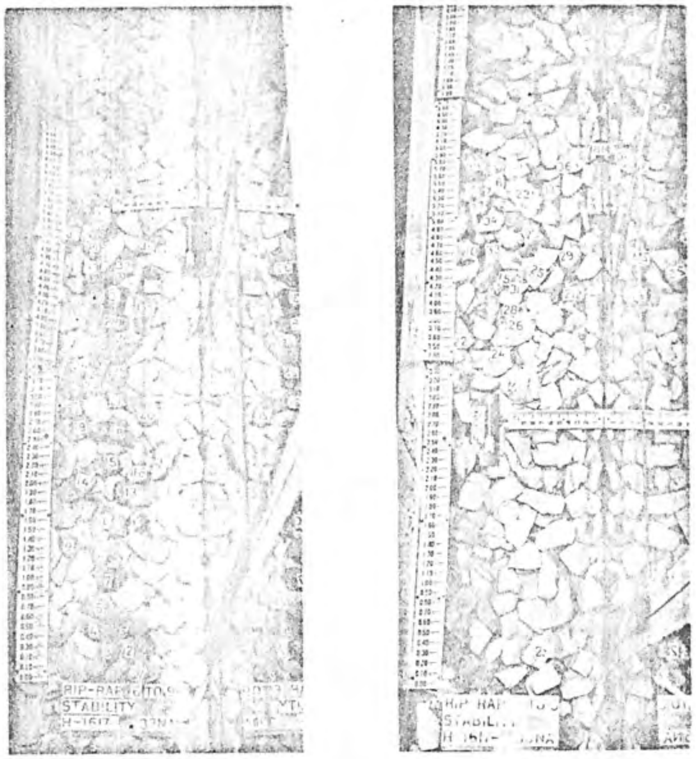

Figure 9A
Test 18
Before and after 3-inch scour
1-1/2- to 3-inch angulars
1-1/2-foot stone layer
22-cubic-foot-per-second flow
Photos PX-D-61623NA and PX-D-61624NA

Figure 9B
Test 20
Before and after 9-inch scour
6- to 9-inch angulars
1-1/2-foot stone layer
22-cubic-foot-per-second flow
Photos PX-D-61625NA and PX-D-61626NA

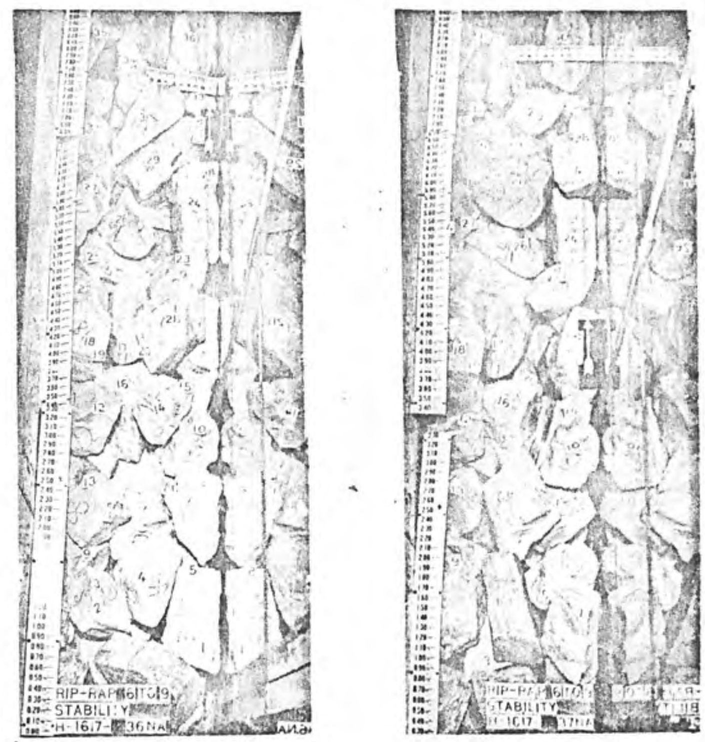

FIGURE 10

SINGLE CHANNEL
ELECTRONIC RECORDER
DATA TAPE

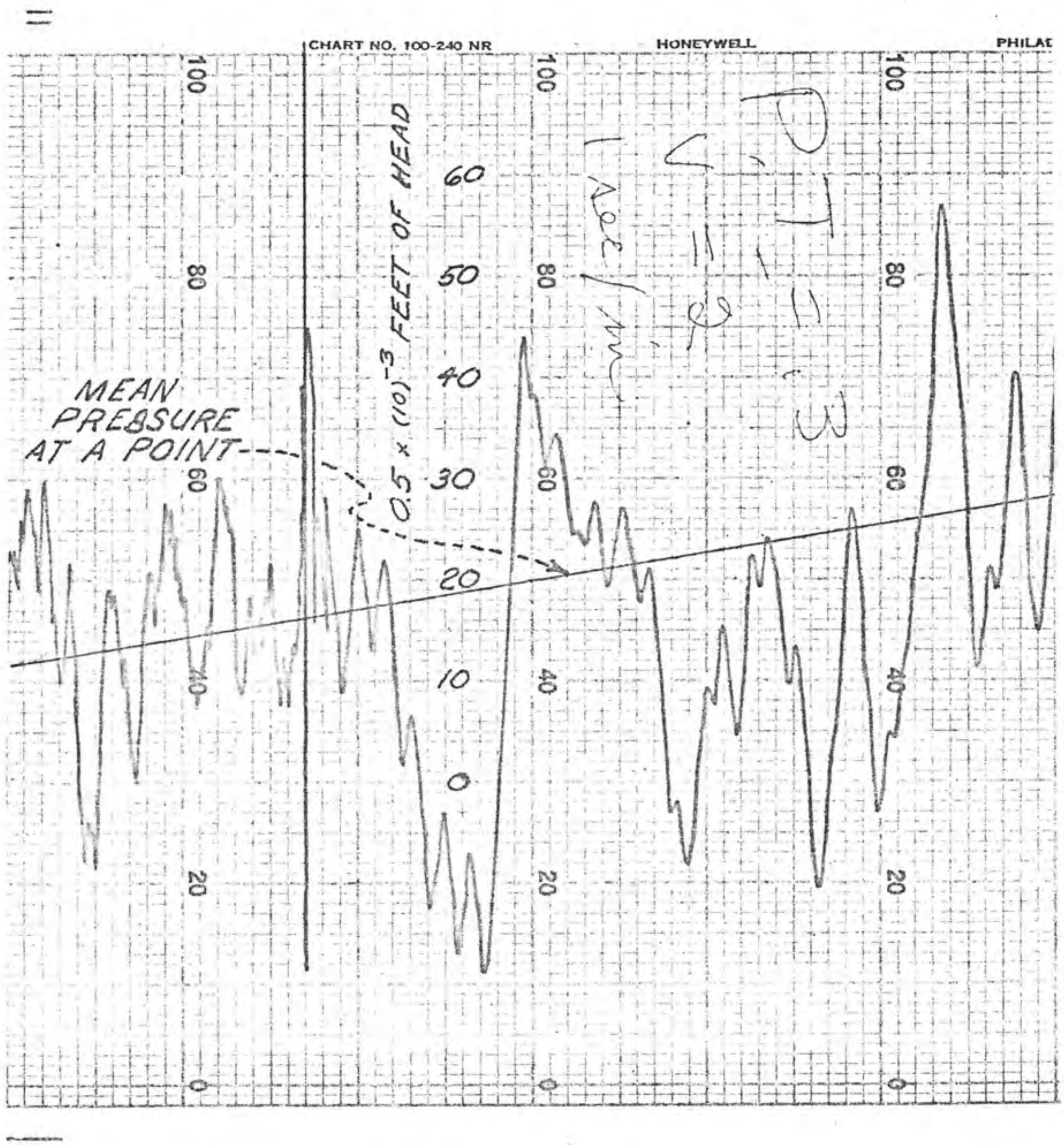

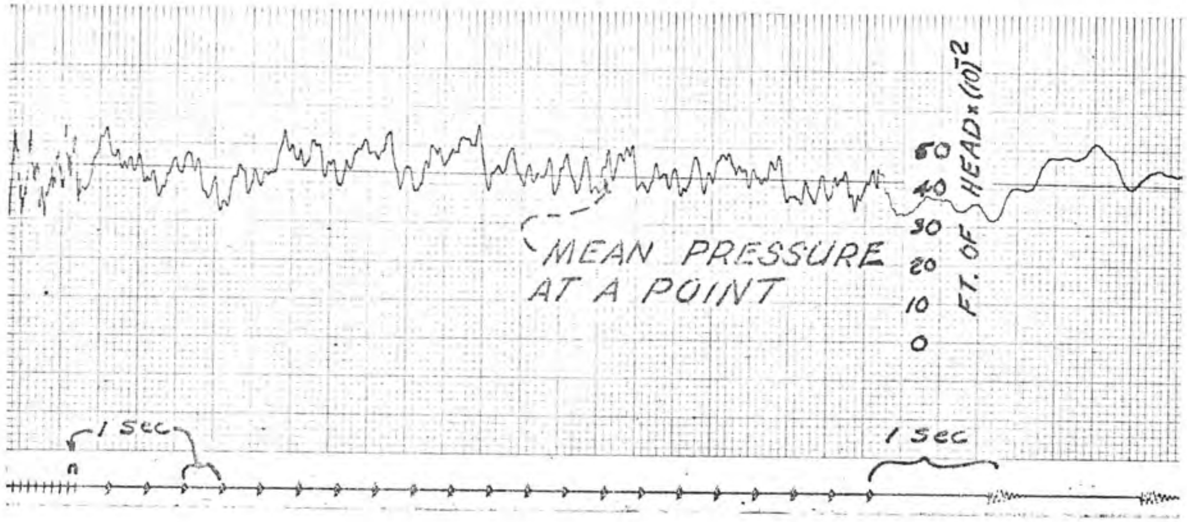

FIGURE 11

SINGLE CHANNEL
ELECTRONIC RECORDER
DATA TAPE

FIGURE 12

DUAL CHANNEL
ELECTRONIC RECORDER
DATA TAPE

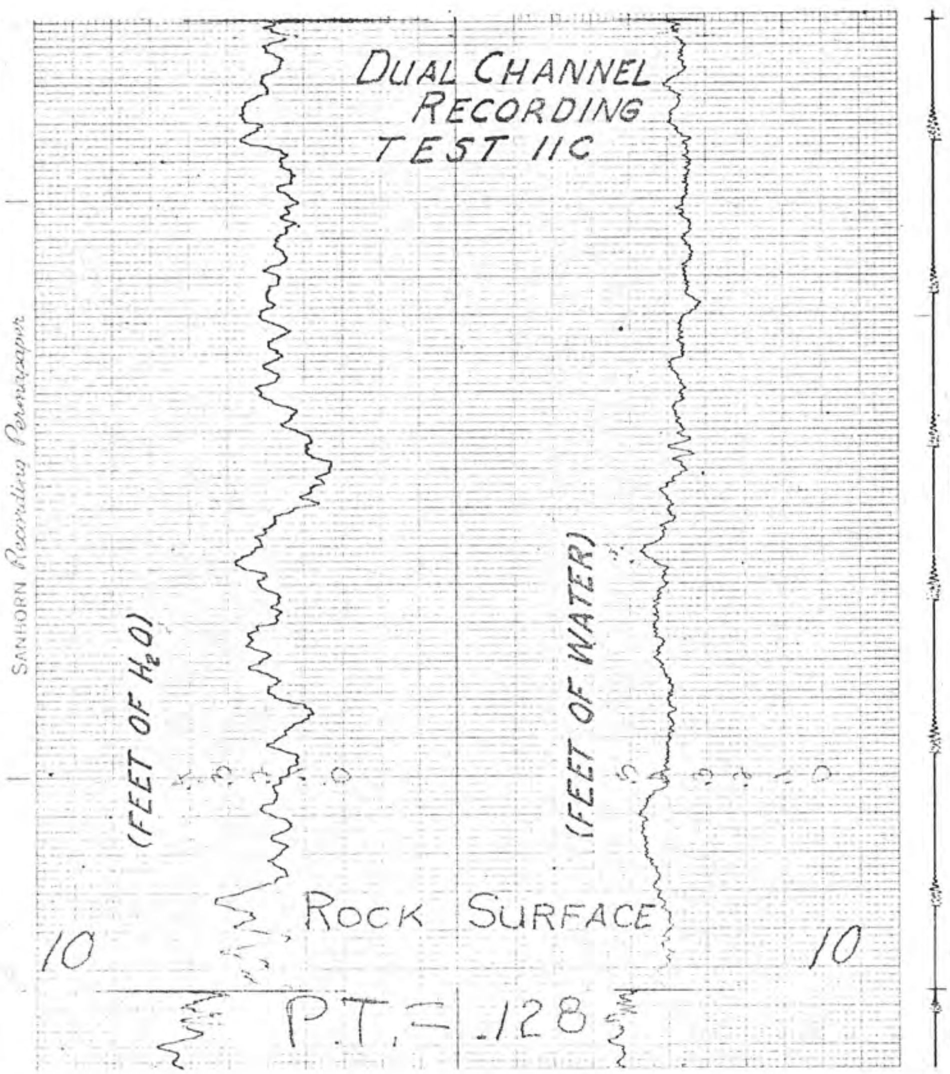

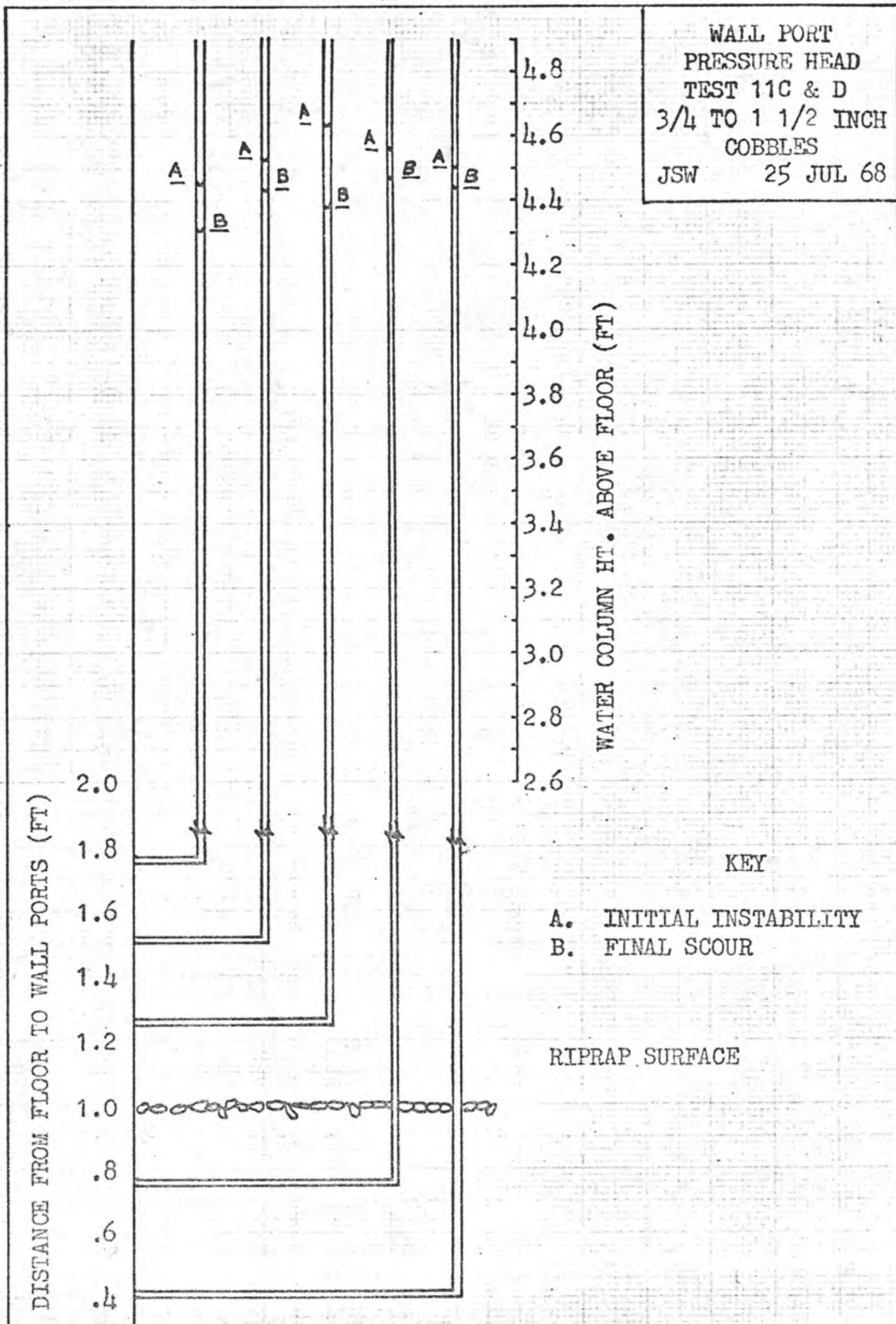
WALL PORT
PRESSURE HEAD
TEST 11C & D
3/4 TO 1 1/2 INCH
COBBLES
JSW 25 JUL 68
A
B
4.8
4.6
4.4
4.2
4.0
3.8
3.6
3.4
3.2
3.0
2.8
2.6
WATER COLUMN HT. ABOVE FLOOR (FT)
DISTANCE FROM FLOOR TO WALL PORTS (FT)
2.0
1.8
1.6
1.4
1.2
1.0
.8
.6
.4
KEY
A. INITIAL INSTABILITY
B. FINAL SCOUR
RIPRAP SURFACE

FIGURE 13

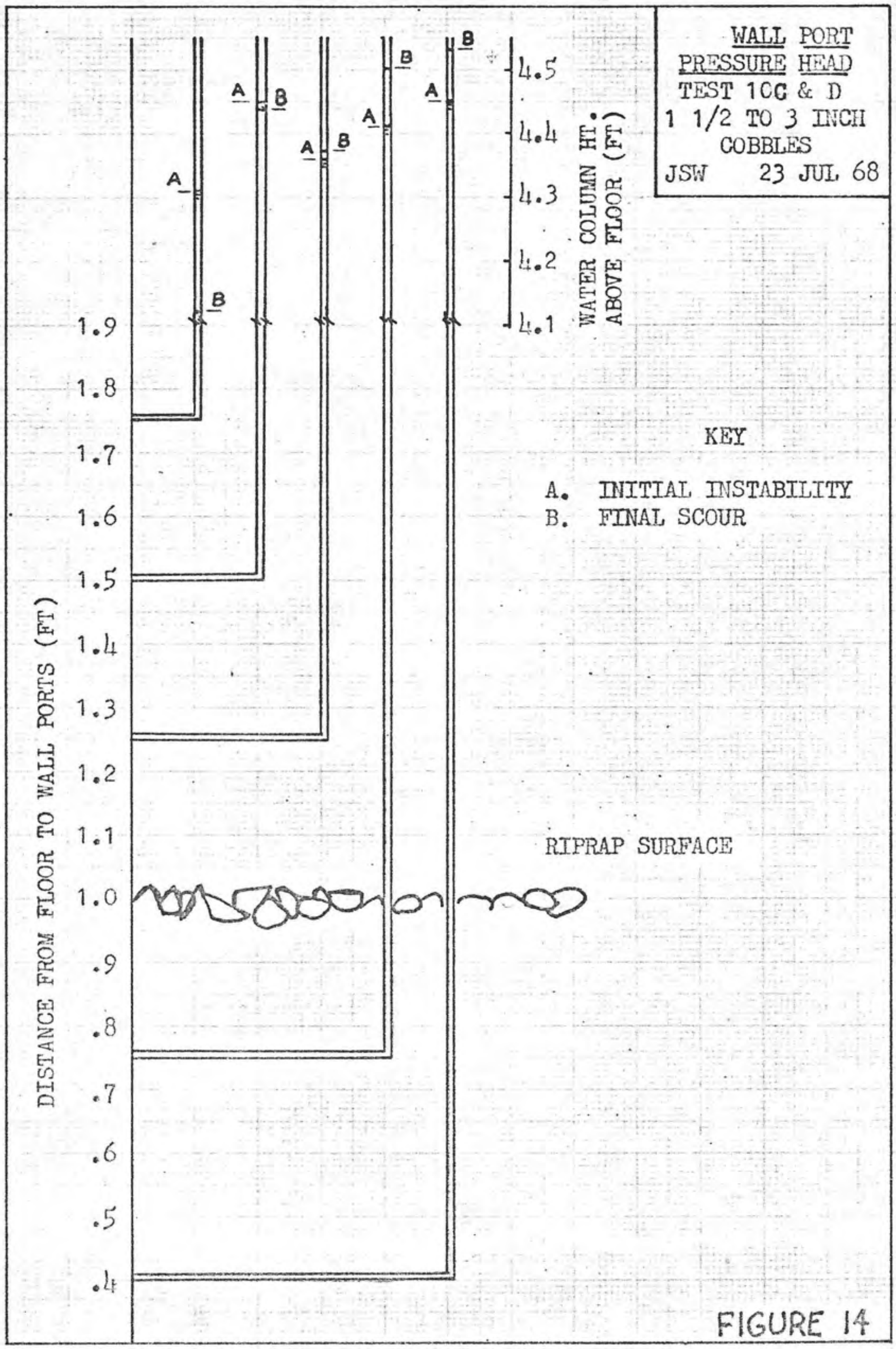
WALL PORT
PRESSURE HEAD
TEST 10C & D
1 1/2 TO 3 INCH
COBBLES
JSW 23 JUL 68
KEY
A. INITIAL INSTABILITY
B. FINAL SCOUR
WATER COLUMN HT. ABOVE FLOOR (FT)
4.5
4.4
4.3
4.2
4.1
DISTANCE FROM FLOOR TO WALL PORTS (FT)
1.9
1.8
1.7
1.6
1.5
1.4
1.3
1.2
1.1
1.0
.9
.8
.7
.6
.5
.4
RIPRAP SURFACE
A
B

FIGURE 14

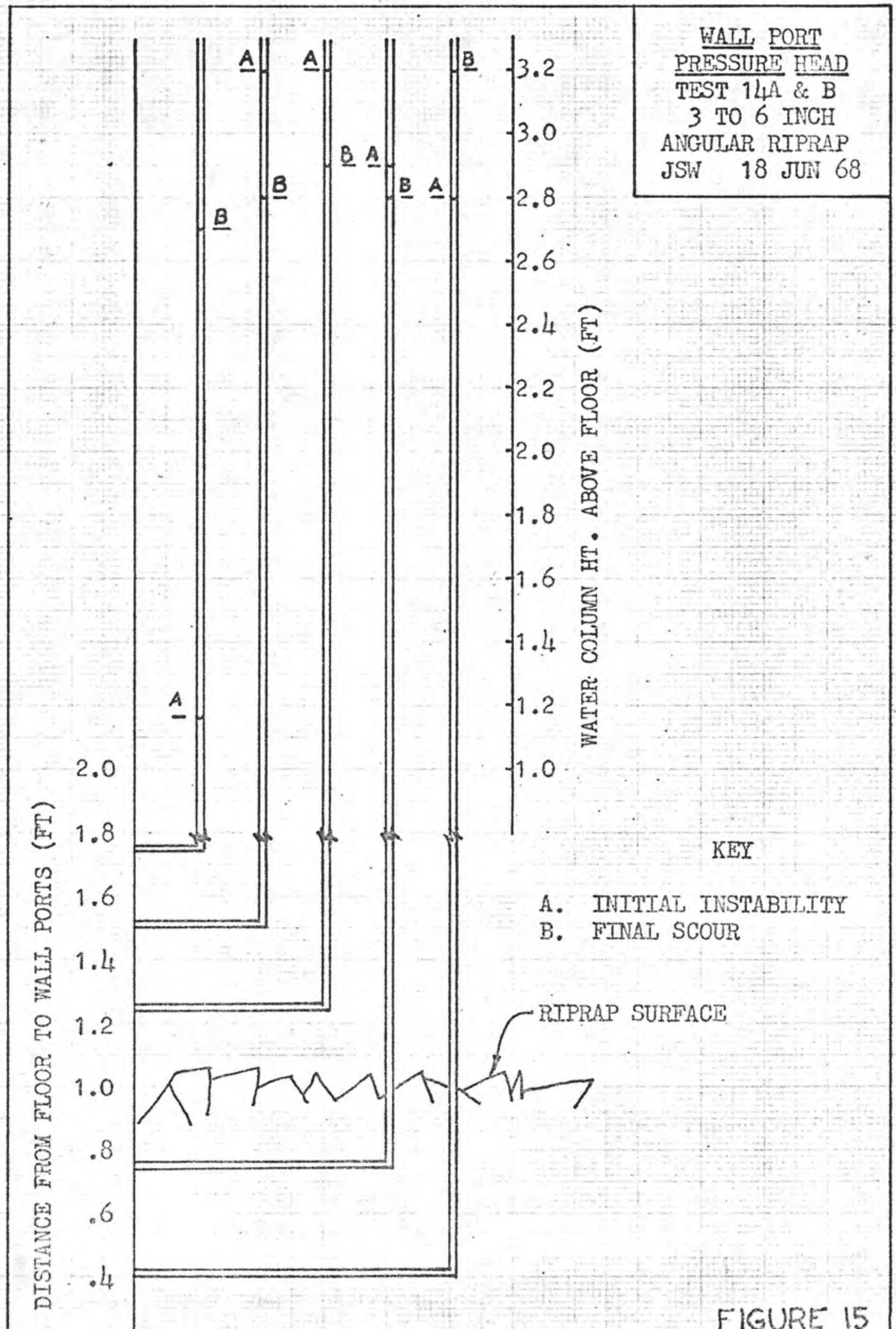
WALL PORT
PRESSURE HEAD
TEST 14A & B
3 TO 6 INCH
ANGULAR RIPRAP
JSW 18 JUN 68
WATER COLUMN HT. ABOVE FLOOR (FT)
3.2
3.0
2.8
2.6
2.4
2.2
2.0
1.8
1.6
1.4
1.2
1.0
DISTANCE FROM FLOOR TO WALL PORTS (FT)
2.0
1.8
1.6
1.4
1.2
1.0
.8
.6
.4
KEY
A. INITIAL INSTABILITY
B. FINAL SCOUR
RIPRAP SURFACE

FIGURE 15

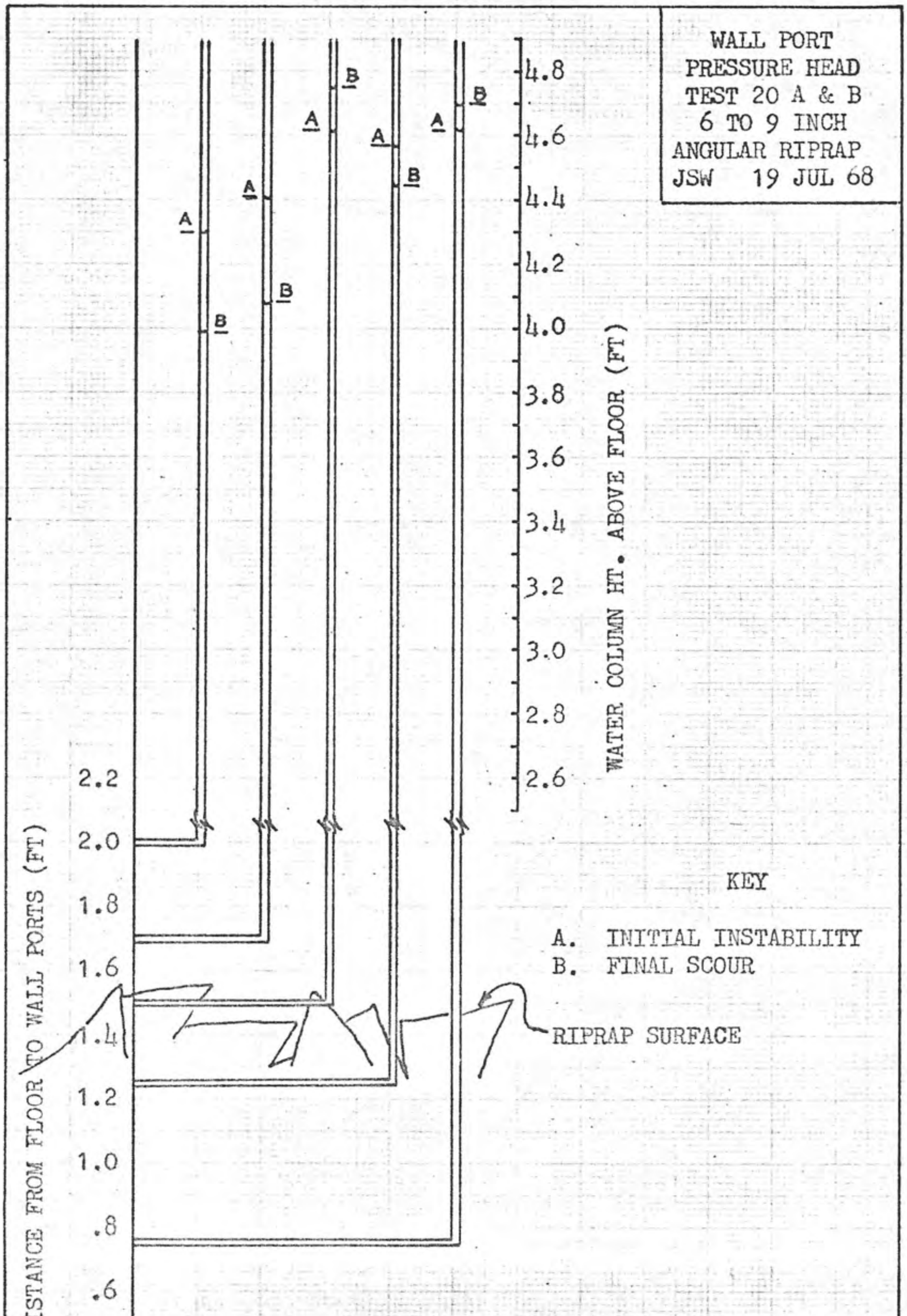

WALL PORT
PRESSURE HEAD
TEST 20 A & B
6 TO 9 INCH
ANGULAR RIPRAP
JSW 19 JUL 68
A
B
4.8
4.6
4.4
4.2
4.0
3.8
3.6
3.4
3.2
3.0
2.8
2.6
WATER COLUMN HT. ABOVE FLOOR (FT)
2.2
2.0
1.8
1.6
1.4
1.2
1.0
.8
.6
DISTANCE FROM FLOOR TO WALL PORTS (FT)
KEY
A. INITIAL INSTABILITY
B. FINAL SCOUR
RIPRAP SURFACE

FIGURE 16

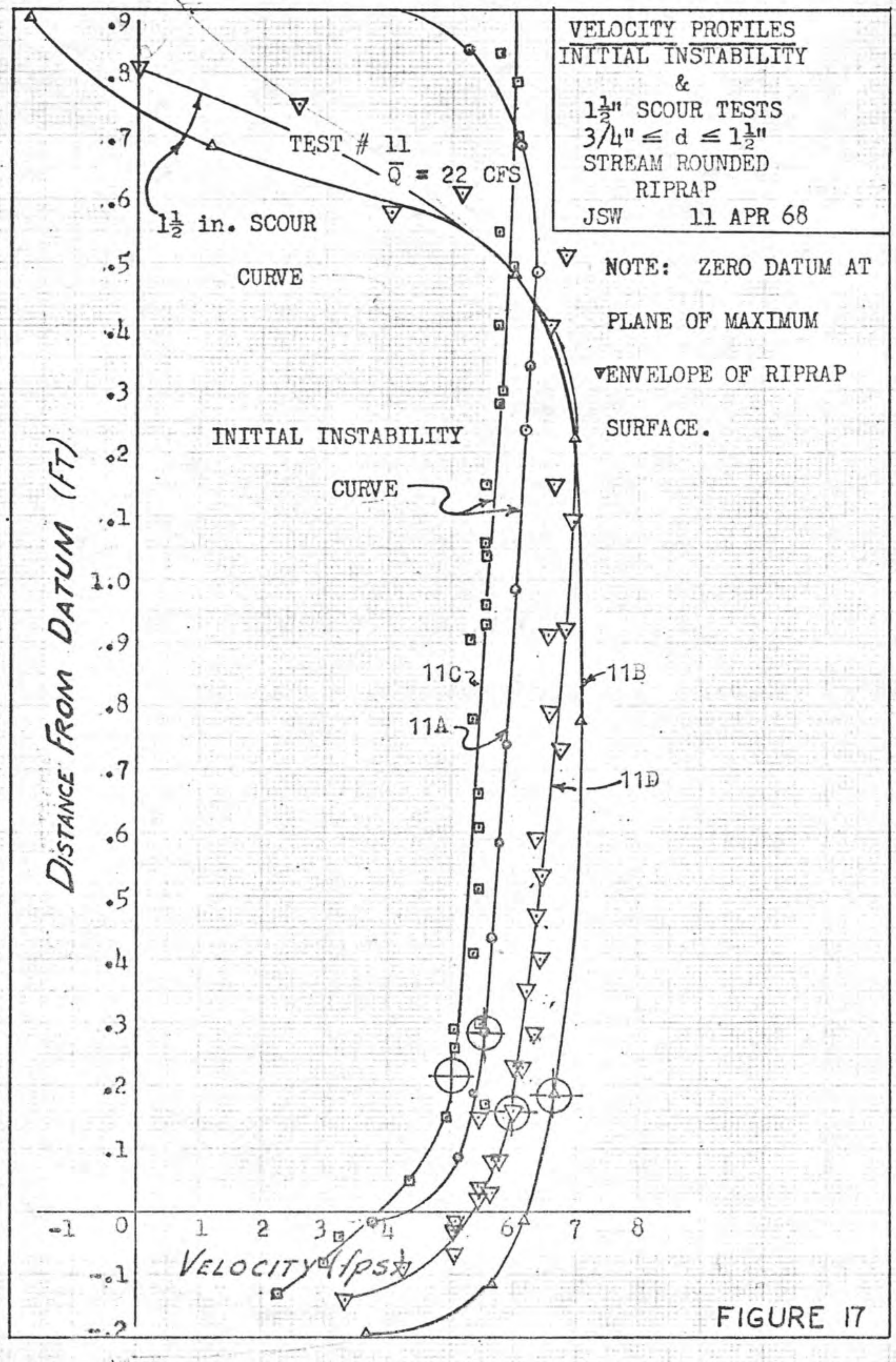
VELOCITY PROFILES
INITIAL INSTABILITY
&
1½" SCOUR TESTS
3/4" ≤ d ≤ 1½"
STREAM ROUNDED
RIPRAP
JSW 11 APR 68
NOTE: ZERO DATUM AT
PLANE OF MAXIMUM
▽ENVELOPE OF RIPRAP
SURFACE.
TEST # 11
Q̄ = 22 CFS
1½ in. SCOUR
CURVE
INITIAL INSTABILITY
CURVE
11C
11A
11B
11D
DISTANCE FROM DATUM (FT)
VELOCITY (fps)
.9
.8
.7
.6
.5
.4
.3
.2
.1
1.0
.9
.8
.7
.6
.5
.4
.3
.2
.1
-.1
-.2
-1
0
1
2
3
4
6
7
8

FIGURE 17

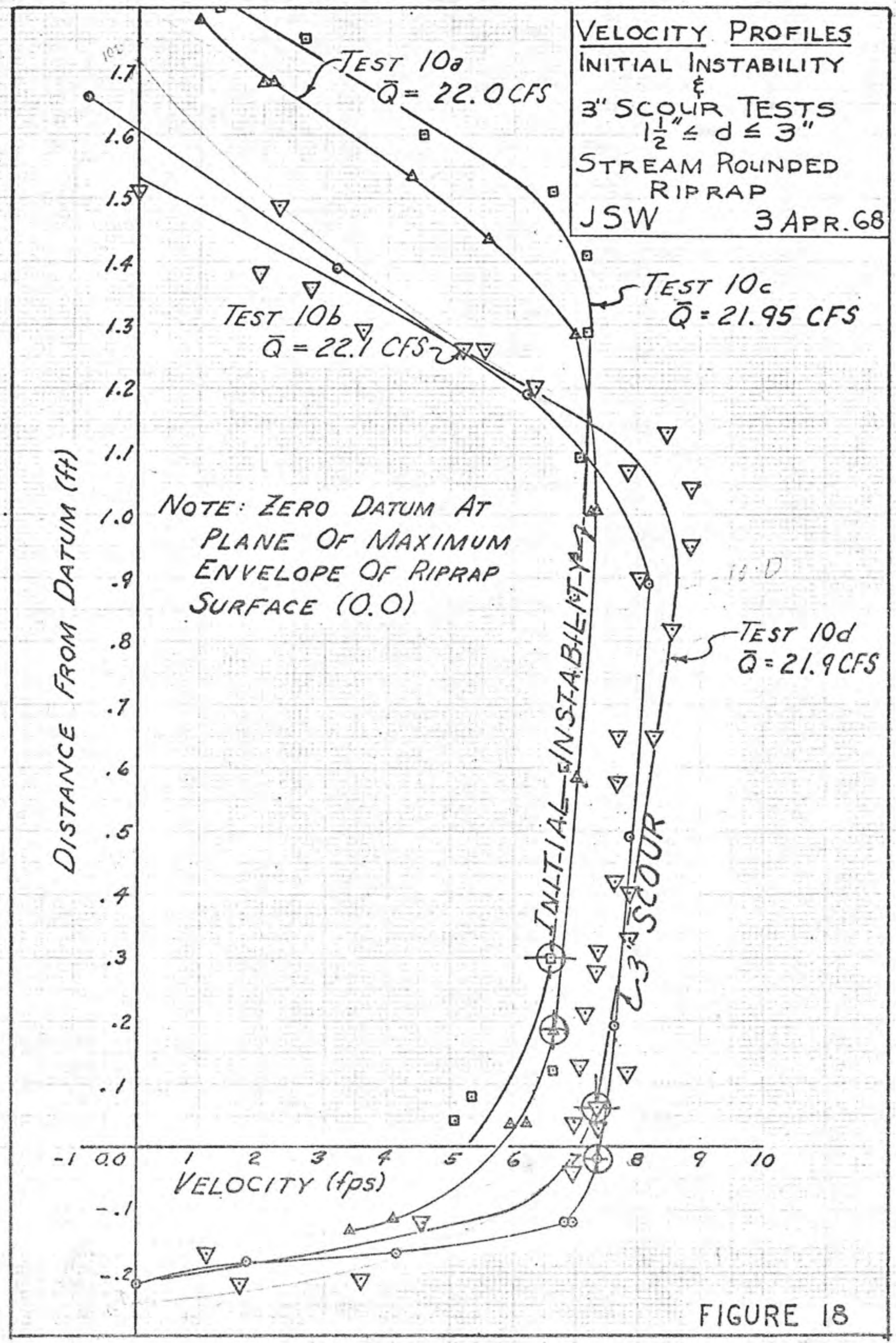

VELOCITY PROFILES
INITIAL INSTABILITY & 3" SCOUR TESTS
$1\frac{1}{2}" \le d \le 3"$
STREAM ROUNDED RIPRAP
JSW 3 APR. 68
TEST 10a $\bar{Q}$ = 22.0 CFS
TEST 10b $\bar{Q}$ = 22.1 CFS
TEST 10c $\bar{Q}$ = 21.95 CFS
TEST 10d $\bar{Q}$ = 21.9 CFS
NOTE: ZERO DATUM AT PLANE OF MAXIMUM ENVELOPE OF RIPRAP SURFACE (0.0)
INITIAL INSTABILITY
3" SCOUR
DISTANCE FROM DATUM (ft)
VELOCITY (fps)

FIGURE 18

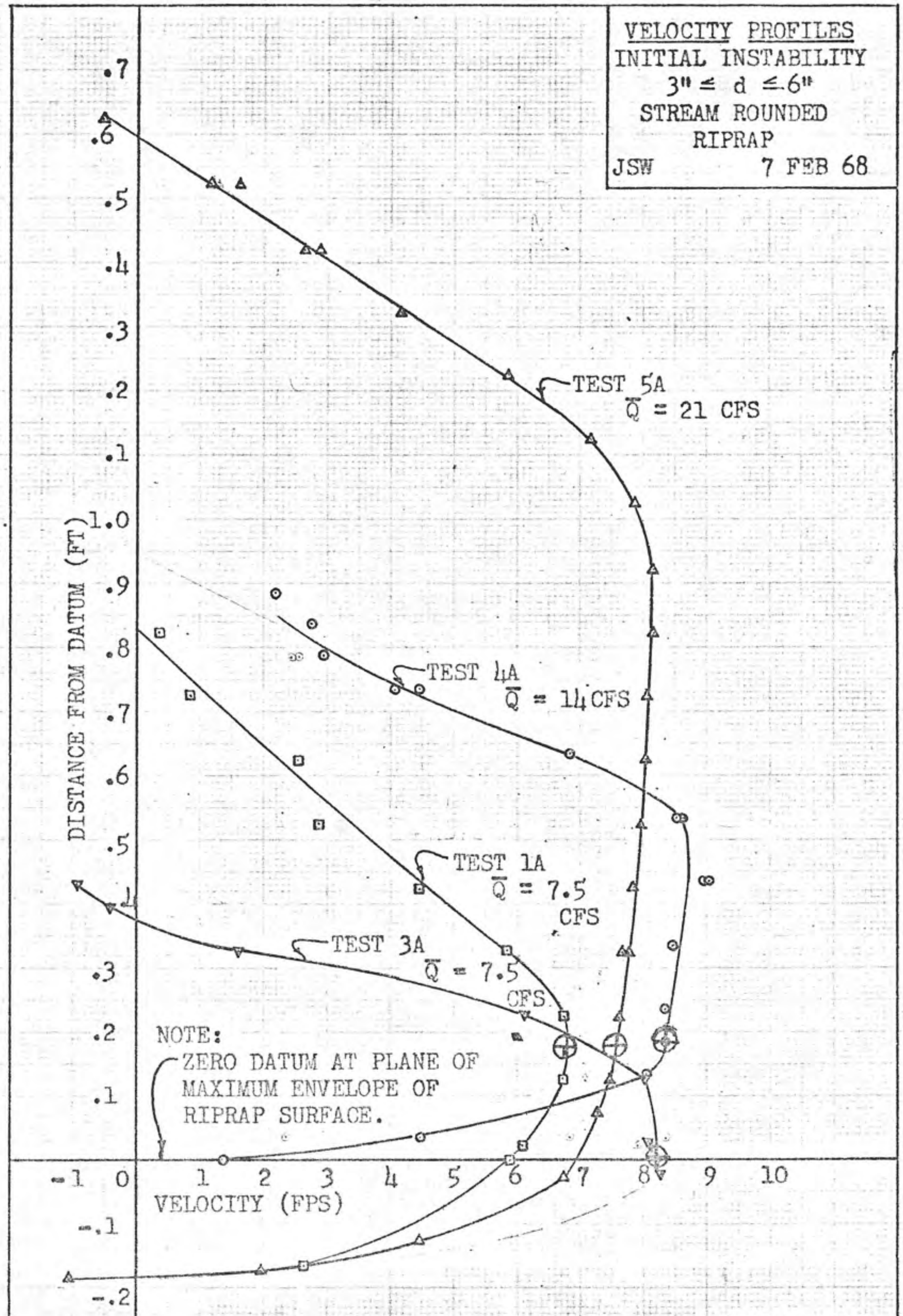
VELOCITY PROFILES
INITIAL INSTABILITY
3" ≤ d ≤ 6"
STREAM ROUNDED
RIPRAP
JSW 7 FEB 68
TEST 5A
Q̄ = 21 CFS
TEST 4A
Q̄ = 14 CFS
TEST 1A
Q̄ = 7.5 CFS
TEST 3A
Q̄ = 7.5 CFS
NOTE:
ZERO DATUM AT PLANE OF MAXIMUM ENVELOPE OF RIPRAP SURFACE.
DISTANCE FROM DATUM (FT)
VELOCITY (FPS)

FIGURE 19

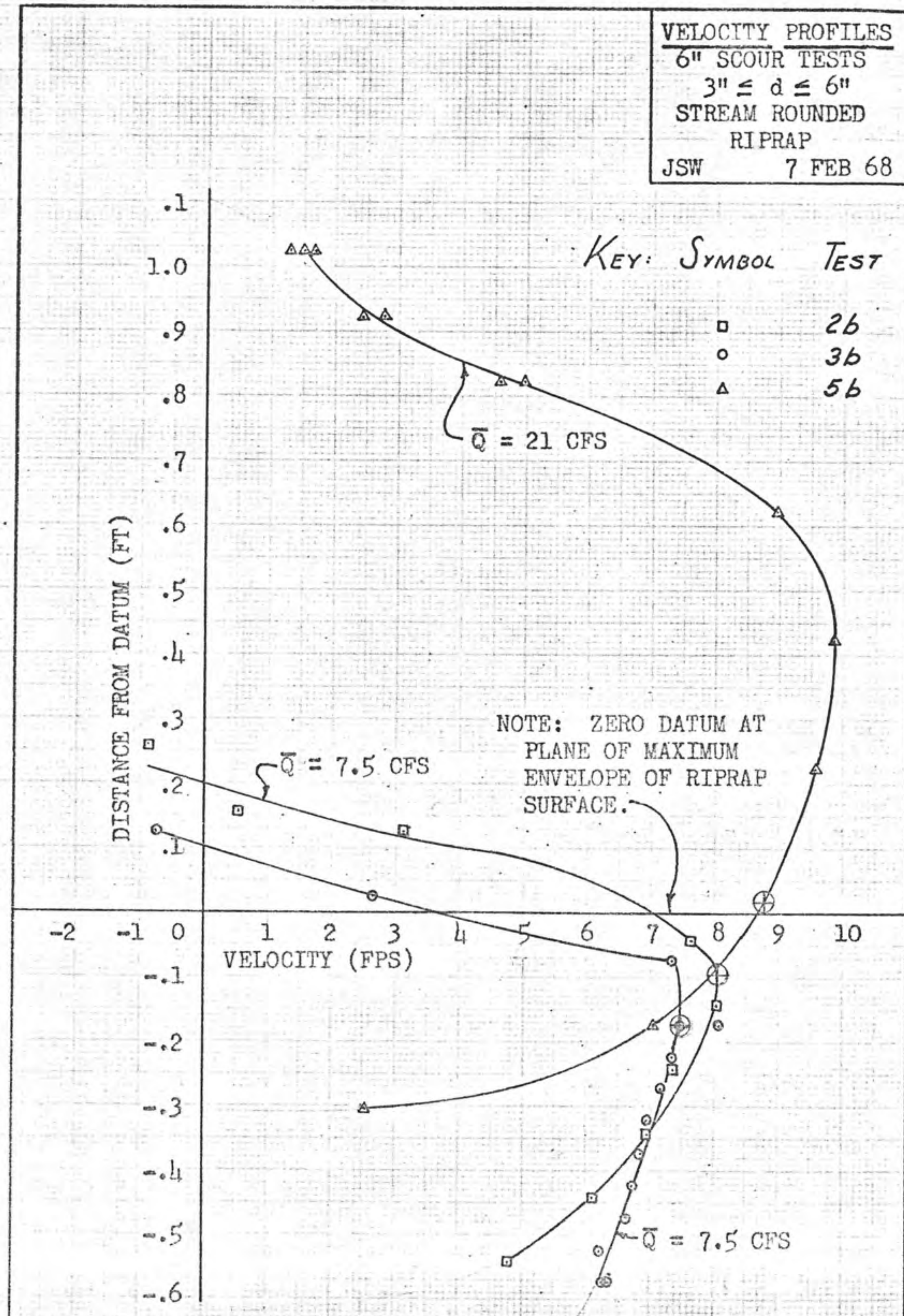
VELOCITY PROFILES
6" SCOUR TESTS
3" ≤ d ≤ 6"
STREAM ROUNDED
RIPRAP
JSW 7 FEB 68
KEY: SYMBOL TEST
2b
3b
5b
Q̄ = 21 CFS
Q̄ = 7.5 CFS
NOTE: ZERO DATUM AT PLANE OF MAXIMUM ENVELOPE OF RIPRAP SURFACE.
Q̄ = 7.5 CFS
DISTANCE FROM DATUM (FT)
VELOCITY (FPS)
1.1
1.0
.9
.8
.7
.6
.5
.4
.3
.2
.1
-.1
-.2
-.3
-.4
-.5
-.6
-2
-1
0
1
2
3
4
5
6
7
8
9
10

FIGURE 20

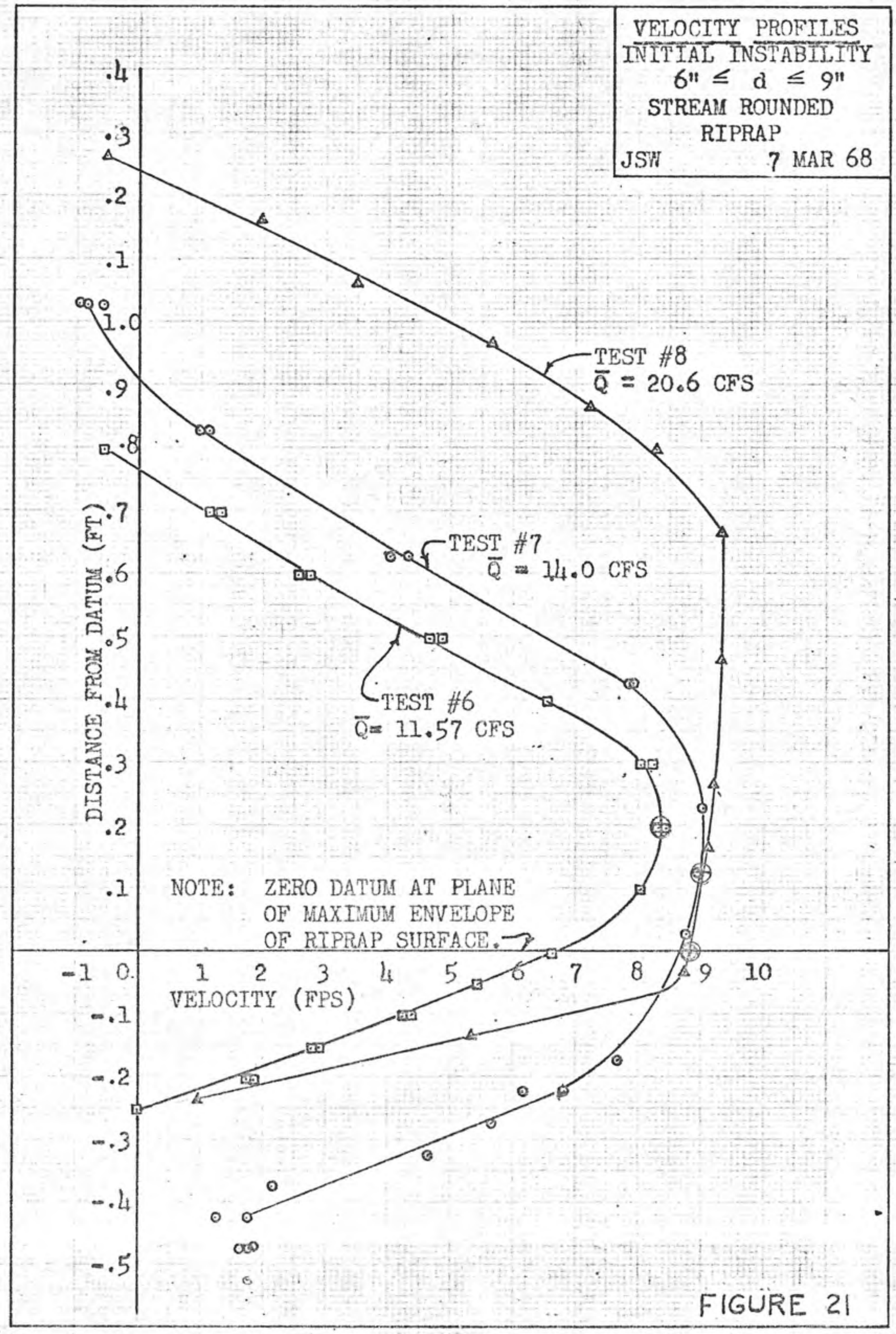
VELOCITY PROFILES
INITIAL INSTABILITY
6" ≤ d ≤ 9"
STREAM ROUNDED
RIPRAP
JSW 7 MAR 68
TEST #8
$\overline{Q}$ = 20.6 CFS
TEST #7
$\overline{Q}$ = 14.0 CFS
TEST #6
$\overline{Q}$ = 11.57 CFS
NOTE: ZERO DATUM AT PLANE OF MAXIMUM ENVELOPE OF RIPRAP SURFACE.
DISTANCE FROM DATUM (FT)
VELOCITY (FPS)
-1
0.
1
2
3
4
5
6
7
8
9
10
1.0
.9
.8
.7
.6
.5
.4
.3
.2
.1
-.1
-.2
-.3
-.4
-.5

FIGURE 21

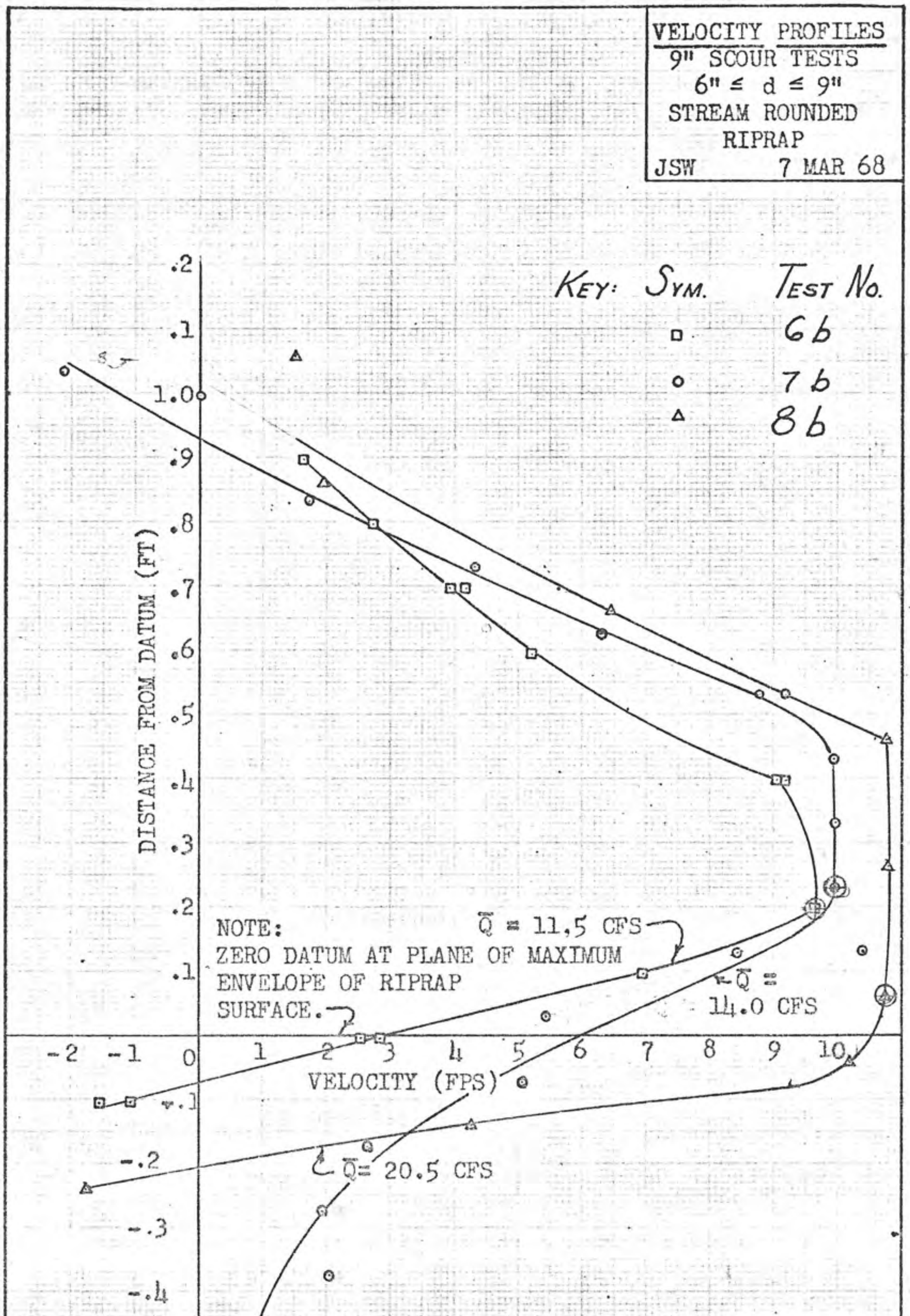
VELOCITY PROFILES
9" SCOUR TESTS
6" ≤ d ≤ 9"
STREAM ROUNDED
RIPRAP
JSW 7 MAR 68
KEY: SYM. TEST NO.
□ 6b
○ 7b
△ 8b
DISTANCE FROM DATUM (FT)
VELOCITY (FPS)
NOTE:
ZERO DATUM AT PLANE OF MAXIMUM
ENVELOPE OF RIPRAP
SURFACE.
Q̄ = 11.5 CFS
Q̄ = 14.0 CFS
Q̄ = 20.5 CFS

FIGURE 22

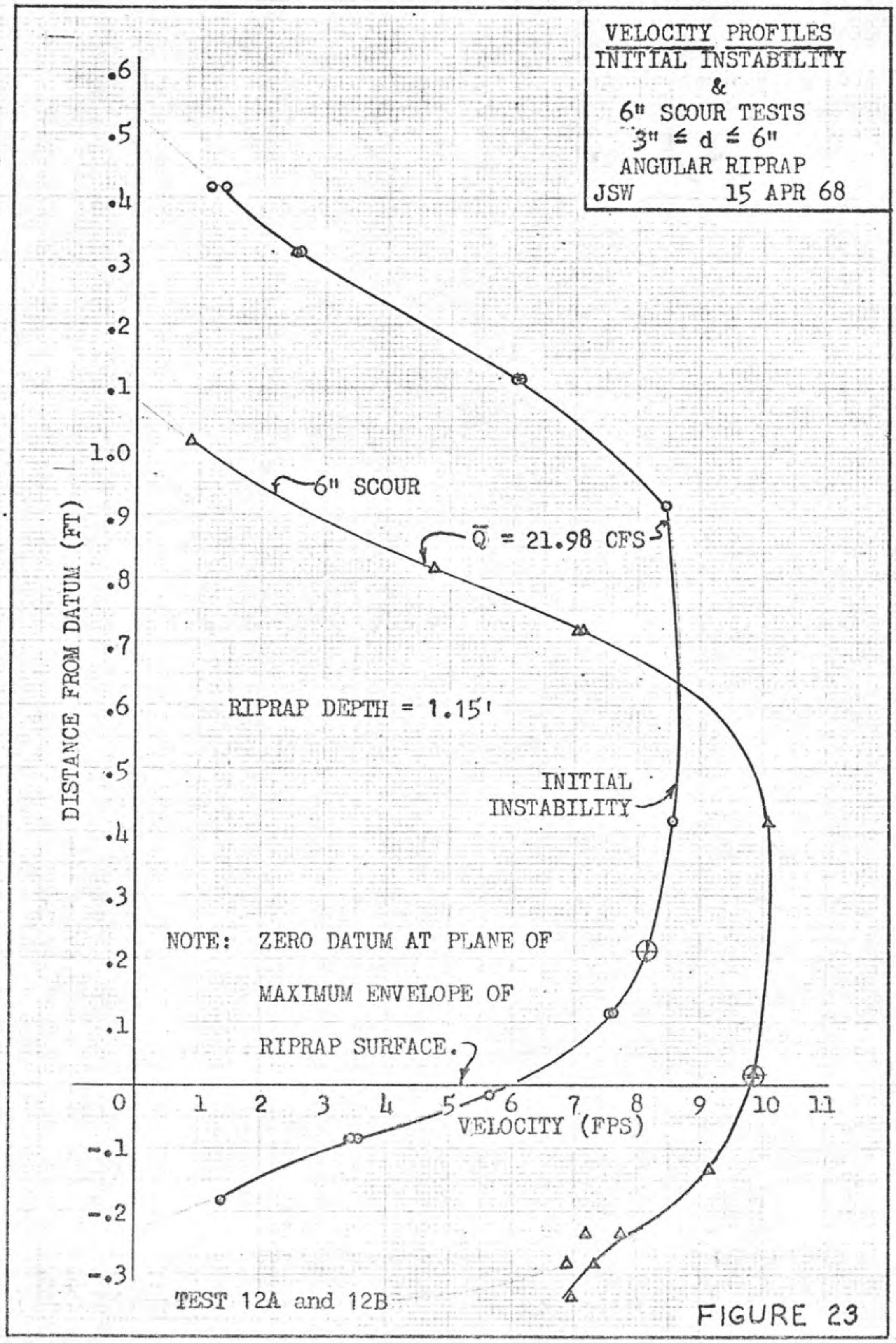

VELOCITY PROFILES
INITIAL INSTABILITY
&
6" SCOUR TESTS
3" ≤ d ≤ 6"
ANGULAR RIPRAP
JSW 15 APR 68
DISTANCE FROM DATUM (FT)
.6
.5
.4
.3
.2
.1
1.0
.9
.8
.7
.6
.5
.4
.3
.2
.1
0
-.1
-.2
-.3
6" SCOUR
Q̄ = 21.98 CFS
RIPRAP DEPTH = 1.15'
INITIAL INSTABILITY
NOTE: ZERO DATUM AT PLANE OF
MAXIMUM ENVELOPE OF
RIPRAP SURFACE.
1 2 3 4 5 6 7 8 9 10 11
VELOCITY (FPS)
TEST 12A and 12B

FIGURE 23

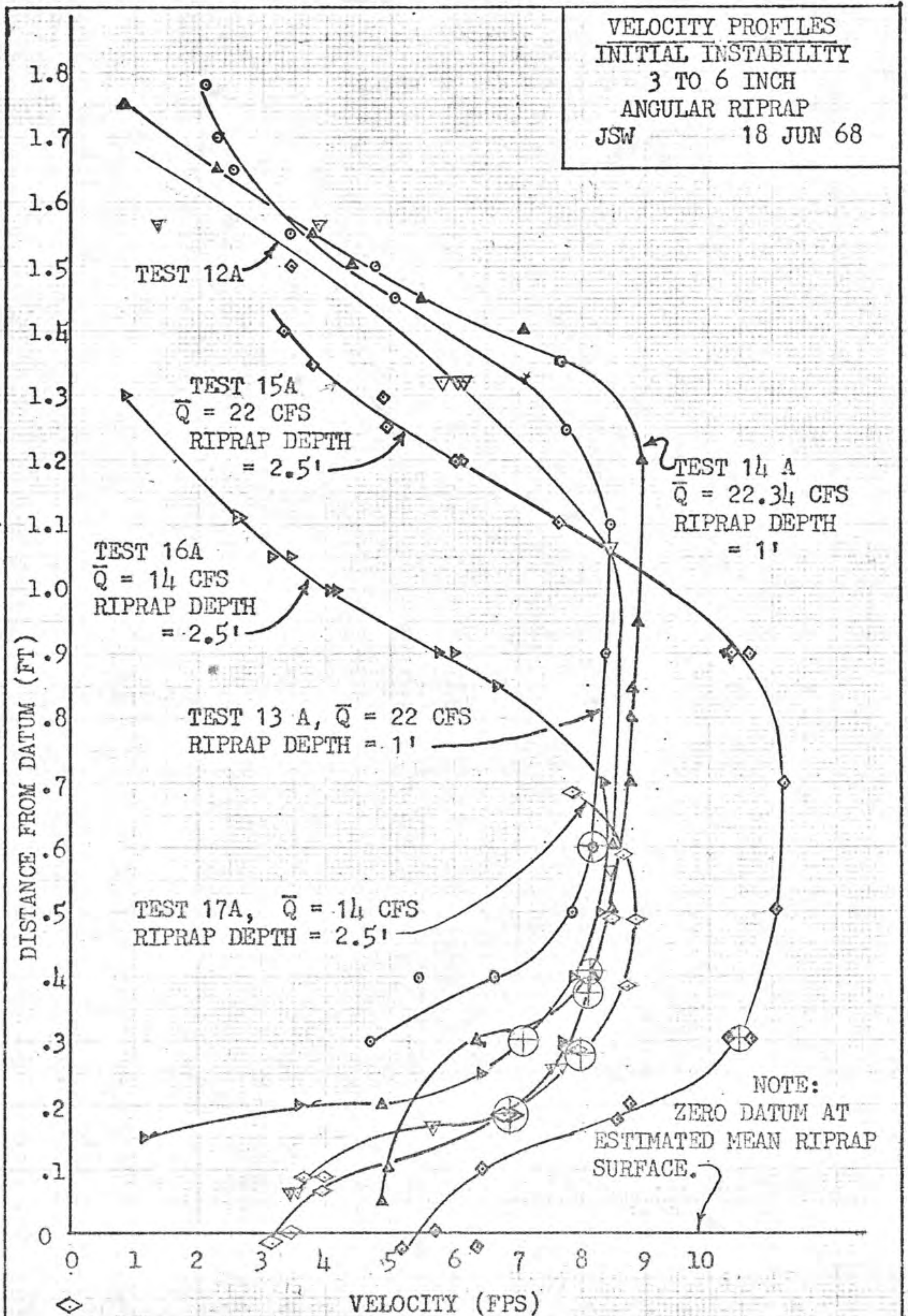

VELOCITY PROFILES
INITIAL INSTABILITY
3 TO 6 INCH
ANGULAR RIPRAP
JSW 18 JUN 68
TEST 12A
TEST 15A
Q̄ = 22 CFS
RIPRAP DEPTH
= 2.5'
TEST 14 A
Q̄ = 22.34 CFS
RIPRAP DEPTH
= 1'
TEST 16A
Q̄ = 14 CFS
RIPRAP DEPTH
= 2.5'
TEST 13 A, Q̄ = 22 CFS
RIPRAP DEPTH = 1'
TEST 17A, Q̄ = 14 CFS
RIPRAP DEPTH = 2.5'
NOTE:
ZERO DATUM AT
ESTIMATED MEAN RIPRAP
SURFACE.
DISTANCE FROM DATUM (FT)
VELOCITY (FPS)

FIGURE 24

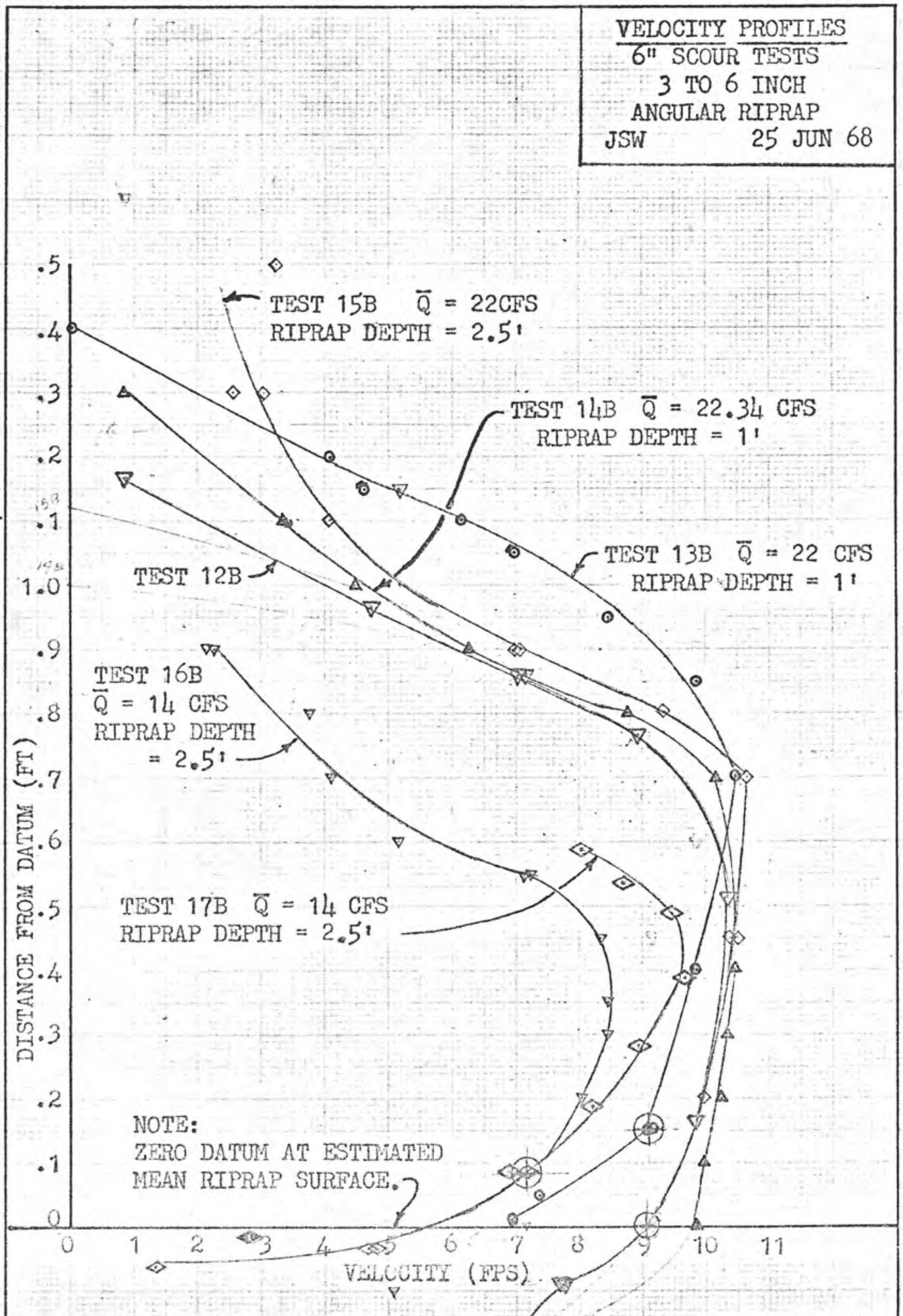
VELOCITY PROFILES
6" SCOUR TESTS
3 TO 6 INCH
ANGULAR RIPRAP
JSW 25 JUN 68
TEST 15B Q̄ = 22CFS
RIPRAP DEPTH = 2.5'
TEST 14B Q̄ = 22.34 CFS
RIPRAP DEPTH = 1'
TEST 13B Q̄ = 22 CFS
RIPRAP DEPTH = 1'
TEST 12B
TEST 16B
Q̄ = 14 CFS
RIPRAP DEPTH
= 2.5'
TEST 17B Q̄ = 14 CFS
RIPRAP DEPTH = 2.5'
NOTE:
ZERO DATUM AT ESTIMATED
MEAN RIPRAP SURFACE.
DISTANCE FROM DATUM (FT)
VELOCITY (FPS)

FIGURE 25

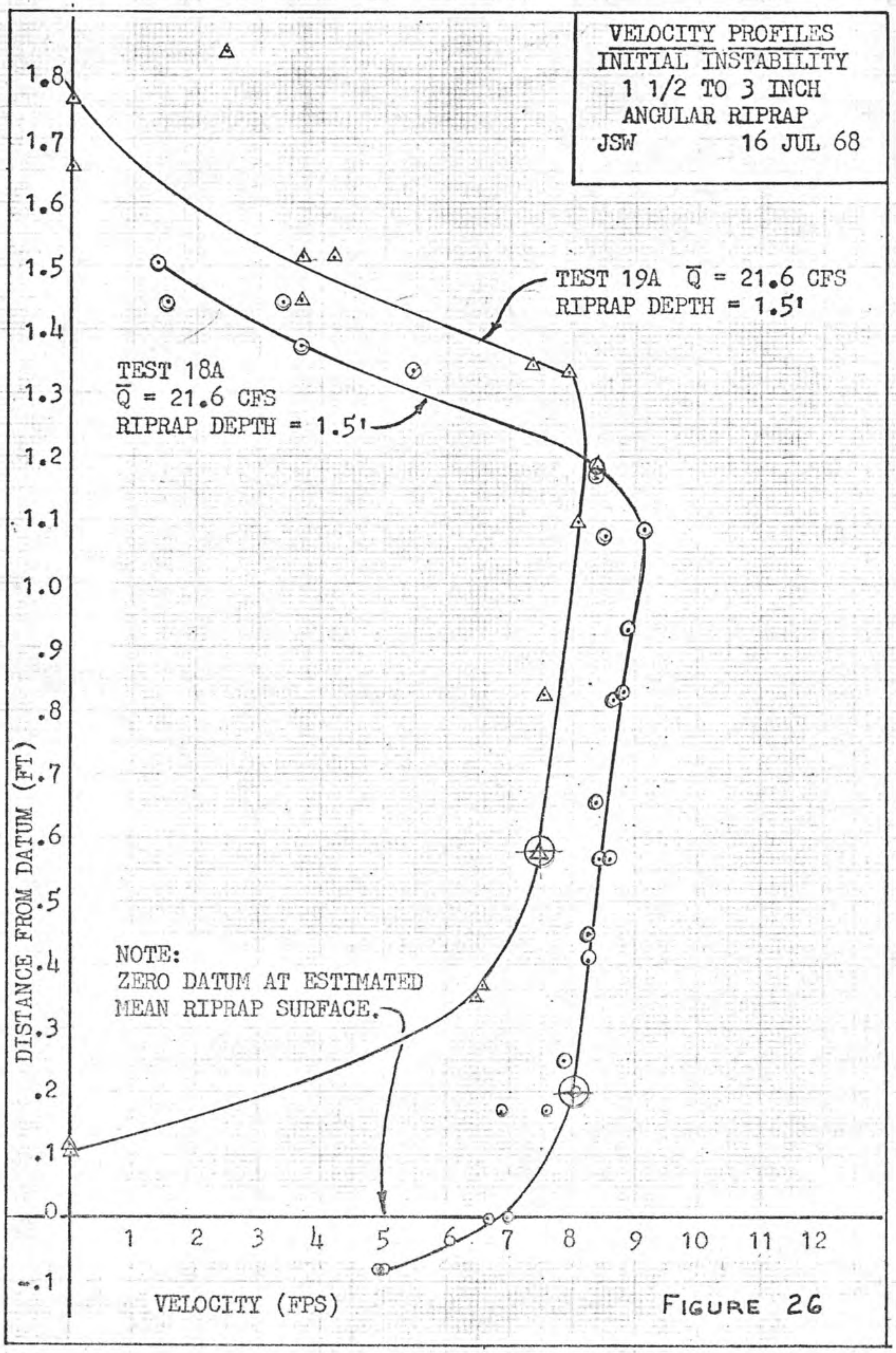
VELOCITY PROFILES
INITIAL INSTABILITY
1 1/2 TO 3 INCH
ANGULAR RIPRAP
JSW 16 JUL 68
TEST 19A $\overline{Q}$ = 21.6 CFS
RIPRAP DEPTH = 1.5'
TEST 18A
$\overline{Q}$ = 21.6 CFS
RIPRAP DEPTH = 1.5'
NOTE:
ZERO DATUM AT ESTIMATED
MEAN RIPRAP SURFACE.
DISTANCE FROM DATUM (FT)
1.8
1.7
1.6
1.5
1.4
1.3
1.2
1.1
1.0
.9
.8
.7
.6
.5
.4
.3
.2
.1
0
-.1
1 2 3 4 5 6 7 8 9 10 11 12
VELOCITY (FPS)

FIGURE 26

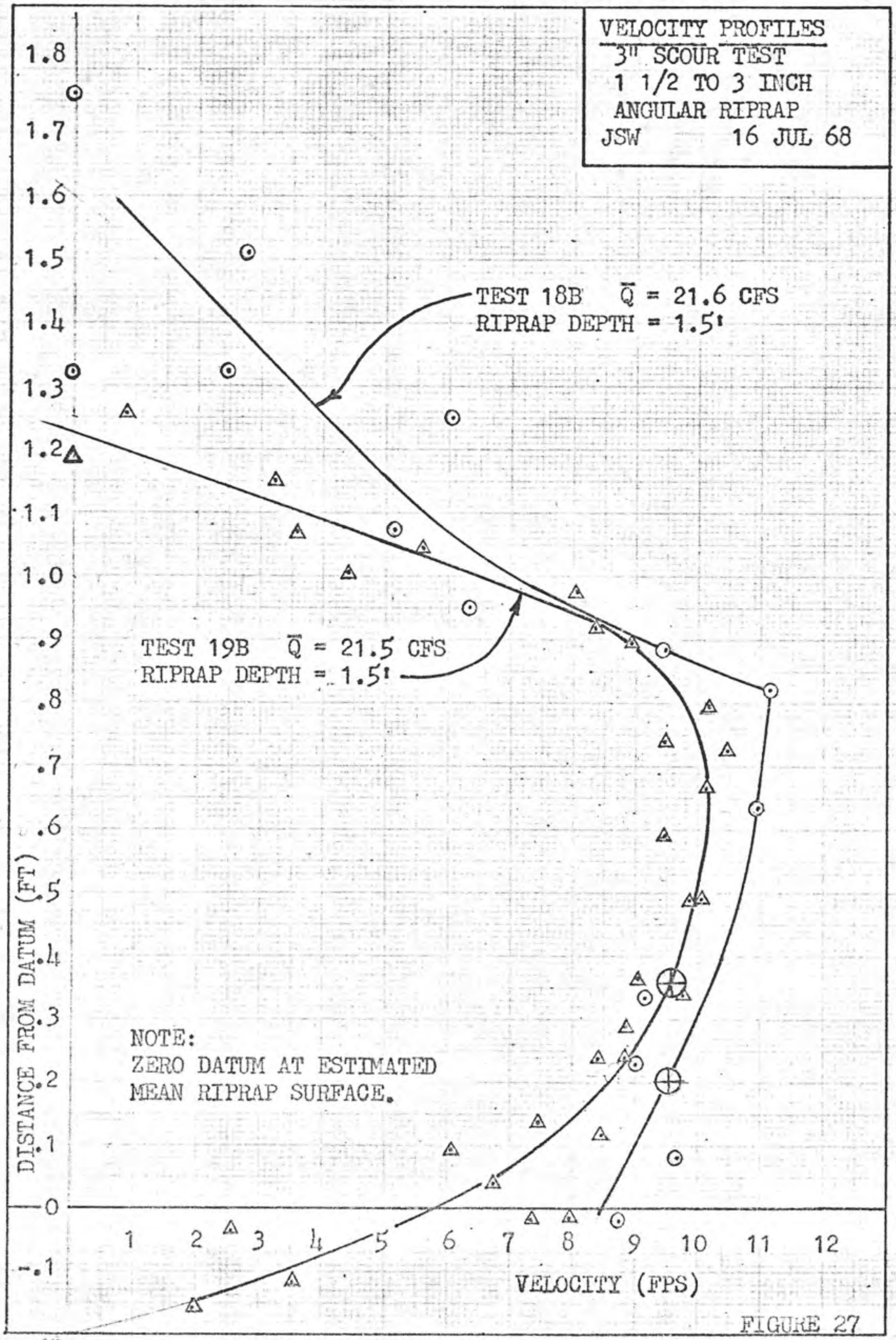
VELOCITY PROFILES
3" SCOUR TEST
1 1/2 TO 3 INCH
ANGULAR RIPRAP
JSW 16 JUL 68
TEST 18B $\bar{Q}$ = 21.6 CFS
RIPRAP DEPTH = 1.5'
TEST 19B $\bar{Q}$ = 21.5 CFS
RIPRAP DEPTH = 1.5'
NOTE:
ZERO DATUM AT ESTIMATED
MEAN RIPRAP SURFACE.
DISTANCE FROM DATUM (FT)
VELOCITY (FPS)
1.8
1.7
1.6
1.5
1.4
1.3
1.2
1.1
1.0
.9
.8
.7
.6
.5
.4
.3
.2
.1
0
-.1
1
2
3
4
5
6
7
8
9
10
11
12

FIGURE 27

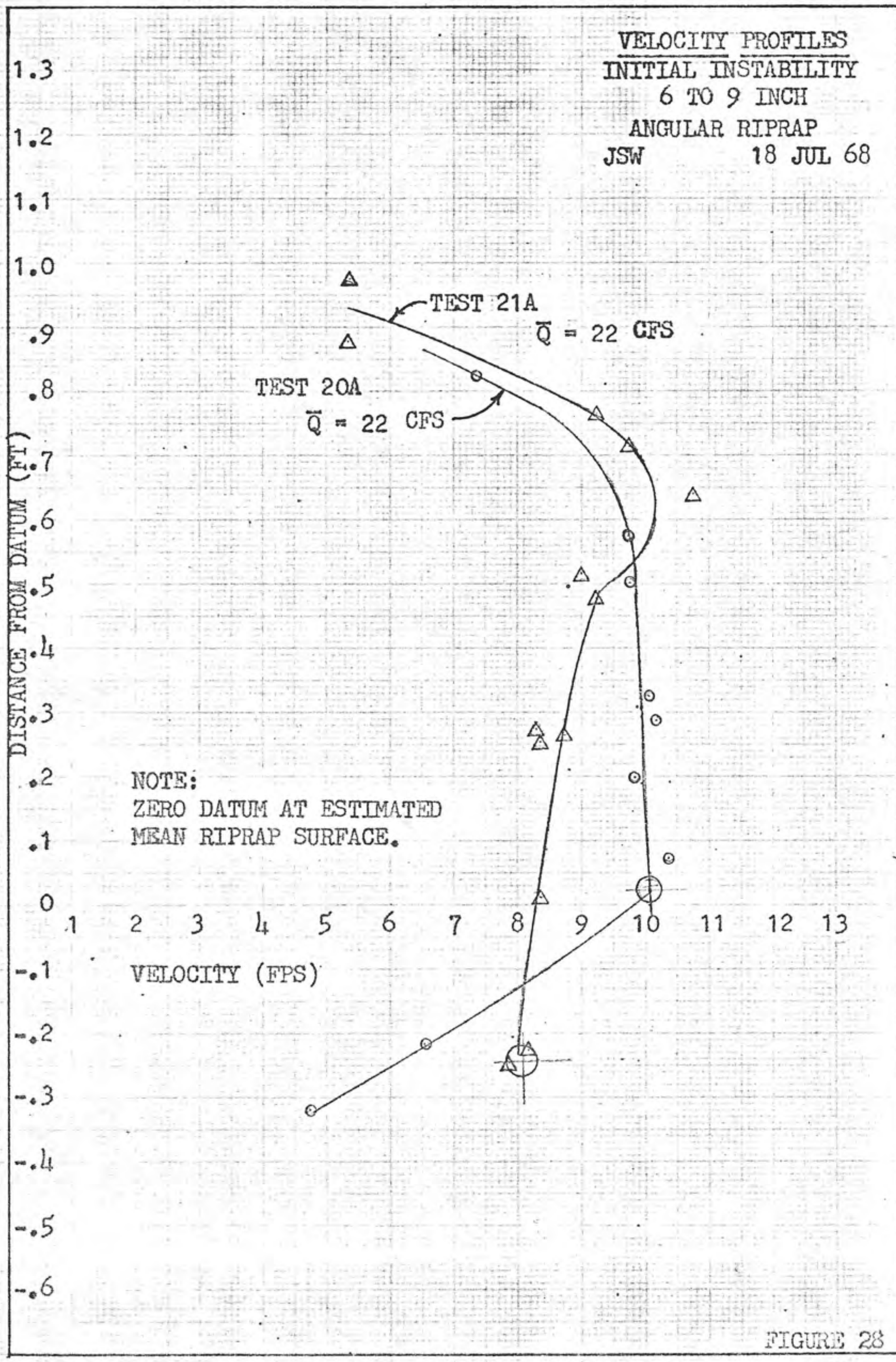
VELOCITY PROFILES
INITIAL INSTABILITY
6 TO 9 INCH
ANGULAR RIPRAP
JSW 18 JUL 68
TEST 21A
$\bar{Q}$ = 22 CFS
TEST 20A
$\bar{Q}$ = 22 CFS
DISTANCE FROM DATUM (FT)
VELOCITY (FPS)
NOTE:
ZERO DATUM AT ESTIMATED
MEAN RIPRAP SURFACE.

FIGURE 28

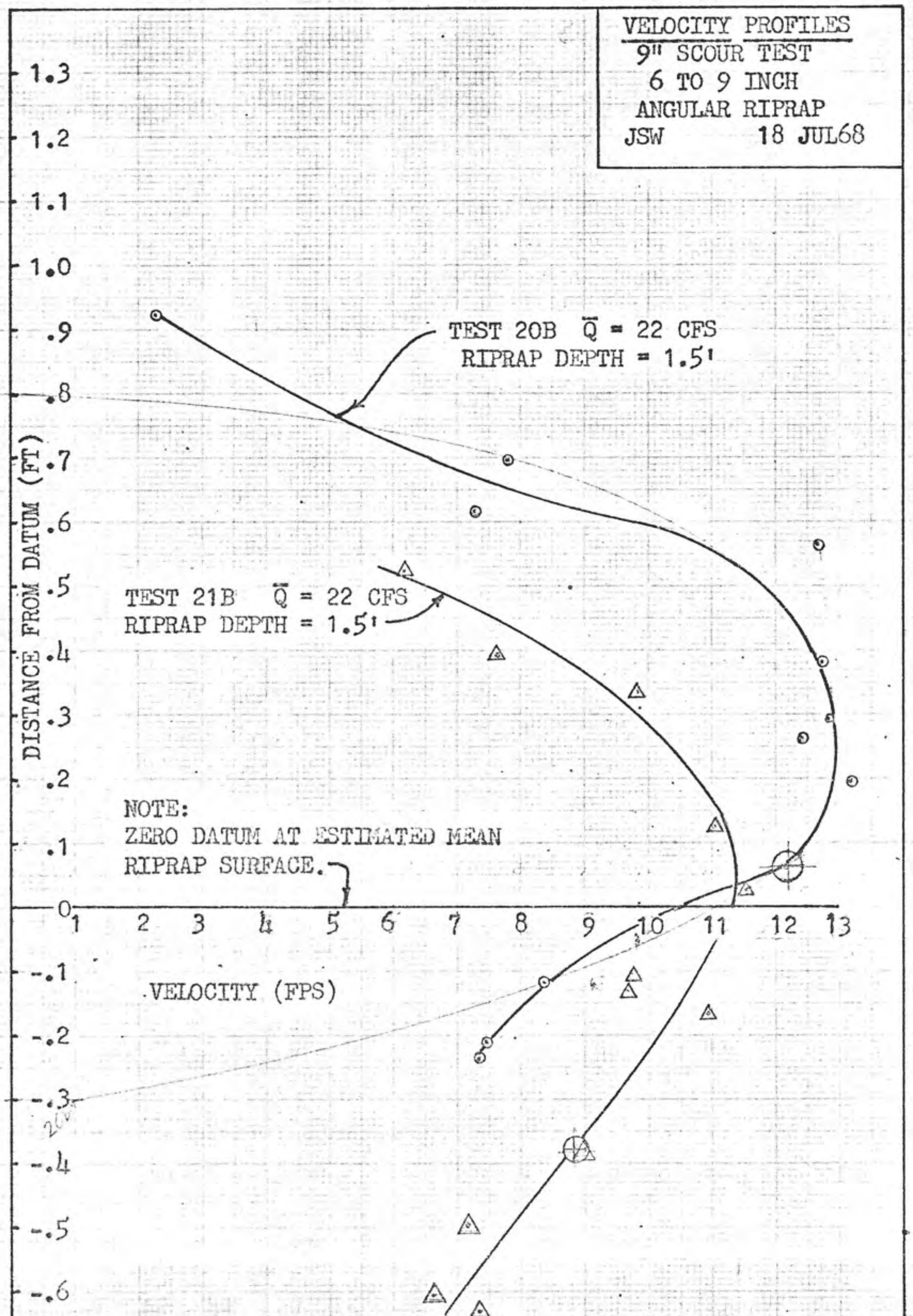
VELOCITY PROFILES
9" SCOUR TEST
6 TO 9 INCH
ANGULAR RIPRAP
JSW 18 JUL68
TEST 20B $\bar{Q}$ = 22 CFS
RIPRAP DEPTH = 1.5'
TEST 21B $\bar{Q}$ = 22 CFS
RIPRAP DEPTH = 1.5'
NOTE:
ZERO DATUM AT ESTIMATED MEAN
RIPRAP SURFACE.
DISTANCE FROM DATUM (FT)
VELOCITY (FPS)
1.3
1.2
1.1
1.0
.9
.8
.7
.6
.5
.4
.3
.2
.1
0
-.1
-.2
-.3
-.4
-.5
-.6
1 2 3 4 5 6 7 8 9 10 11 12 13

FIGURE 29

FIGURE 30. CROSS SECTIONS FOR FINAL SCOUR AT POINT OF MAXIMUM JET CONTRACTION

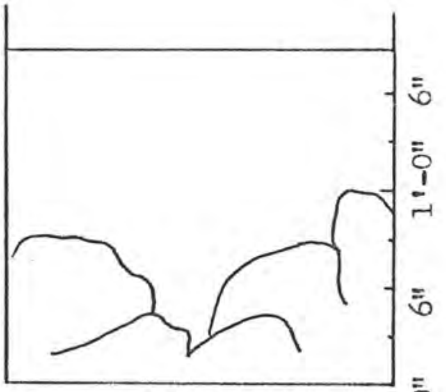

TEST 7
6" ≤ d ≤ 9"
STREAM ROUNDS
BAFFLE SETTING = 1.7'
ABOVE FLOOR

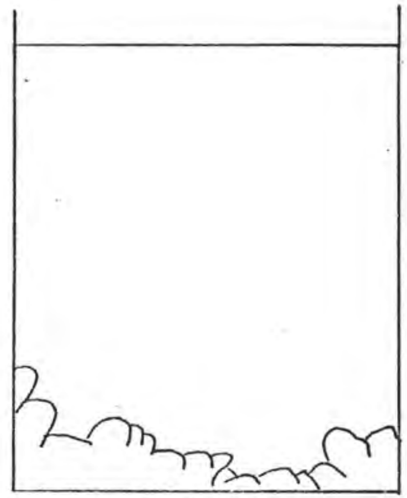

TEST 10
$1\frac{1}{2}$" ≤ d ≤ 3"
STREAM ROUNDS
BAFFLE SETTING = 2.29'
ABOVE FLOOR

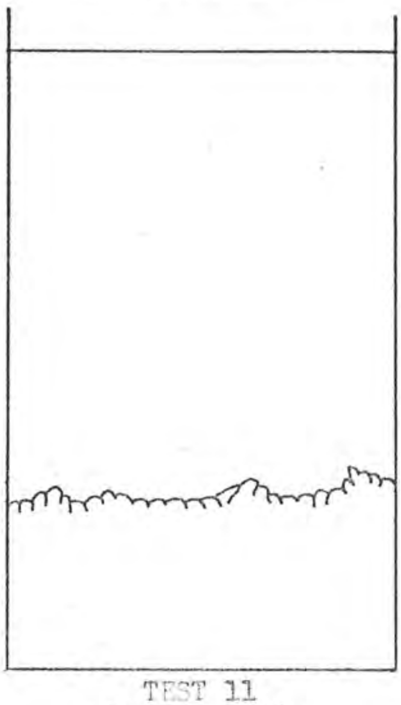

TEST 11
3/4" ≤ d ≤ $1\frac{1}{2}$"
STREAM ROUNDS
BAFFLE SETTING = 3.17'
ABOVE FLOOR

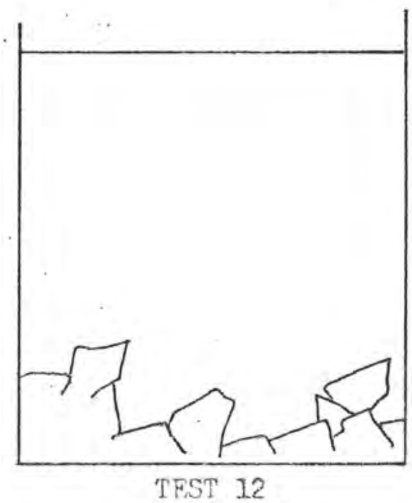

TEST 12
3" d 6"
QUARRY ANGULAR
BAFFLE SETTING = 2.12'
ABOVE FLOOR

FIGURE. 31. CROSS SECTIONS FOR FINAL SCOUR AT POINT OF MAXIMUM JET CONTRACTION

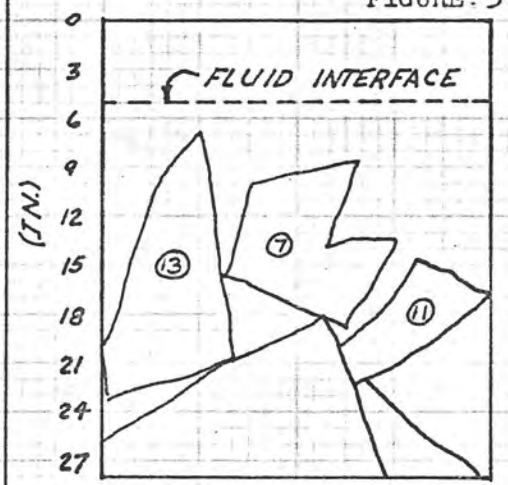

A. TEST 20B
6 TO 9 INCH
ANGULAR RIPRAP
BAFFLE SETTING = 2.3'
ABOVE FLOOR

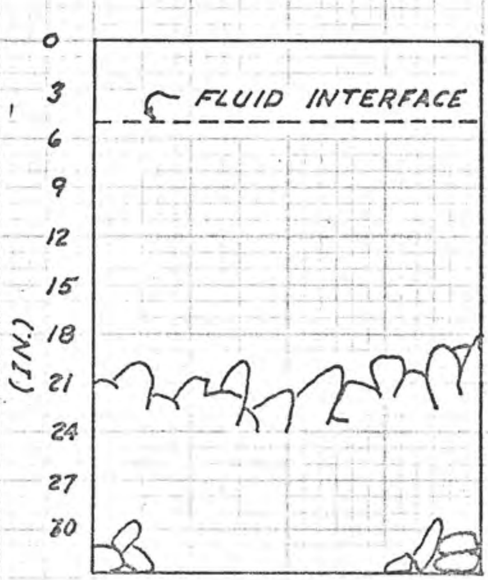

B. TEST 10D
1 1/2 TO 3 INCH
COBBLES
BAFFLE SETTING = 2.71'
ABOVE FLOOR

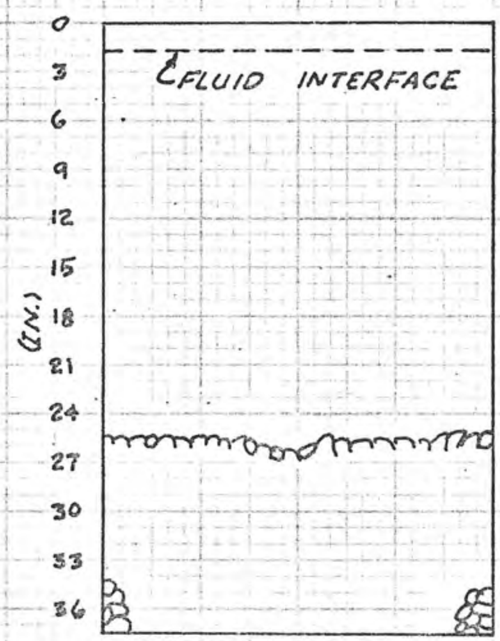

C. TEST 11D
3/4 TO 1 1/2 INCH
COBBLES
BAFFLE SETTING = 3.13'
ABOVE FLOOR

FIGURE 31 . CROSS SECTIONS FOR FINAL SCOUR AT POINT OF MAXIMUM JET CONTRACTION

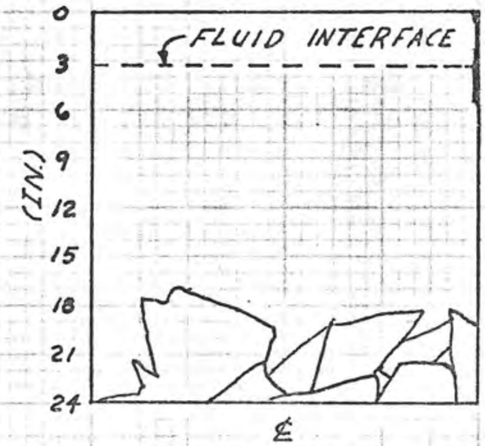

A. TEST 14B
3 TO 6 INCH
ANGULAR RIPRAP
BAFFLE SETTING = 2.0'
ABOVE FLOOR

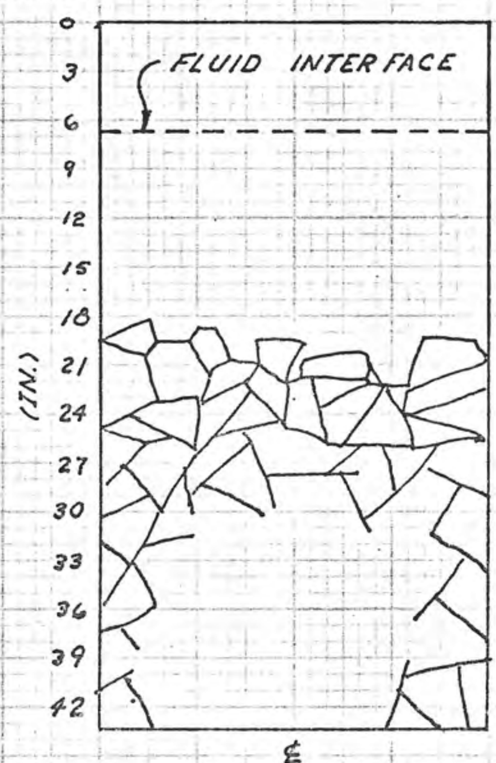

B. TEST 15B
3 TO 6 INCH
ANGULAR RIPRAP
BAFFLE SETTING = 3.62'
ABOVE FLOOR

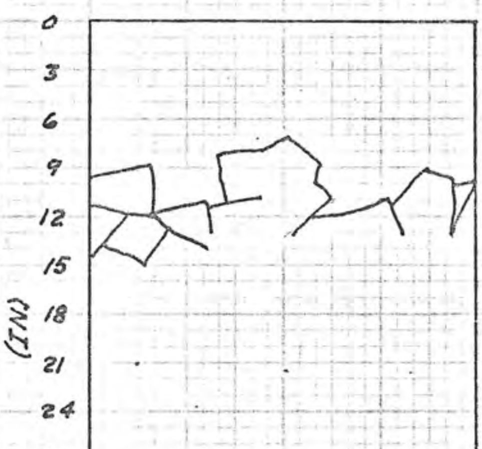

C. TEST 16B
3 TO 6 INCH
ANGULAR RIPRAP
BAFFLE SETTING = 3.0'
ABOVE FLOOR

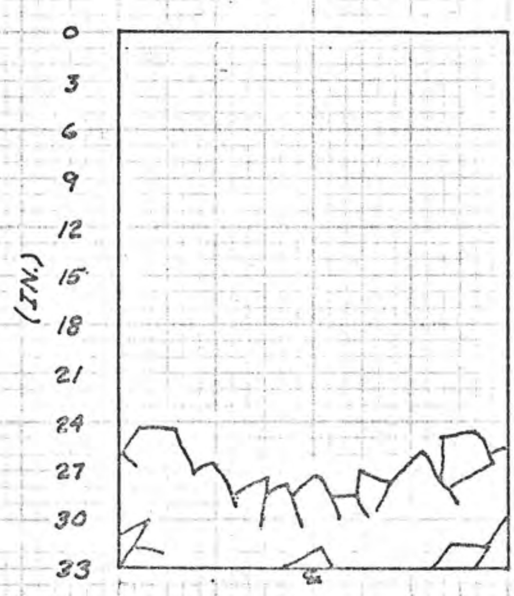

D. TEST 19B
1 1/2 TO 3 INCH
ANGULAR RIPRAP
BAFFLE SETTING = 2.75'

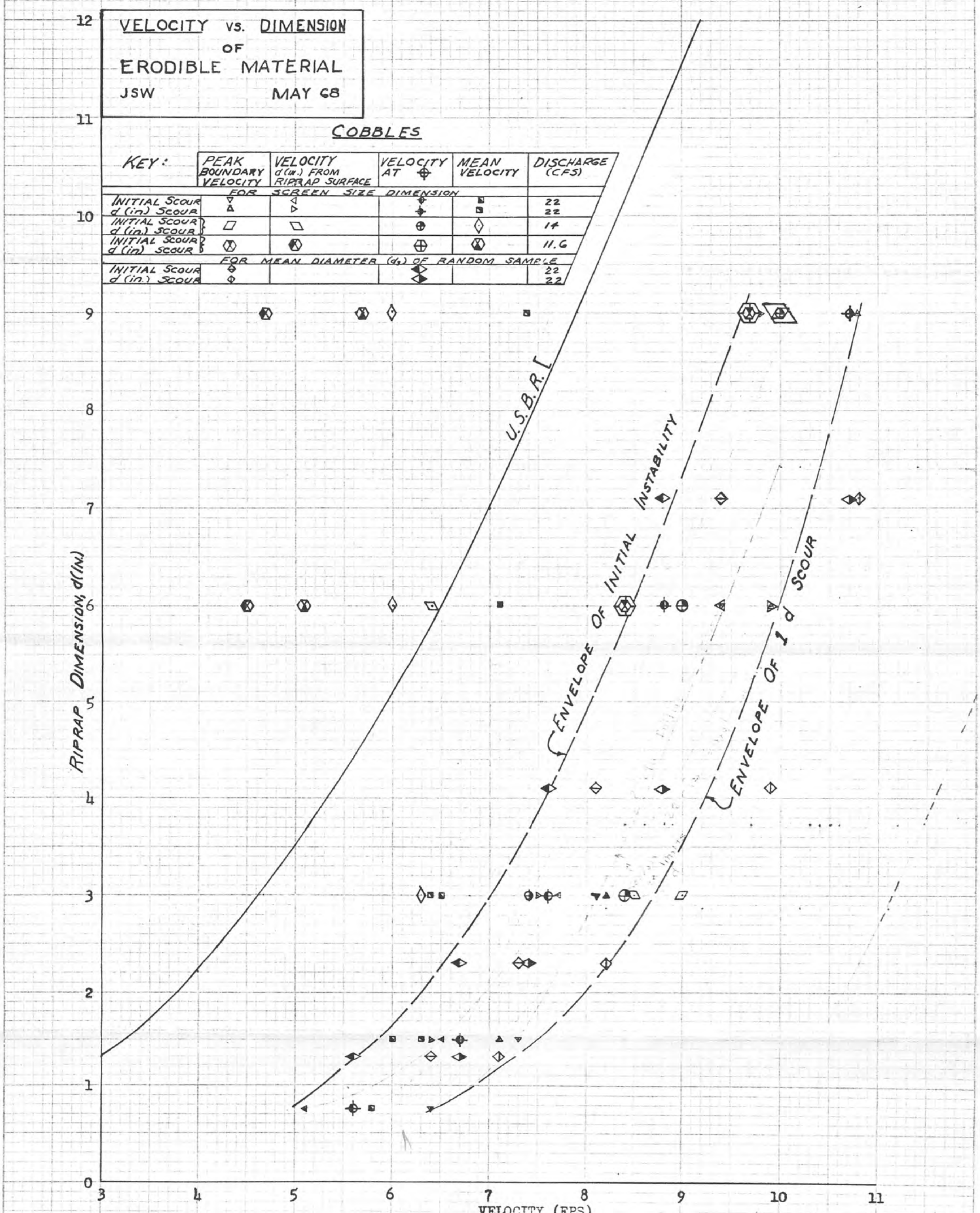
VELOCITY vs. DIMENSION OF ERODIBLE MATERIAL
JSW MAY 68
COBBLES
KEY:
PEAK BOUNDARY VELOCITY
VELOCITY d(in.) FROM RIPRAP SURFACE
VELOCITY AT ⊕
MEAN VELOCITY
DISCHARGE (CFS)
FOR SCREEN SIZE DIMENSION
INITIAL SCOUR
d (in) SCOUR
22
22
14
11.6
FOR MEAN DIAMETER (d₁) OF RANDOM SAMPLE
22
22
U.S.B.R.
ENVELOPE OF INITIAL INSTABILITY
ENVELOPE OF 1 d SCOUR
RIPRAP DIMENSION, d(IN.)
VELOCITY (FPS)

FIGURE 32

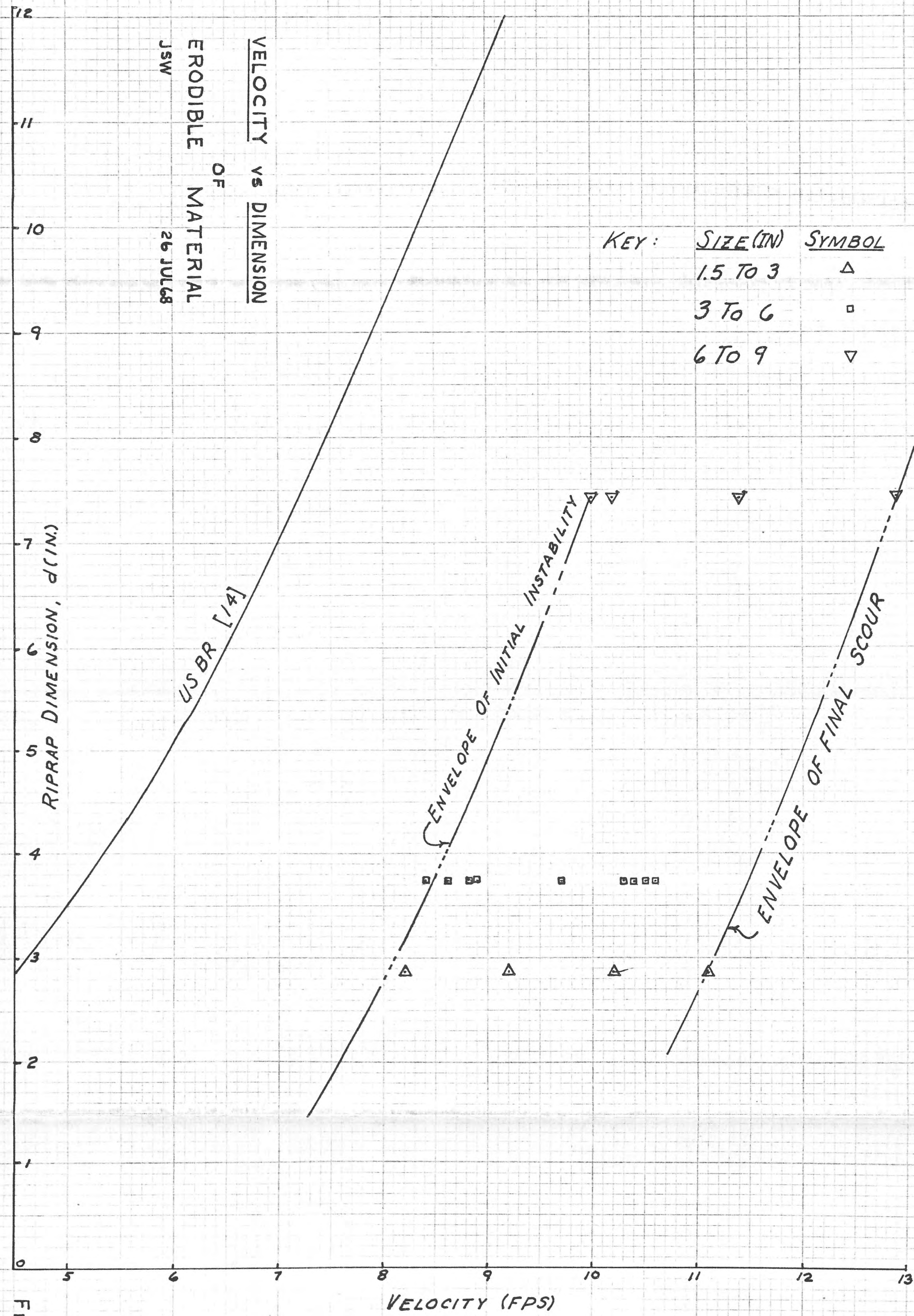
VELOCITY vs DIMENSION OF ERODIBLE MATERIAL
JSW 26 JUL 68
KEY: SIZE (IN) SYMBOL
1.5 TO 3 △
3 TO 6 □
6 TO 9 ▽
USBR [14]
ENVELOPE OF INITIAL INSTABILITY
ENVELOPE OF FINAL SCOUR
RIPRAP DIMENSION, d (IN.)
VELOCITY (FPS)
0
1
2
3
4
5
6
7
8
9
10
11
12
13

FIGURE 33

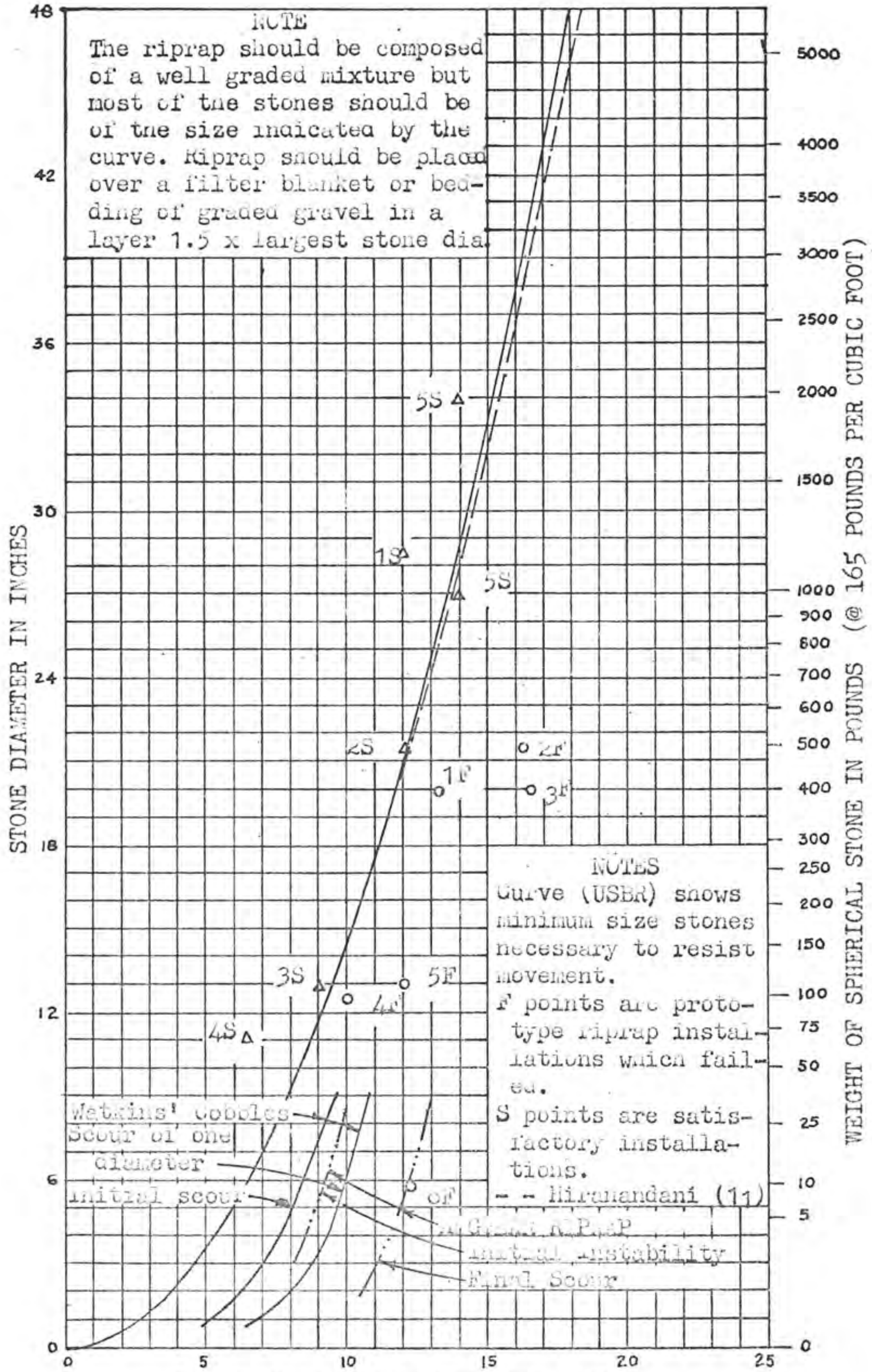

BOTTOM VELOCITY IN FEET PER SECOND

FIGURE 34

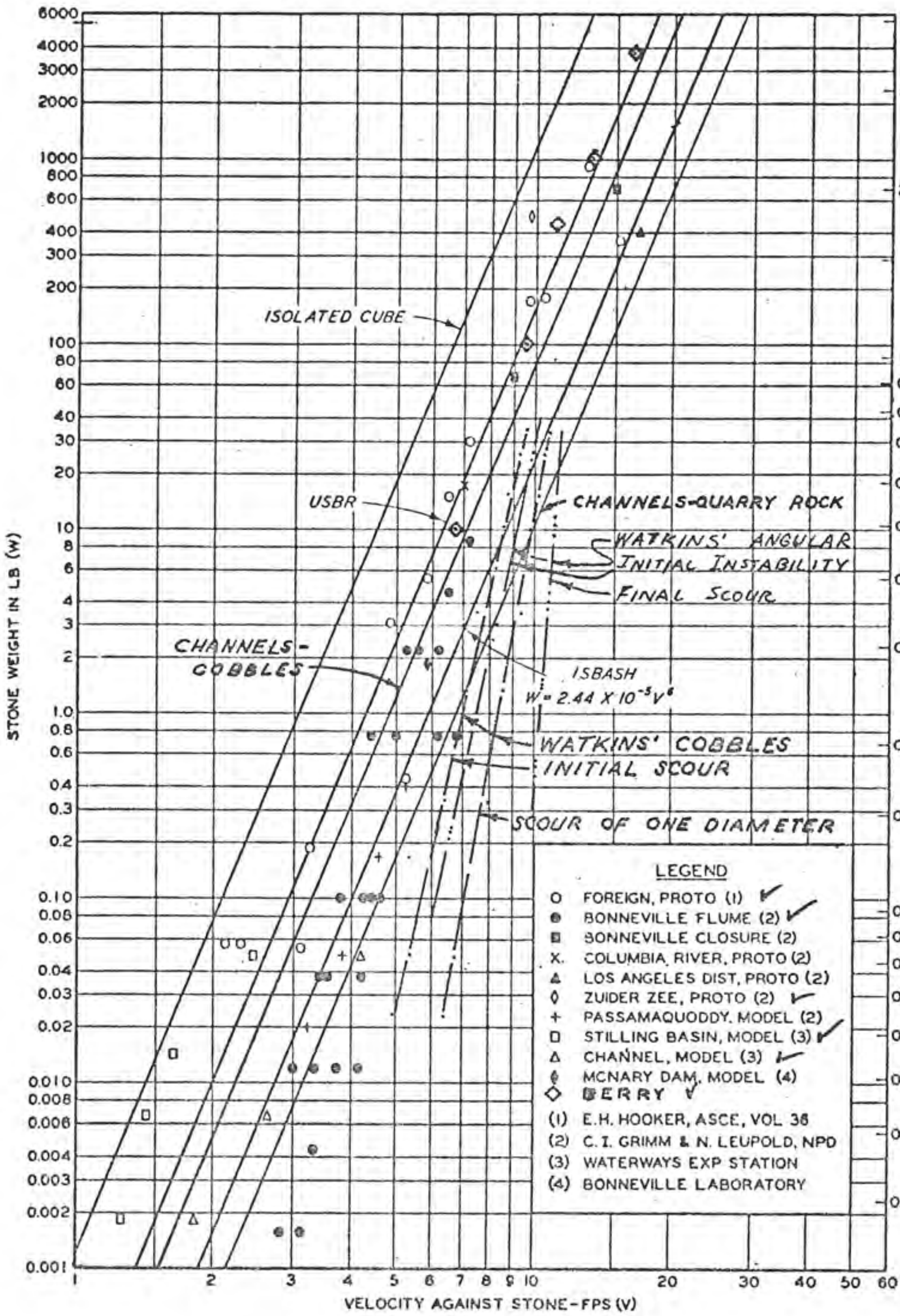

Note: ✓ V based on V_s, others on V_m

NOTE: SPECIFIC WEIGHT OF ROCK = 165 LB/CU FT.

FIGURE 35

RIVER CLOSURES

VELOCITY VS STONE WEIGHT

HYDRAULIC DESIGN CHART 712-1

CURVES USED BY EPR AND US ARMY CE

REVISED 8-58 WES 6-57

FIGURE 36

ANDERSSON'S SUMMARY OF VELOCITY CURVES
REQUIRED DIAMETER OF STONE AS A FUNCTION OF MEAN VELOCITY

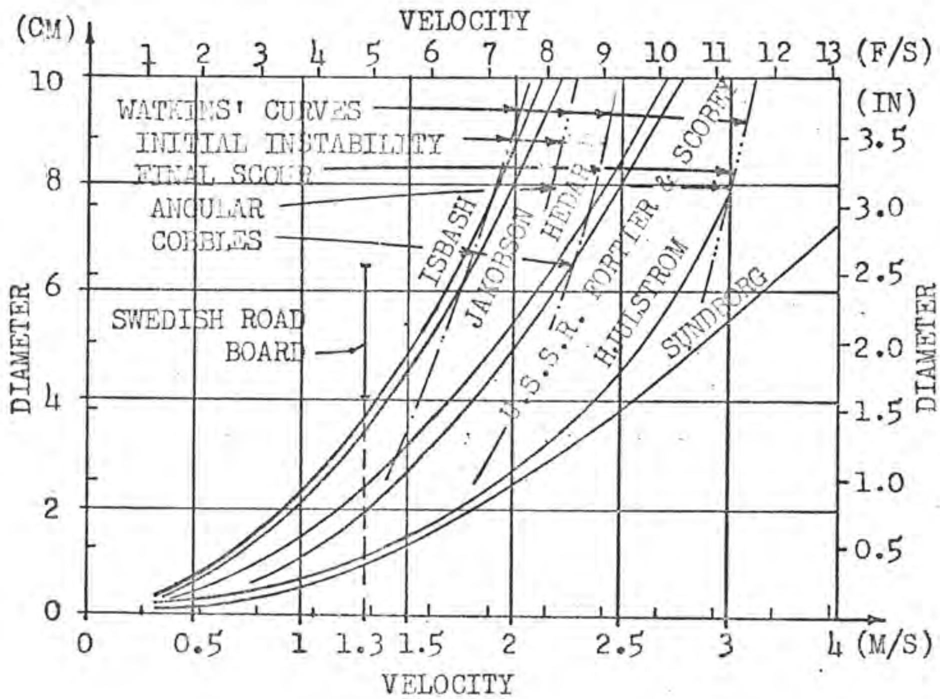

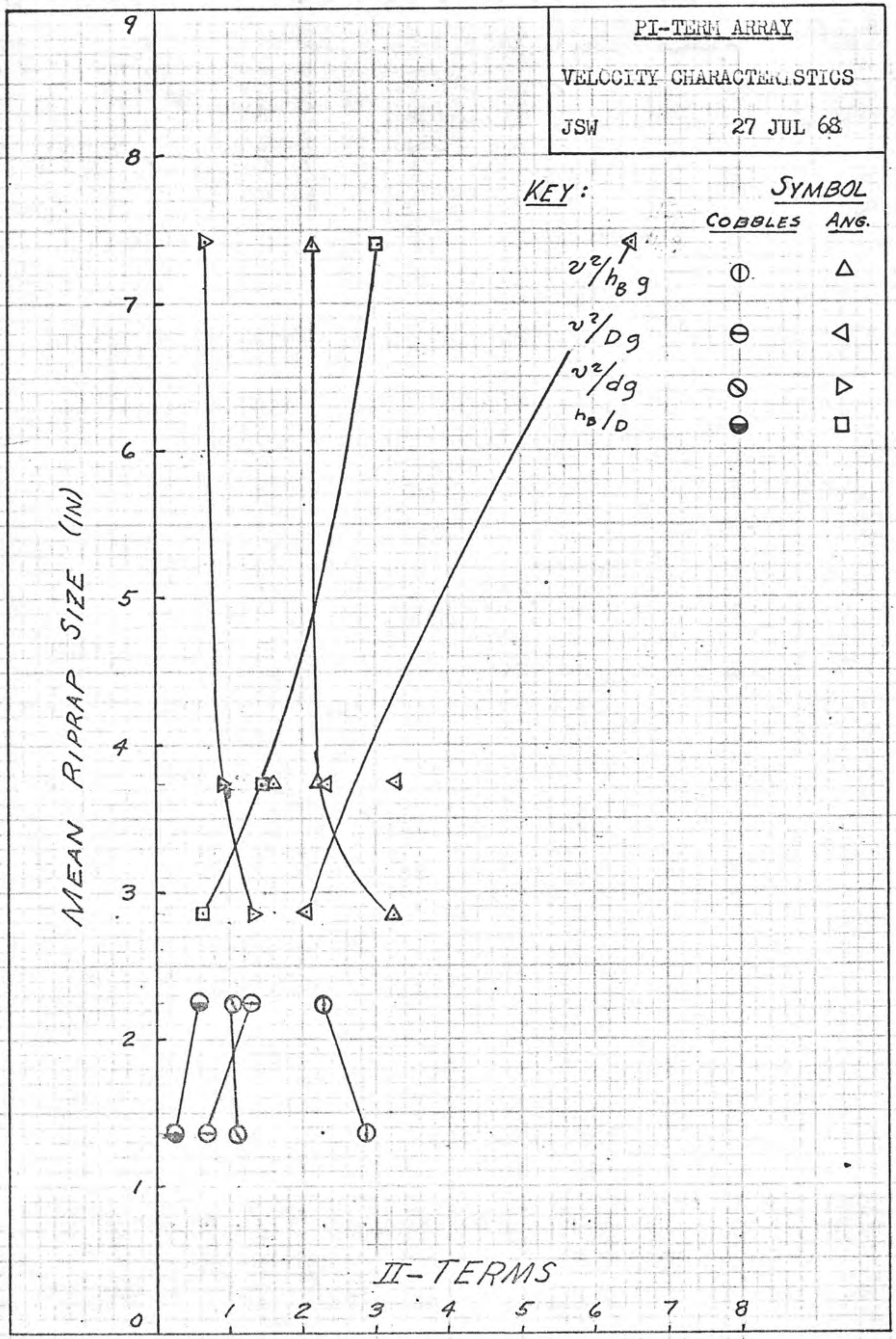
PI-TERM ARRAY
VELOCITY CHARACTERISTICS
JSW
27 JUL 68
KEY:
SYMBOL
COBBLES
ANG.
v²/h_B g
v²/Dg
v²/dg
h_B/D
MEAN RIPRAP SIZE (IN)
Π-TERMS
0
1
2
3
4
5
6
7
8
9

FIGURE 37

APPENDIX

COMPUTOR PROGRAM ENTITLED "RIPSHA"

```
10 DIM S(50), Z(50), X(50), V(50), U$(50)
20 READ N
30 FØR J = 1 TØ N
40 READ A,B,C,W,H1,H2
50 LET V(J) = 0.670857*(H2 - H1)
60 LET Z(J) = B/A
70 LET X(J) = C/B
80 LET S(J) = (C *B)/ A↑2
90 NEXT J
100 LET K1 = K2 = K3 = K4 = 0
110 FØR J = 1 TØ N
120 IF Z(J) > 0.667 THEN 200
130  IF  X(J) < 0.667 THEN 170
140  LET K2 = K2 + 1
150 LET U$(J) = "II"
160  GØ TØ 260
170 LET K1 = K1 + 1
180 LET U$(J) = "I"
190 GØ TØ 260
200 IF  X(J) < 0.667 THEN 240
210 LET K4 = K4 + 1
220 LET U$(J) = "IV"
230 GØ TØ 260
240 LET K3 = K3 + 1
250 LET U$(J) = "III"
260 NEXT J
270 LET S1 =S2 =S3 =S4 =S5 =S6 =S7 =S8 =S9 =T1 =0
280 FØR J = 1 TØ N
290 IF S(J) > 0.1 THEN 320
300 LET T1 = T1 + 1
310 GØ TØ 570
320 IF S(J) > 0.2 THEN 350
330 LET S8 = S8 +1
340 GØ TØ 570
350 IF S(J) > 0.3 THEN 380
360 LET S9 = S9 + 1
370 GØ TØ 570
380 IF S(J) > 0.4 THEN 410
390 LET S1 = S1 +1
400 GØ TØ 570
410 IF S(J) > 0.5 THEN 440
420 LET S2 = S2 + 1
430 GØ TØ 570
440 IF S(J) > 0.6 THEN 470
450 LET S3 = S3 + 1
460 GØ TØ 570
```

COMPUTOR PROGRAM ENTITLED "RIPSHA", continued

```
470 IF S(J) > 0.7THEN 500
480 LET S4 = S4 + 1
490 GØ TØ 570
500 IF S(J) > 0.8 THEN 530
510 LET S5 = S5 + 1
520 GØ TØ 570
530 IF S(J) > 0.9 THEN 560
540 LET S6 = S6 + 1
550 GØ TØ 570
560 LET S7 = S7 + 1
570 NEXT J
580 LET T1 = 100 * (T1/N)
590 LET S9 = 100 * (S9/N)
600 LET S8 = 100 * (S8/N)
610 LET S1 = 100 * (S1/N)
620 LET S2 = 100* (S2/N)
630 LET S3 = 100* (S3/N)
640 LET S4 = 100* (S4/N)
650 LET S5 = 100* (S5/N)
660 LET S6 = 100* (S6/N)
670 LET S7 = 100* (S7/N)
680 LET J3 = 1
690 PRINT
700 PRINT "RØCK", "ZING", "BC/A↑2", "VØL"
710 LET M1 = J3
720 PRINT "NUMBER", "CLASS", "SPHERICITY", "CU FT"
730 LET J3 = 1
740 FØR J = M1 TØ N

750 LET J3 = J3 + 1
760 PRINT J, U$(J), S(J), V(J)
770 IF J3 > 20 THEN 690
780 NEXT J
790 PRINT
795 PRINT "  ", "  ", "TABLE"
800 PRINT
```

COMPUTOR PROGRAM ENTITLED "RIPSHA", continued

```
805 PRINT
810 PRINT
815 PRINT "  ", "ZING CLASSIFICATIØNS:  PER CENT PER CATEGØRY"
820 PRINT "  ", "---- ---------------"
825 PRINT  "  ", "I", "II", "III", "IV"
830 PRINT "   ", "DISK", "SPHERICAL", "BLADE", "RØDLIKE"
835 PRINT "PERCENT", ((K1*100)/N),((K2*100)/N),((K3*100)/N);
840 PRINT ((K4*100)/N)
845 PRINT
850 PRINT "SPHERICITY CLASSIFICATIØN = (C*B)/A↑2"
855 PRINT "--------------------------------------"
860 PRINT "PER CENT - 0.0 TØ 0.1 = "; T1
865 PRINT "PER CENT - 0.1 TØ 0.2 = "; S8
870 PRINT "PER CENT - 0.2 TØ 0.3 = "; S9
875 PRINT "PER CENT - 0.3 TØ 0.4 = "; S1
880 PRINT "PER CENT - 0.4 TØ 0.5 = "; S2
885 PRINT "PER CENT - 0.5 TØ 0.6 = "; S3
890 PRINT "PER CENT - 0.6 TØ 0.7 = "; S4
895 PRINT "PER CENT - 0.7 TØ 0.8 = "; S5
900 PRINT "PER CENT - 0.8 TØ 0.9 = "; S6
905 PRINT "PER CENT - 0.9 TØ 1.0 = "; S7
910 PRINT
915 GØ TØ 20
1000 DATA 36
9999 END
```

COMPUTOR PROGRAM ENTITLED "RIPRAP"

```
10 DIM P(50),F(50), Ø(50), D(50), V(50)
20 DIM W(50), G(50)
30 DIM E(40), A(40), B(40), C(40), M(40)
40 READ N,Y
50 LET G1 = 0
60 FØR J = 1 TØ N
70 READ A, B, C, W, H1, H2
74 IF J > 16 THEN 80
76 LET W = W - 0.11
80 LET V(J) = 0.670857*(H2-H1)
90 LET G(J) = W/V(J)
100 LET G1 = G1 + G(J)
110 LET W(J) = W
112 LET A(J) = A
114 LET B(J) = B
116 LET C(J) = C
120 NEXT J
130 LET G = G1/N
140 FØR J = 1 TØ N
150 LET D(J) = (W(J)/(.76*G))↑.3333
160 LET D(J)= 12* D(J)
170 LET E(J) = (A(J)+B(J)+C(J))/3
180 LET P(J) = E(J)/D(J)
190 LET F(J) = E(J)/Y
200 LET M(J) = (A(J)*B(J)*C(J))/12↑3
210 LET Ø(J) =V(J)/M(J)
220 NEXT J
230 LET D1 = 0
240 FØR J = 1 TØ N
250 LET D1 = D1 + D(J)
260 NEXT J
270 LET J2 = 1
280 PRINT
290 PRINT " ", " ", "TABLE"
300 PRINT
```

COMPUTOR PROGRAM ENTITLED "RIPRAP", continued

```
310 PRINT " ", "PIE TERMS FØR PHYSICAL CHARACTERISTICS ØF RIPRAP"
320 LET M1 = J2
330 PRINT
340 LET J2 = 1
350 PRINT "WHERE DIA=DIAMETER ØF SPHERE ØF WEIGHT EQUAL TØ RØCK SAMPLE"
360 PRINT "PIE 1 IS RATIØ ØF MEAN AXIS DIM AND DIA ØF = WT SPHERE"
370 PRINT "PIE 2 IS RATIØ ØF MEAN AXIS DIM AND SIGNIFICANT DEPTH"
380 PRINT "PIE 3 IS RATIØ ØF RØCK VØLUME AND ABC RECTANGULAR SØLID"
390 PRINT
400 PRINT "RØCK","DIA","PIE 1","PIE 2","PIE 3"
410 PRINT "NUMBER","INCHES"
420 FØR J = M1 TØ N
430 LET J2 = J2 + 1
440 PRINT J,D(J),P(J),F(J),Ø(J)
450 IF J2 > 20 THEN 280
460 NEXT J
470 PRINT "MEAN DIA ØF = WEIGHT SPHERE";(D1/N);" INCHES"
480 PRINT
490 GØ TØ 40
998 REM   INSERT DATA IN LINE 1000:  N, Y, G
1005 REM   AXIAL DIMENSIØNS (IN)   WEIGHT  HT ØF EQ CYL
1007 REM      A       B       C  LBS     H1      H2
9999 END
```

COMPUTOR PROGRAM ENTITLED "AREVEL"

```
10 DIM  A(20),D(20),G(20), Q(20),V(20),T(20),F(20),E(20),U(20),H(20)
15 DIM L(10),P(10),R(10),S(10), X(10), Y(10), C(10)
20 READ N
22 FØR J = 1 TØ N
24 READ D(J)
28 NEXT J
30 FØR J=1 TØ N
40 READ T(J),Ø(J),P(J),R(J),S(J),X(J),Y(J),C(J),Q(J)
50 LET A(J) = P(J)-Ø(J)
60 LET L(J) = A(J)/2
70 LET A(J) =.5 * A(J)
80 LET V(J) = ((S(J) - R(J))*0.645)/D(J)
90 LET F(J)=V(J)* A(J)
100 LET Q(J) = .5 * Q(J)
110 LET G(J) = Q(J)-F(J)
130 LET H(J) = X(J) - Y(J)
140 LET U(J) = (1/SQR(1-(Y(J)/X(J))↑2)) * SQR(2*32.2*H(J))
150 LET E(J) = U(J)*C(J)*A(J)
160 NEXT J
170 PRINT
180 PRINT " ", " ", "TABLE"
190 PRINT
200 PRINT " ", " ", "DISCHARGE"
210 PRINT
220 PRINT "WHERE","G = FLØW IN CUBIC FEET PER SECØND IN GRAVEL"
230 PRINT " ",  "Q = TØTAL DISCHARGE FØR UNIT WIDTH SECTIØN"
240 PRINT " ","F = DISCHARGE IN JET CØMPUTED BY THE CØNTINUITY EQUATIØN"
250 PRINT " ", "E = DISCHARGE IN JET CØMPUTED BY EQUATIØN 3.16"
260 PRINT
270 PRINT "TEST","DISCHARGE","TØTAL","DISCHARGE","DISCHARGE"
280 PRINT "NUMBER","IN","DISCHARGE","F","E"
290 PRINT "   ","RIPRAP","IN"," "," "
300 PRINT "   ",  "G","FLUME"," "," "
```

COMPUTOR PROGRAM ENTITLED "AREVEL", (continued)

```
310 PRINT " ","(CFS/FT)","(CFS/FT)","(CFS/FT)","(CFS/FT)"
320 PRINT
330 FØR J = 1 TØ N
340 PRINT T(J),G(J),Q(J), F(J), E(J)
350 NEXT J
360 PRINT
370 PRINT
380 PRINT " "," ","TABLE"
390 PRINT
400 PRINT " ","CØMPARISØN ØF VELØCITY CØMPUTATIØN"
410 PRINT
420 PRINT"WHERE V = MEAN VELØCITY ØF JET BY VELØCITY PRØFILE AVERAGING"
430 PRINT TAB(7);"U = MEAN JET VELØCITY BY EQUATIØN 3.15"
435 PRINT " " ,"L = MEAN DEPTH ØF JET ABØVE RIPRAP SURFACE"
440 PRINT
450 PRINT "TEST","V", "U", "L"
460 PRINT "NUMBER","(FPS)","(FPS)"
470 PRINT
480 FØR J= 1 TØ N
490  PRINT T(J), V(J), U(J), L(J)
500 NEXT J
510 GØ TØ 20
520 DATA 6
525 DATA 1,75, 1.96, 1.35, 1.35, 1.42, 1.66
530 DATA 10, 81.70, 83.78, 77.30,  95.52, 4.10, 3.090, .81000, 21.85
540 DATA 11,  99.78, 99.90, 06.04, 23.77, 3.85, 3.314, .89000, 22.09
550 DATA 14, 12.14, 14.82, 80.02, 90.34, 4.20, 2.057, .83330, 22.30
560 DATA 15, 06.51, 08.72, 90.34, 108.12, 3.70, 2.112, .65120, 22.00
570 DATA 19, 94.05, 97.80, 14.85, 31.00, 3.80, 2.619, .83188, 21.47
580 DATA 20, 88.76, 90.07, 54.55, 73.95, 5.14, 2.683, .67860, 21.82
1000 END
```

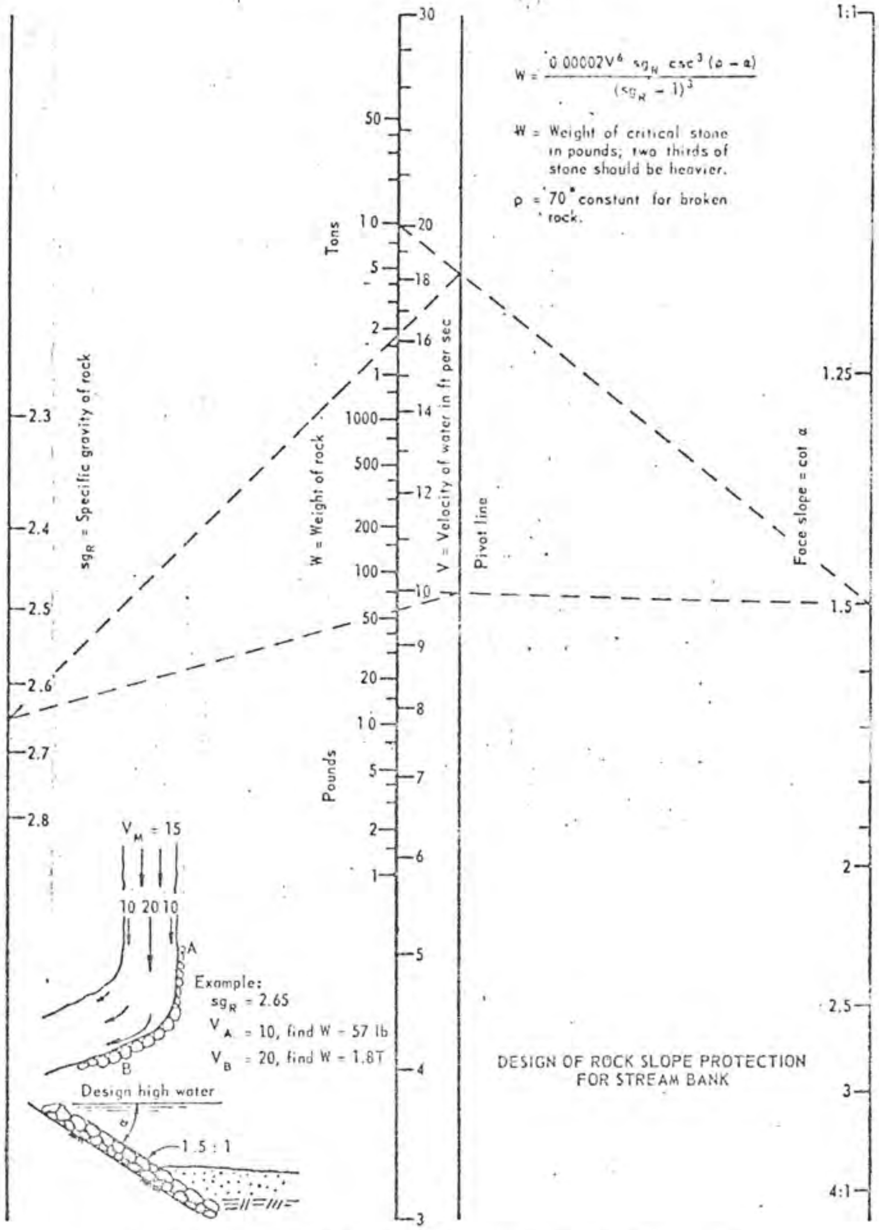

CHART D. Nomograph for design of stream-bank rock slope protection.

TABLE 4. EFFECT OF EXTREME RANGE OF SHAPE ON SIZE OF SPECIFIED REVETMENT STONES

Shape	Shape ratios		Shape factor V/Vm	$j = \frac{V}{l^3}$	$k = \frac{l}{\sqrt[3]{W}}$ for	
	r	s			$sg = 2.4$ $d = 150$	2.8 175
Spheroidal	1.00	1.00	.52	.52	.23	.22
Lenticular	.33	1.00	.52	.17	.34	.32
Ellipsoidal	.33	.33	.52	.058	.49	.46
Cylindrical	.33	.33	.785	.087	.42	.40
Discoidal	.33	1.00	.785	.26	.30	.28
Cuboidal	1.00	1.00	.19	.19	.33	.31
Tetragonal	.33	.75	.26	.082	.43	.41
Slabal	.33	.97	.28	.092	.41	.39
Conoidal	1.00	1.00	.26	.26	.30	.28
Pyramidal	1.00	1.00	.33	.33	.27	.26
Tetrahedral	.33	.38	.17	.062	.68	.63
Normal cube	1.00	1.00	1.00	1.00	.188	.179

For this purpose, the characteristic shapes are assumed to be the extremes within the definitions of shapes and specifications for permissible elongation. Such shapes may occur, but they will not be dominant, except possibly the slabal shape in rock broken from laminar formations, and the lenticular shape common to cobbles.

Axial length is also taken as an extreme. The effect of this is most striking for the cuboidal shape. If axes were taken normal to faces of a cube, the volume is l^3, but if l is the diagonal of the cube, its volume is $.19l^3$. The normal cube is listed at bottom of the table to emphasize this difference.

Maximum Length

Table 4 expresses the volume of extreme shapes in two ways: (1) as a shape factor, or ratio to the enveloping prism, and (2) as a ratio to the cube of the longest dimension.

For the latter, the table shows k for the relation $V = j\,l^3$, and since $W = Vd$,

$$l = \sqrt[3]{W/jd} = k\,\sqrt[3]{W} \quad \text{where} \quad k = 1/\sqrt[3]{jd}$$

Values of k for extremes of density are tabulated in the last two columns.

To illustrate use of k, consider a 4-ton stone, for which the cube root of the weight in pounds is 20. Using a density of 175 pcf, if the stone is a perfect cube, its side is 20 x .179 = 3.58 ft. If a sphere, its diameter is 20 x .22 = 4.4 ft. If lenticular with vertical diameter only a third of its horizontal diameter, the latter is 20 x .32 = 6.4 ft. Specifications will even allow a shape 20 x .46 = 9.2 ft long.

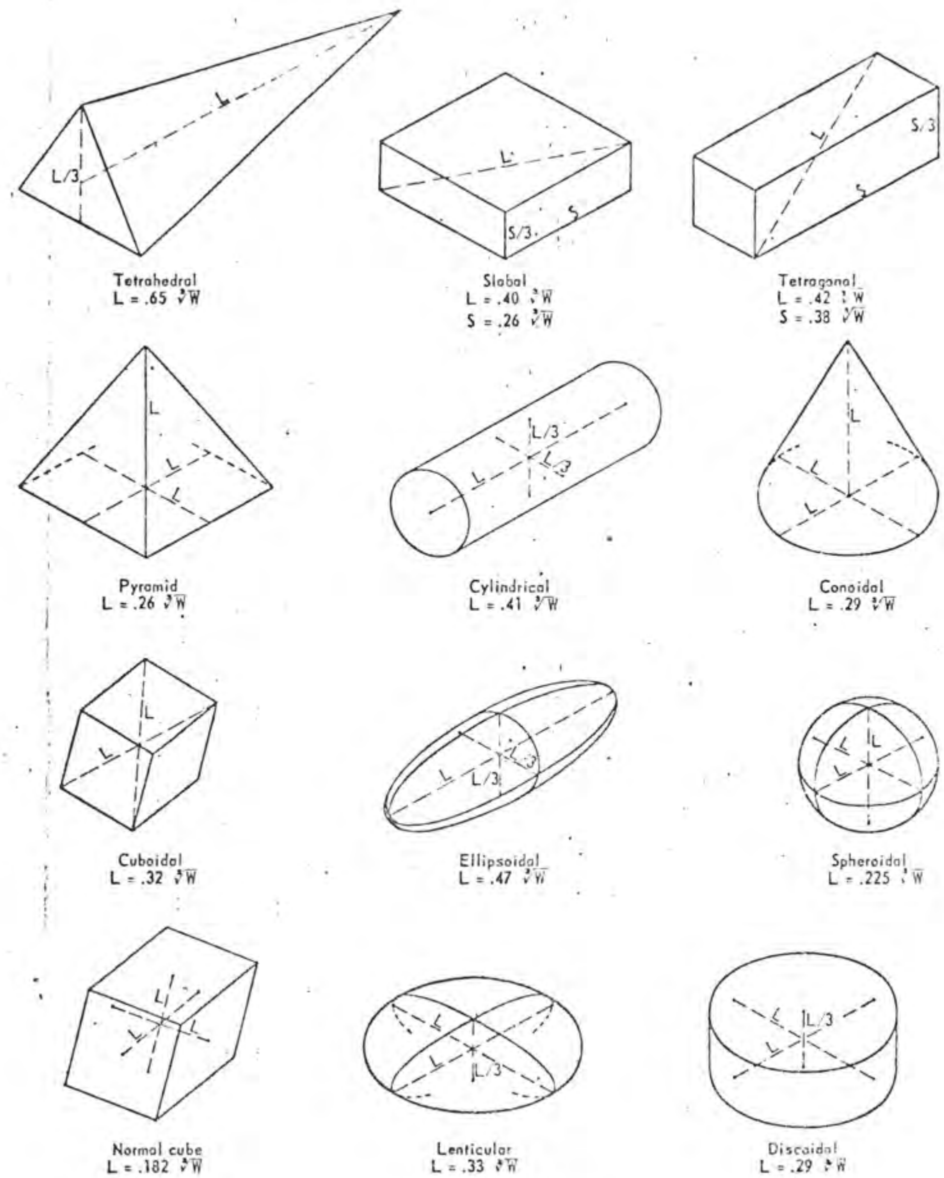

FIGURE 157.
Effect of extreme range of shape on size of specified revetment stones.